

7. SITE 289

The Shipboard Scientific Party¹

SITE DATA

Date Occupied: 31 May 1973 (1630)

Date Departed: 8 June 1973 (1130)

Time on Site: 187 hours

Position:

Latitude: 00°29.92'S

Longitude: 158°30.69'E

Water Depth (from sea level): 2206 meters (echo sounding)

Bottom Felt At: 2224 meters (drill pipe)

Penetration: 1271 meters

Number of Holes: 1

Number of Cores: 133

Total Length of Cored Section: 1271 meters

Total Core Recovered: 712.6 meters

Percentage of Core Recovery: 56%

Oldest Sediment Cored:

Depth below sea floor: 1262.5 meters

Nature: Limestone and altered ash

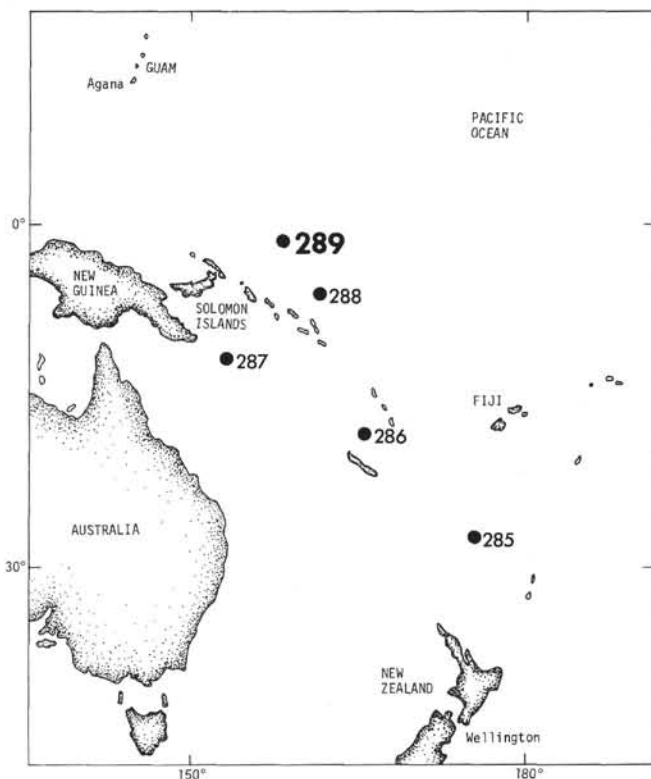
Age: Aptian

Basement:

Depth below sea floor: 1262.5 meters (drilled)

Nature: Basalt

Principal Results: Extrusive basalt, pre-early Aptian (1271-1262 m); Early Cretaceous (Aptian) to late Eocene Radiolaria-bearing limestone, siliceous limestone nanno-foram chalk, nodular chert, and tuff (1262-969 m); late Eocene to Pleistocene nanno-foram ooze and chalk (969-0 m). At Site 289 on the northern part of the Ontong-Java Plateau the Pleistocene to early Oligocene sequence is continuous and contains a diverse microflora and microfauna with good to excellent preservation. Very minor chert was detected in the early Miocene with the major appearance in middle Eocene accompanied by the loss of Radiolaria from the sediments. Less chert was observed at this site than at Site 288. Plateau elevation has been relatively constant above the foram solution depth, with the exception of a



deeper interval in the Campanian as seen also at Site 288. At least six substantial stratigraphic breaks are present in the section. These occur between Rupelian (lower Oligocene) and Bartonian; Lutetian (middle Eocene) and Ypresian; Ypresian and Thanetian (upper Paleocene); Thanetian and Danian (lower Paleocene); lower Danian and Maestrichtian; and Aptian and Campanian. The Eocene/Oligocene break is similar to that reported in the Tasman and Coral seas.

BACKGROUND AND OBJECTIVES

¹James E. Andrews, University of Hawaii, Honolulu, Hawaii (Co-chief scientist); Gordon Packham, University of Sydney, N.S.W., Australia (Co-chief scientist); James V. Eade, New Zealand Oceanographic Institute, Wellington, New Zealand; Brian K. Holdsworth, The University of Keele, Staffordshire, England; David L. Jones, U.S. Geological Survey, Menlo Park, California; George DeVries Klein, University of Illinois, Champaign-Urbana, Illinois; Loren W. Kroenke, University of Hawaii, Honolulu, Hawaii; Tsunemasa Saito, Lamont-Doherty Geological Observatory, Palisades, New York; Samir Shafik, University of Adelaide, Adelaide, South Australia; Douglas B. Stoeser, University of Oregon, Eugene, Oregon (now at Cambridge Astrophysical Observatory, Cambridge, Mass.); Gerrit J. van der Lingen, New Zealand Geological Survey, Christchurch, New Zealand.

The Ontong-Java Plateau has a very thick and, so far as was known, continuous sequence of biogenic sediments that extends back to at least the middle Eocene (Site 64) (Winterer, Riedel, et al., 1971). The principal objective was to core the section continuously to provide a standard section for the tropical biostratigraphy and to extend the sequence down below the chert as far as possible. In the vicinity of Site 289 (160 km north of Site 64) the basement reflector is about 0.1 sec below the chert reflector. In view of the result of drilling at Site 288, where the acoustic basement was

found to be limestones and cherts at least Aptian in age at the base, it was important that the acoustic basement should be penetrated at Site 289.

Apart from the nature of the basement at Site 288 other data relevant to the determination of this basement are:

- 1) The acoustic basement on the plateau shows only little evidence of layering;
- 2) The magnetic anomalies are of low amplitude;
- 3) On the track to Site 288 from the Solomon Islands the anomalies appear to trend at 060°T .

This trend of the magnetic anomalies, if correct, differs slightly from the 80°T trend of the Mesozoic Phoenix anomalies (Larson and Chase, 1972) to the east, and the Ontong-Java anomaly amplitude is more subdued. The smaller amplitude might be due to the anomalies originating on the Ontong-Java Plateau in an equatorial region or the anomalies being damped by lava flows. Since the anomalies in the vicinity of Site 288 are also of low amplitude, there is no obvious reason why the acoustic basement should be different from that at Site 289. If the increasing age of the Phoenix anomalies to the north is correct and the same rate of spreading applies, the basement at Site 289 should be 15 m.y. older than at Site 288, i.e., greater than 121 m.y. (assuming no fracture zones intervene). The limestone sequence below the top of the acoustic basement should be about 60 meters thicker than at Site 288. The lack of seismic penetration of basement may be attributable to the strong return of energy from the chert horizon and the top of the acoustic basement.

OPERATIONS

The track from Site 288 to Site 289 was arranged to cross Site 64 and approach the proposed location on a course of 000° (Figure 1). This provided a degree of correlation between sites and a control for expected stratigraphy at Site 289. The approach profile is shown in Figure 2.

The beacon was dropped underway at 1632, 31 May 1973. Because of the extreme regularity of the plateau, this was accomplished without the usual initial crossing of the site. Because of excellent performance at Site 167 a four-cone sealed bearing bit with chisel teeth was chosen, and results were more than satisfactory. Between 0055, 1 June and 2345, 7 June a total of 133 cores were cut in a program of continuous coring to a depth of 1271 meters subbottom. Recovery averaged 56% for the entire section, decreasing downward from 100% in the upper section of the hole as intercalated more lithified zones were encountered. Recovery in hard limestones near the base of the hole was also poor due to the unusual style of bit failure. Normally, bearing failure occurs first and results in undersized cores. In this case the ends of the cones, which cut the core to size, were worn back before the bearings failed, with the result that cores were cut oversize and would jam in the throat of the core barrel. A final basalt section was found jammed in the throat of the bit on pulling the string.

Coring results are summarized in Table 1. It was interesting to note in experimenting with the extended inner barrel that the contact between two cored intervals

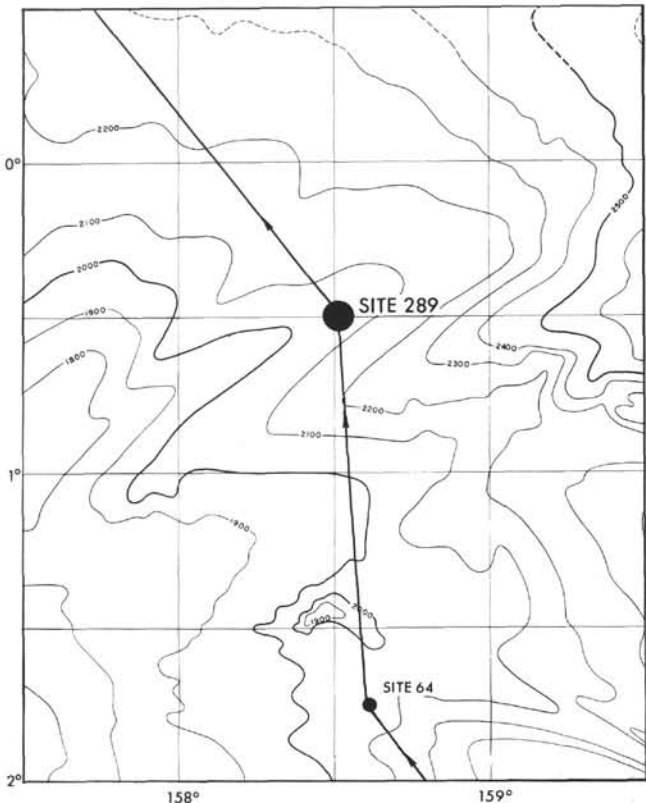


Figure 1. Location of Site 289 (Leg 30) and Site 64 (Leg 7) on the Ontong-Java Plateau. Contour in hundreds of meters. (Bathymetric map from Kroenke, 1972.)

was sampled (see Figure 3). The extended inner barrel achieved greater recovery, but the cores were highly fractured (apparently due to wandering at the base of the hole), and the volume of samples returned was small compared to standard cores and hindered sampling programs.

An on-site sonobuoy was shot (Figure 4; see also Correlation of Reflection Profiles with Drilling Results section). The site was departed at 1130, 8 June 1973.

LITHOLOGY

Site 289, on the Ontong-Java Plateau, was drilled in a water depth of 2224 meters and cored continuously to 1271 meters. One hundred thirty-three cores were obtained and a total of 712.6 meters of sediments and igneous rocks was recovered (708.6 m of sediment; 4.1 m of igneous rock).

The cored sequence is divided into three units. The sedimentary section ranges in age from Pleistocene to Lower Cretaceous (Aptian). The basal igneous unit consists of a single basalt flow predating the sedimentary succession (Figures 5 and 25). The composition of the sediments as determined from smear slides is given in Appendix A and plotted in Figure 6.

The units are (in descending order):

Unit 1 (0.969.0 m): Nanno-foram ooze, interbedded nanno-foram ooze and nanno-foram chalk. Pleistocene to late Eocene.

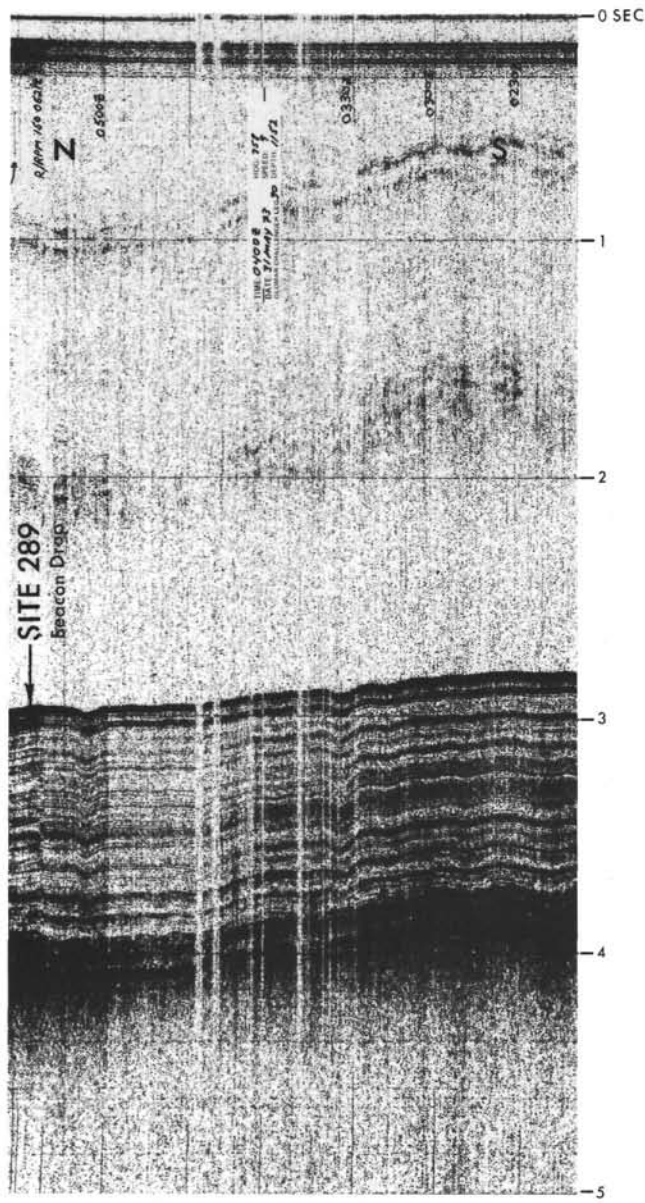


Figure 2. Seismic profile taken on D/V Glomar Challenger on approach to Site 289.

Unit 2 (969.0-1262.0 m): Radiolarian-bearing limestone, siliceous limestone, nanno-foram chalk, nanno-foram limestone, nodular chert, tuff. Late Eocene to Early Cretaceous. Two subunits are recognized as follows:

Subunit 2A (969.0-1231.0 m). Radiolarian-bearing limestone, siliceous limestone, nanno-foram chalk, nanno-foram limestone, nodular chert. Late Eocene to Late Cretaceous.

Subunit 2B (1231.0-1262.0 m). Limestone and tuff. Late Cretaceous to Early Cretaceous.

Unit 3 (1262.0-1271.0 m). Early Cretaceous, early Aptian.

Unit 1: Nanno-foram Ooze and Interbedded Nanno-foram Ooze and Nanno-foram Chalk

Unit 1, recovered from Cores 289-1 through 289-102, consists of a 969.0-meter thick succession of nanno-foram ooze and interbedded nanno-foram chalk. Highly disturbed soft ooze occurs from the core top to 250 meters below the mudline, whereas interbedded semilithified chalk and both disturbed, soft and undisturbed, stiff ooze occur from 350.0 to 969.0 meters below the mudline.

The ooze and chalk are characterized by the same colors and mineral and biogenic components. White is the dominant color and light gray is subordinate. Accessory colors include black (mostly as spots or in parallel laminae), greenish-white, greenish-gray, yellowish-gray, and medium gray. Trace quantities of pale purple are confined to parallel laminae in the upper part of the interbedded ooze and chalk sequence. Reexamination of core sections 52 days after departure from Site 289 disclosed the alteration of tints of greenish-gray, pale purple, and medium gray to white and yellowish-gray.

Foraminifera and nannofossils are dominant and together comprise up to 99% of the total components present. Accessory components include Radiolaria and micarb; trace quantities of feldspar, pyrite, volcanic glass, opaque minerals, heavy minerals, sponge spicules, and silicoflagellates occur (Appendix A). Texturally, the oozes are silty clays and clayey silts with the foraminifera and Radiolaria comprising the sand and silt sizes, whereas the nannofossils comprise the clay sizes (see Appendix B). Shipboard insoluble residue analysis (Figure 7) and shore-based calcium-carbonate determinations show Unit 1 carbonate sediments to contain in excess of 90% calcium carbonate with the exception of 289-55, CC, where only 87.5% CaCO₃ was recorded. This lower CaCO₃ content at Sample 289-55, CC coincides with a higher Radiolaria content (Appendix A). The remainder of the insoluble residues consists of volcanic glass, a finding in agreement with X-ray determination of the amorphous content of the carbonates (Zemmels, this volume).

Accessory quantities of light to medium gray chert nodules of fine pebble size were observed in Cores 289-32, 289-33, and 289-102.

Hydrogen sulfide gas occurs in some of the ooze in Cores 289-7 through 289-28. It occurs mostly in ooze which contains swirled mixtures of white, black, yellowish-gray, and medium gray, but is absent from white chalk and white ooze. Black spots and both yellowish-gray and medium gray layers containing pyrite are associated with the H₂S-bearing sediment. Smear-slide petrography disclosed the association of both gas bubbles (possibly H₂S) and pyrite within chambers of foraminifera tests (Figure 8).

Sedimentary structures were observed in the lower and better indurated oozes and chalks. They include parallel laminae, color bands up to 3 cm thick, flaser bedding, lenticular bedding, and wavy bedding.

TABLE 1
Coring Summary, Site 289

Core	Date (June 1973)	Time	Depth From Drill Floor (m)	Depth Below Sea Floor (m)	Length Cored (m)	Length Recovered (m)	Recovery (%)
1	1	0055	2224.0-2233.5	0.0-9.5	9.5	9.0	100
2	1	0140	2233.5-2243.0	9.5-19.0	9.5	9.0	95
3	1	0220	2243.0-2252.5	19.0-28.5	9.5	9.5	100
4	1	0305	2252.5-2262.0	28.5-38.0	9.5	9.0	95
5	1	0345	2262.0-2271.5	38.0-47.5	9.5	9.0	95
6	1	0425	2271.5-2281.0	47.5-57.0	9.5	8.6	91
7	1	0510	2281.0-2290.5	57.0-66.5	9.5	9.0	95
8	1	0550	2290.5-2300.0	66.5-76.0	9.5	9.5	100
9	1	0635	2300.0-2309.5	76.0-85.5	9.5	9.4	99
10	1	0725	2309.5-2319.0	85.5-95.0	9.5	7.2	76
11	1	0815	2319.0-2328.5	95.0-104.5	9.5	7.2	76
12	1	0905	2328.5-2338.0	104.5-114.0	9.5	8.0	84
13	1	0950	2338.0-2347.5	114.0-123.5	9.5	5.0	53
14	1	1035	2347.5-2357.0	123.5-133.0	9.5	9.4	99
15	1	1125	2357.0-2366.5	133.0-142.5	9.5	5.7	60
16	1	1225	2336.5-2376.0	142.5-152.0	9.5	9.1	96
17	1	1315	2376.0-2385.5	152.0-161.5	9.5	8.9	94
18	1	1405	2385.5-2395.0	161.5-171.0	9.5	6.9	73
19	1	1455	2395.0-2404.5	171.0-180.5	9.5	5.6	58
20	1	1540	2404.5-2414.0	180.5-190.0	9.5	9.2	97
21	1	1635	2414.0-2423.5	190.0-199.5	9.5	2.9	31
22	1	1730	2423.5-2433.0	199.5-209.0	9.5	4.8	51
23	1	1825	2433.0-2442.5	209.0-218.5	9.5	9.0	95
24	1	1920	2442.5-2452.0	218.5-228.0	9.5	8.6	91
25	1	2020	2452.0-2461.5	228.0-237.5	9.5	6.9	72
26	1	2105	2461.5-2471.0	237.5-247.0	9.5	9.5	100
27	1	2155	2471.0-2480.5	247.0-256.5	9.5	8.7	92
28	1	2245	2480.5-2490.0	256.5-226.0	9.5	9.5	100
29	1	2340	2490.0-2499.5	266.0-275.5	9.5	4.6	48
30	2	0025	2499.5-2509.0	275.5-285.0	9.5	4.1	43
31	2	0115	2509.0-2518.5	285.0-294.5	9.5	8.6	91
32	2	0205	2518.5-2528.0	294.5-304.0	9.5	7.3	77
33	2	0255	2528.0-2537.5	304.0-313.5	9.5	9.2	97
34	2	0350	2537.5-2547.0	313.5-323.0	9.5	9.0	95
35	2	0445	2547.0-2556.5	323.0-332.5	9.5	5.2	55
36	2	0545	2556.5-2566.0	332.5-342.0	9.5	9.4	99
37	2	0635	2566.0-2575.5	342.0-351.5	9.5	9.5	100
38	2	0730	2575.5-2585.0	351.5-361.0	9.5	9.5	100
39	2	0820	2585.0-2594.5	361.0-370.5	9.5	9.5	100
40	2	0920	2594.5-2604.0	370.5-380.0	9.5	9.4	99
41	2	1005	2604.0-2613.5	380.0-389.5	9.5	2.8	29
42	2	1100	2613.5-2623.0	389.5-399.0	9.5	9.5	100
43	2	1205	2623.0-2632.5	399.0-408.5	9.5	9.5	100
44	2	1310	2632.5-2642.0	408.5-418.0	9.5	9.4	99
45	2	1410	2642.0-2651.5	418.0-427.5	9.5	9.4	99
46	2	1510	2651.5-2661.0	427.5-437.0	9.5	2.4	25
47	2	1605	2661.0-2670.5	437.0-446.5	9.5	8.9	94
48	2	1700	2670.5-2680.0	446.5-456.0	9.5	9.7	102
49	2	1755	2680.0-2689.5	456.0-465.5	9.5	9.5	100
50	2	1910	2689.5-2699.0	465.5-475.0	9.5	9.7	102
51	2	2020	2699.0-2708.5	475.0-484.5	9.5	8.7	92
52	2	2150	2708.5-2718.0	484.5-494.0	9.5	9.6	101
53	2	2255	2718.0-2727.5	494.0-503.5	9.5	4.9	52
54	3	0000	2727.5-2737.0	503.5-513.0	9.5	5.2	55
55	3	0105	2737.0-2746.5	513.0-522.5	9.5	9.5	100
56	3	0200	2746.5-2756.0	522.5-532.0	9.5	5.8	61
57	3	0325	2756.0-2765.5	532.0-541.5	9.5	9.1	96
58	3	0420	2765.5-2775.0	541.5-551.0	9.5	9.8	103
59	3	0505	2775.0-2784.5	551.0-560.5	9.5	2.8	29
60	3	0600	2784.5-2794.0	560.5-570.0	9.5	8.3	87
61	3	0655	2794.0-2803.5	570.0-579.5	9.5	9.6	101
62	3	0755	2803.5-2813.0	579.5-589.0	9.5	3.1	33
63	3	0840	2813.0-2822.5	589.0-598.5	9.5	2.9	31
64	3	0930	2822.5-2832.0	598.5-608.0	9.5	3.6	38
65	3	1020	2832.0-2841.5	608.0-617.5	9.5	4.1	43
66	3	1145	2841.5-2851.0	617.5-627.0	9.5	4.5	47

TABLE 1 - *Continued*

Core	Date (June 1973)	Time	Depth From Drill Floor (m)	Depth Below Sea Floor (m)	Length Cored (m)	Length Recovered (m)	Recovery (%)
67	3	1250	2851.0-2860.5	627.0-636.5	9.5	9.6	101
68	3	1350	2860.5-2870.0	636.5-646.0	9.5	7.9	83
69	3	1540	2870.0-2879.5	646.0-655.5	9.5	7.5	79
70	3	1640	2879.5-2889.0	655.5-665.0	9.5	9.6	101
71	3	1745	2889.0-2898.5	665.0-674.5	9.5	7.6	80
72	3	1900	2898.5-2908.0	674.5-684.0	9.5	8.4	88
73	3	2005	2908.0-2917.5	684.0-693.5	9.5	7.1	75
74	3	2110	2917.5-2927.0	693.5-703.0	9.5	9.5	100
75	3	2220	2927.0-2936.5	703.0-712.5	9.5	5.0	53
76	3	2345	2936.5-2946.0	712.5-722.0	9.5	6.3	66
77	4	0055	2946.0-2955.5	722.0-731.5	9.5	1.6	17
78	4	0200	2955.5-2965.0	731.5-741.0	9.5	4.3	45
79	4	0305	2965.0-2974.5	741.0-750.5	9.5	3.9	41
80	4	0410	2974.5-2984.0	750.5-760.0	9.5	4.8	51
81	4	0510	2984.0-2993.5	760.0-769.5	9.5	1.8	19
82	4	0620	2993.5-3003.0	769.5-779.0	9.5	4.6	48
83	4	0720	3003.0-3012.5	779.0-788.5	9.5	1.9	20
84	4	0815	3012.5-3022.0	788.5-798.0	9.5	2.2	23
85	4	0930	3022.0-3031.5	798.0-807.5	9.5	1.5	16
86	4	1035	3031.5-3041.0	807.5-817.0	9.5	7.7	81
87	4	1155	3041.0-3050.5	817.0-826.5	9.5	1.8	19
88	4	1310	3050.5-3060.0	826.5-836.0	9.5	3.3	35
89	4	1420	3060.0-3069.5	836.0-845.5	9.5	6.2	65
90	4	1530	3069.5-3079.0	845.5-855.0	9.5	3.7	39
91	4	1650	3079.0-3088.5	855.0-864.5	9.5	7.0	74
92	4	1800	3088.5-3098.0	864.5-874.0	9.5	1.2	13
93	4	1905	3098.0-3107.5	874.0-883.5	9.5	5.4	57
94	4	2015	3107.5-3117.0	883.5-893.0	9.5	4.8	51
95	4	2130	3117.0-3126.5	893.0-902.5	9.5	1.8	19
96	4	2255	3126.5-3136.0	902.5-912.0	9.5	0.6	6
97	5	0015	3136.0-3145.5	912.0-921.5	9.5	4.0	42
98	5	0130	3145.5-3155.0	921.5-931.0	9.5	3.6	38
99	5	0300	3155.0-3164.5	931.0-940.5	9.5	7.6	80
100	5	0425	3164.5-3174.0	940.5-950.0	9.5	1.6	17
101	5	0540	3174.0-3183.5	950.0-959.5	9.5	2.8	29
102	5	0705	3183.5-3193.0	959.5-969.0	9.5	0.9	9
103	5	0805	3193.0-3202.5	969.0-978.5	9.5	1.5	16
104	5	0910	3202.5-3212.0	978.5-988.0	9.5	0.1	1
105	5	1010	3212.0-3221.5	988.0-997.5	9.5	0.1	1
106	5	1130	3221.5-3231.0	997.5-1007.0	9.5	7.3	77
107	5	1330	3231.0-3240.5	1007.0-1016.5	9.5	2.2	23
108	5	1450	3240.5-3250.0	1016.5-1026.0	9.5	1.4	15
109	5	1600	3250.0-3259.5	1026.0-1035.5	9.5	0.4	4
110	5	1730	3259.5-3269.0	1035.5-1045.0	9.5	0.6	6
111	5	1930	3269.0-3278.5	1045.0-1054.5	9.5	4.0	42
112	5	2145	3278.5-3288.0	1054.5-1064.0	9.5	0.2	2
113	6	0025	3288.0-3297.5	1064.0-1073.5	9.5	0.5	5
114	6	0305	3297.5-3307.0	1073.5-1083.0	9.5	0.3	3
115	6	0600	3307.0-3316.5	1083.0-1092.5	9.5	1.3	14
116	6	0800	3316.5-3326.0	1092.5-1102.0	9.5	0.4	4
117	6	1000	3326.0-3335.5	1102.0-1111.5	9.5	0.1	1
118	6	1140	3335.5-3345.0	1111.5-1121.0	9.5	1.0	11
119	6	1400	3345.0-3354.5	1121.0-1130.5	9.5	0.3	3
120	6	1625	3354.5-3360.0	1130.5-1136.0	5.5	1.1	20
121	6	2110	3360.0-3369.5	1136.0-1145.5	9.5	2.4	25
122	6	2345	3369.5-3379.0	1145.5-1155.0	9.5	2.0	21
123	7	0115	3379.0-3388.5	1155.0-1164.5	9.5	1.2	13
124	7	0235	3388.5-3398.0	1164.5-1174.0	9.5	1.8	19
125	7	0400	3398.0-3407.5	1174.0-1183.5	9.5	0.6	6
126	7	0525	3407.5-3417.0	1183.5-1193.0	9.5	0.2	2
127	7	0700	3417.0-3426.5	1193.0-1202.5	9.5	0.2	2
128	7	0825	3426.5-3436.0	1202.5-1212.0	9.5	0.5	5
129	7	1010	3436.0-3445.5	1212.0-1221.5	9.5	0.4	6
130	7	1130	3445.5-3455.0	1221.5-1231.0	9.5	<0.1	1
131	7	1555	3455.0-3483.5	1231.0-1259.5	28.5	4.5	16
132	7	1925	3483.5-3493.0	1259.5-1269.0	9.5	4.7	49
133	7	2315	3493.0-3495.0	1269.0-1271.0	2.0	0.4	20
Total				1271.0	712.6	56	

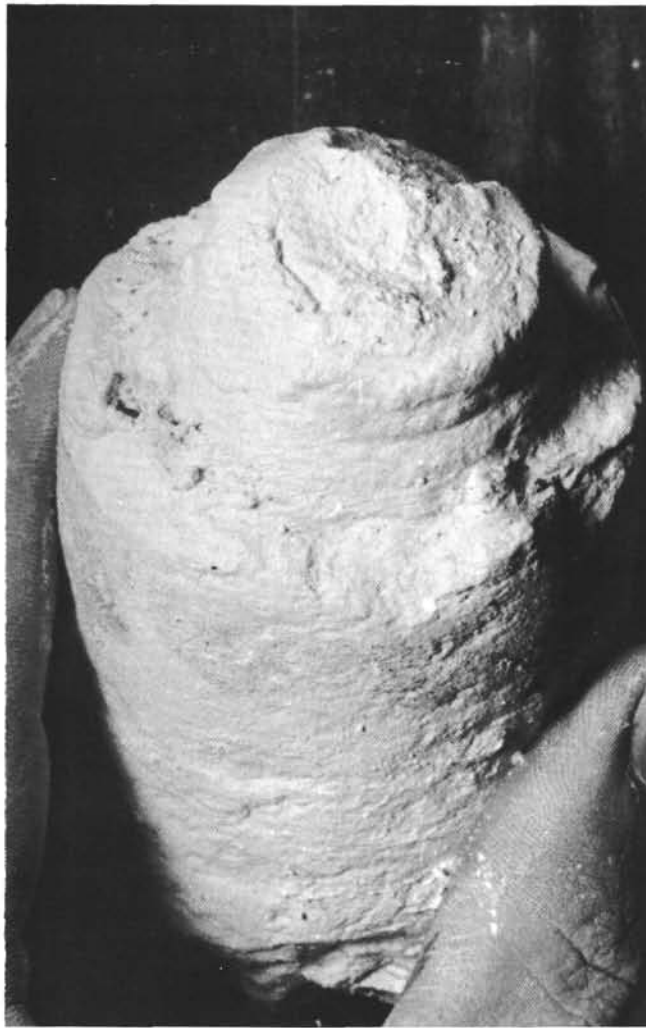


Figure 3. Junction between Cores 289-91 and 92 from top of Core 289-92. The upper core was taken using an extended innerbarrel and the lower one as taken using a conventional core barrel.

Biogenic structures include small horizontal and vertical burrows, including *Zoophycos* (Cores 289-63 to 65).

Foraminifera in Unit 1 are extremely well preserved (see Paleontology) and show no evidence of either solution or reworking by bottom currents. The environment of deposition of Unit 1 is oceanic, middle bathyal, and above the foram solution depth. Biogenic productivity was high during deposition of Unit 1.

Bottom current velocities were sufficiently high to generate current ripples (preserved only as wavy beds). However, flaser drapes over the ripples indicate these currents to be characterized by an alternation of bedload and suspension deposition. Tidal currents are characterized by such an alternation. Oceanic bottom currents with both a tidal velocity and directional fluctuation have been observed in water depths of 2000 to 2500 meters by Lonsdale et al., (1972a, b). Perhaps similar current systems operated at Site 289 during deposition of Unit 1 to produce flaser, lenticular, and wavy bedding. Alternatively, periodic storm activity

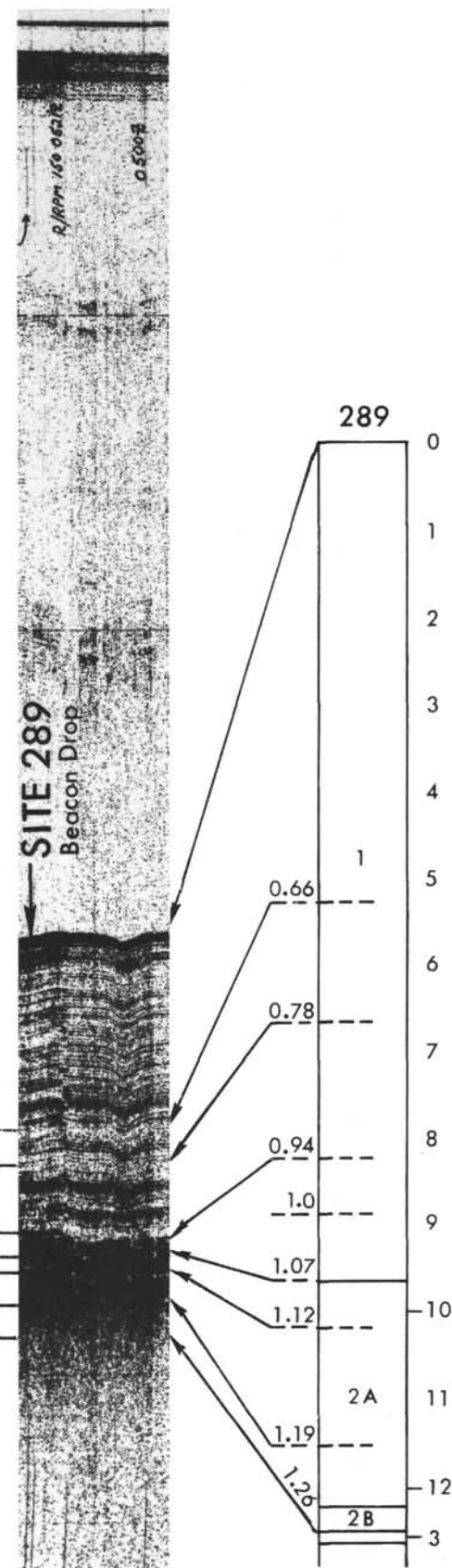


Figure 4. Part of seismic profile shown in Figure 1 with column showing correlation of reflectors with lithologic units.

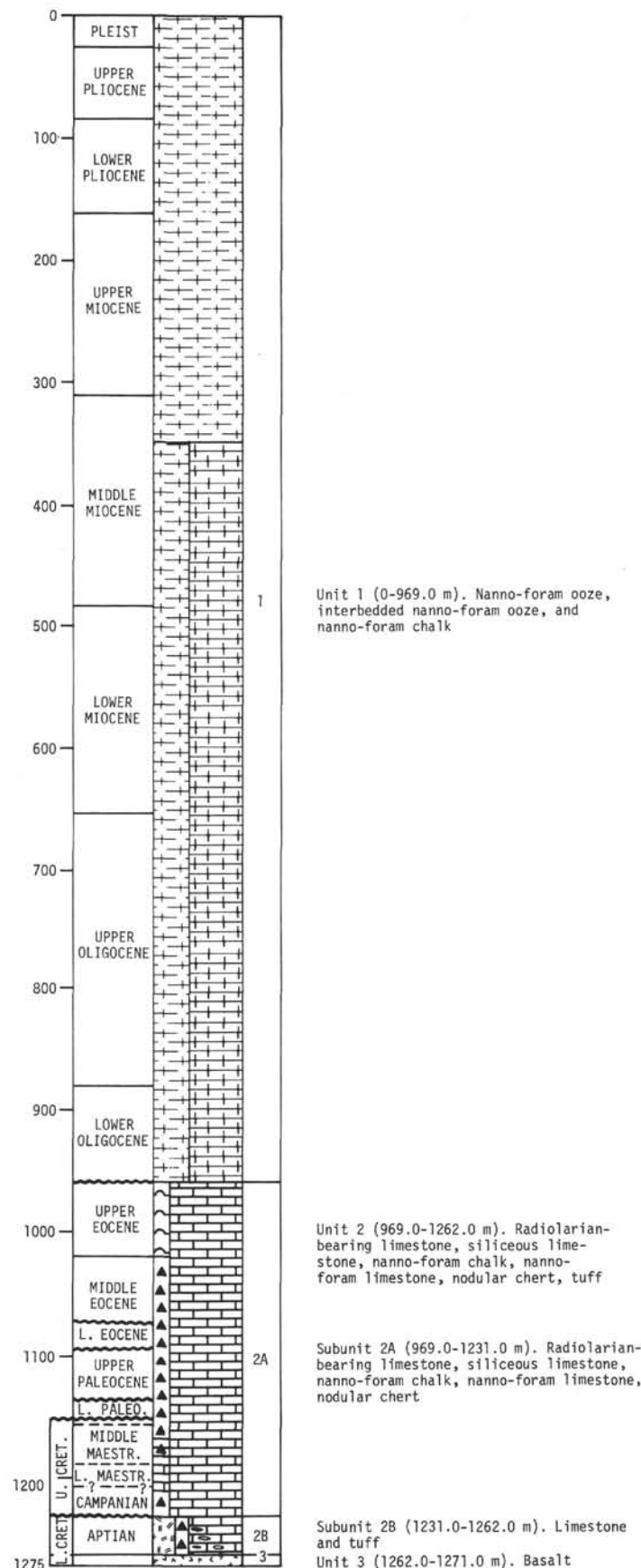


Figure 5. Stratigraphic column, Site 289.

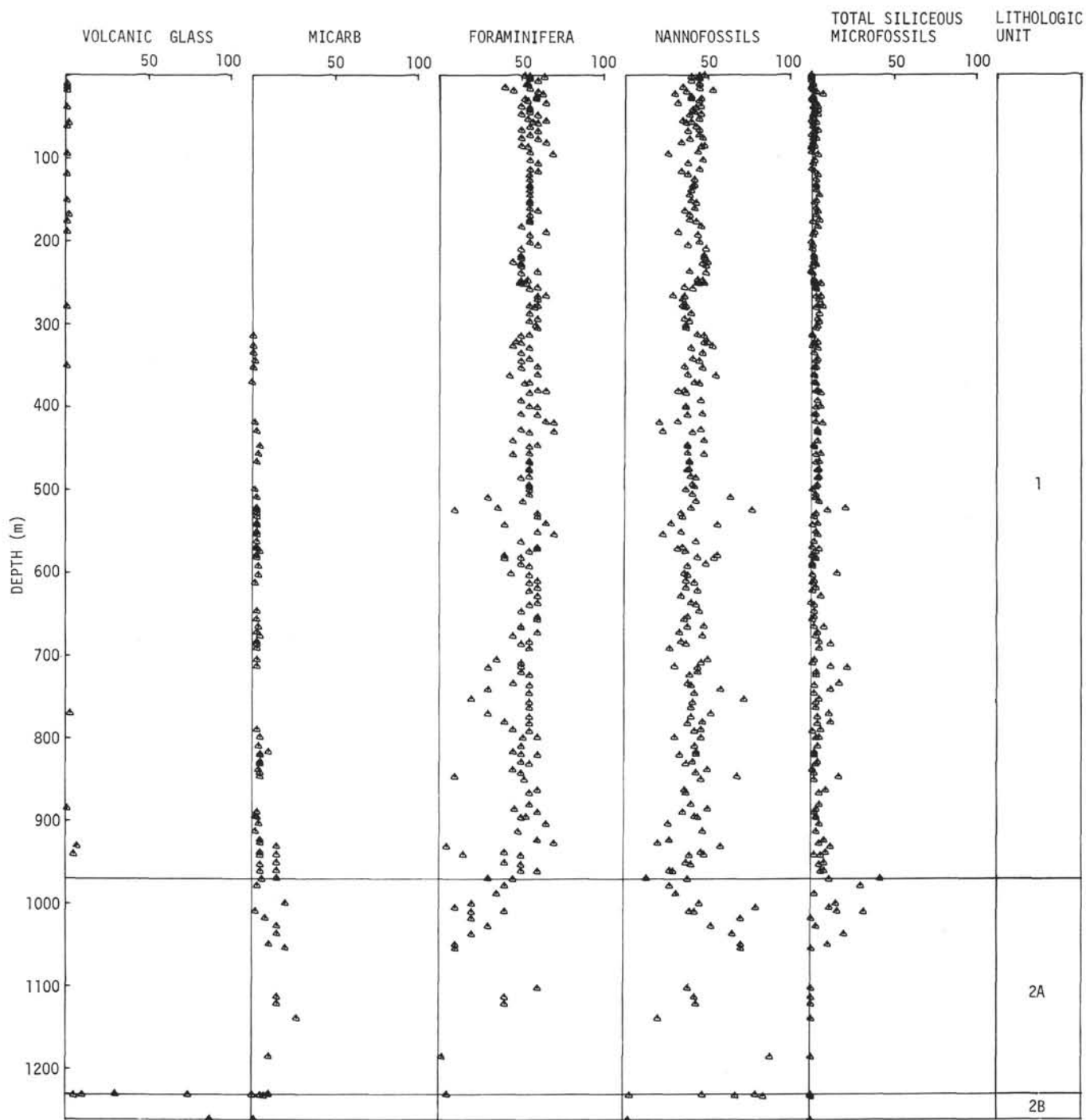


Figure 6. *Sediment composition as determined in smear slides, Site 289.*

may produce such flaser beds (McCave, 1970) although proof of effective bed shear by storms at depths of 2000 to 2500 meters is lacking.

Although an Eocene-Oligocene hiatus is recognized between Cores 289-101 and 102, no lithologic change was observed on either side of the biostratigraphic discontinuity.

Unit 2: Chalk, Ooze, Limestone, Radiolarian-bearing Limestone, Chert Nodules, Tuff

Unit 2, recovered from Cores 289-103 through 289-132, consists of a 293.0-meter thick succession of soft, disturbed nanno ooze, and semilithified nanno chalk, and nanno-foram limestones, nanno limestones,

radiolarian-bearing limestones, siliceous limestones, nodular cherts, and tuff. Unit 2 is separated from Unit 1 by the appearance of radiolarian-bearing limestone in Core 289-103; these grade downward into siliceous limestones interbedded with nodular cherts. Unit 2 is divided further into two subunits according to the

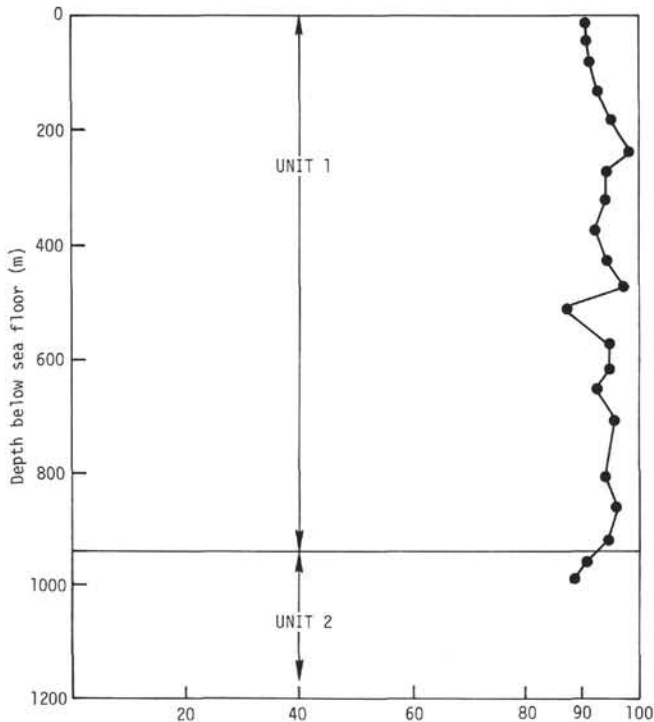
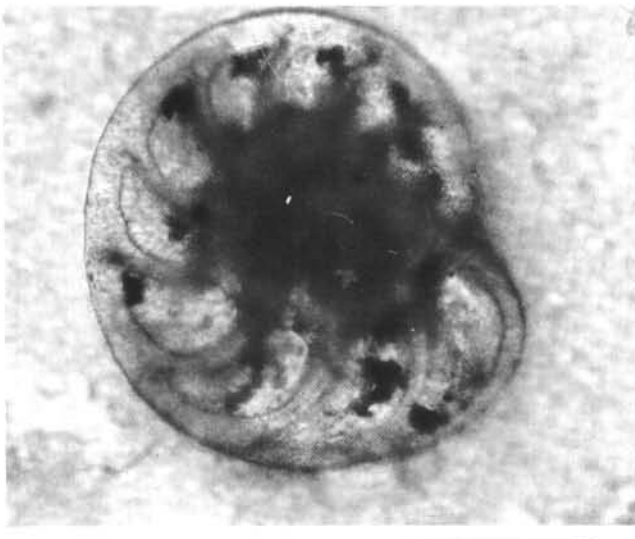


Figure 7. Percent calcium carbonate determined from shipboard insoluble residue analysis, Site 289.



presence of tuff layers and volcanic glass and zeolites within the limestones.

Subunit 2A

Subunit 2A, recovered from Cores 289-103 through 289-130, consists of 262 meters of interbedded nanno-foram ooze, nanno-foram chalk, nanno-foram limestones, radiolarian-rich and radiolarian-bearing limestones, and nodular chert. The carbonate rocks are white, very light gray, light gray, and medium gray. Olive-gray, black, and greenish-gray components occur in accessory quantities, usually as parallel, flaser, or wavy beds. The principal components are foraminifera, nannofossils (Figure 9) and Radiolaria (these only from 969.0 to 1025.5 m). Accessory components include micarb and sponge spicules; trace quantities of pyrite, volcanic glass and feldspar occur (Appendix A). Shipboard insoluble residue determinations (Figure 7) show Subunit 2A carbonate rocks to contain about 85% calcium carbonate, a figure in agreement with the radiolarian content (Appendix A). A radiolarian-rich horizon at Sample 289-110, 1-134 contains only 51% calcium carbonate.

Sedimentary structures in Subunit 2A include parallel laminae, flaser bedding, wavy bedding, and lenticular bedding. These laminae and bedding types differ from those in lighter colored limestones by dark olive-gray, black and greenish-gray laminae. Most of the darker laminae contain predominant zeolite and altered volcanic ash. X-ray analysis (Zemmels, this volume) indicates these dark layers to contain significant quantities of sepiolite and palygorskite and pyrite, accessory quantities of mica, montmorillonite, and chlorite, and trace quantities of potassium-feldspar and quartz. The flaser bedding is continuous and bifurcated in contrast to similar-appearing features in bioturbated zones in these

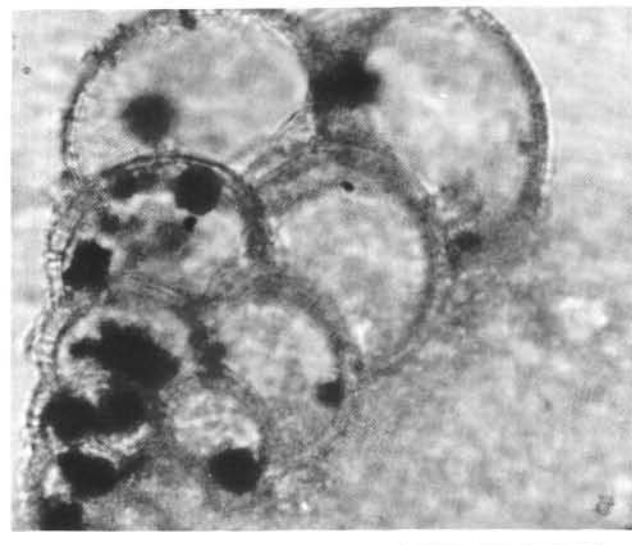


Figure 8. (a) Photomicrograph of smear slide 289-25-5, 88 cm showing pyrite partially filling chambers of foraminifera test. Nanno-foram ooze, Unit 1, Site 289. Scale bar is 0.25 mm long. (b) Photomicrograph, same smear slide showing pyrite partially filling chambers of foraminiferal test with a geopel fabric. Nanno-foram ooze, Unit 1, Site 289. Scale bar is 0.25 mm long.

cores, which are disrupted and lack bifurcation. The continuous flaser beds drape lenticular zones; such flaser drapes are absent in bioturbated horizontal burrow zones cross-sections of which may be mistaken for lenticular bedding.

Stylolites are common to Subunit 2A, particularly in the lower half. These stylolites are developed along ash layers and appear to be associated with dissolved foraminifera (see Paleontology section).

Bioturbation is extremely common to this unit and consists mostly of horizontal traces and vertical burrows, ranging in diameter from 2 mm to 1 cm.

Chert nodules of varying size characterize Subunit 2A. They are medium light gray, medium gray, medium grayish-blue, medium dark gray, light gray, and red. These nodules interfinger with enclosing limestone beds and complex patterns of intergrowths were observed. Some intervals resemble "graphic" intergrowths of quartz and feldspar common to pegmatitic granites (Figure 10). Chert also occurs commonly as a secondary pore-fill in tests of foraminifera (Figures 11, 12, 13). X-ray analysis (Zemmels, this volume) shows the chert to contain cristobalite in one sample (289-111-1, 128). The chert is clearly of replacement origin; an origin and replacement sequence as reported by Heath (1973), Heath and Moberly (1971), and Greenwood (1973) is duplicated at Site 289.

Faunal components in Subunit 2A include foraminifera, nannofossils, and Radiolaria. The foraminifera are recrystallized (see Paleontology section) in Cores 289-108 through 289-127; foraminifera in Cores 289-128 through 289-130 show evidence of solution.

Hiatuses are found (see Paleontology section) at the base of Cores 289-113, 289-115, 289-120-1, and 289-122-1. Lithologic changes occur only at the base of Core 289-115. Above that hiatus, white and gray siliceous limestones with flaser and lenticular bedding and bioturbation are interbedded with grayish-blue, gray, and



Figure 9. Photomicrograph of nanno-foram limestone (sand and silt size) and "micritic" matrix of nannofossils, Unit 2A, Site 289. Polarized light; scale bar is 0.25 mm long.

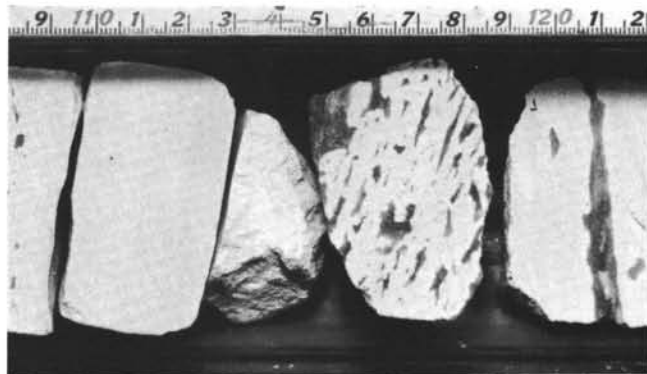


Figure 10. Graphic replacement intergrowth of chert in limestone, 289-115-1, Unit 2A, Site 289.

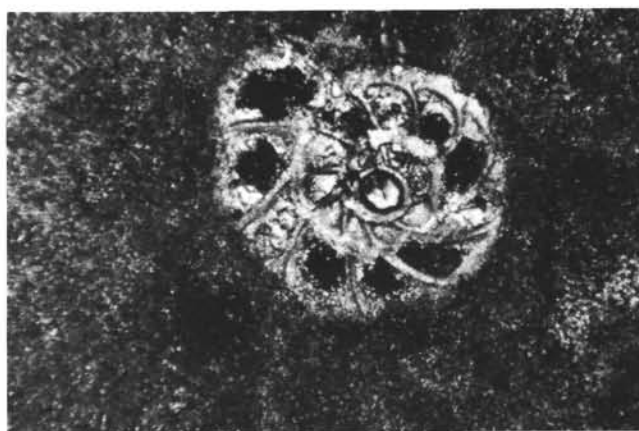


Figure 11. Chert pore-filling in foraminifera test set in micritic matrix of nanno-fossils in nanno-foram limestone. 289-108-1, 51 cm, Unit 2A, Site 289. Crossed nicols; scale bar is 0.25 mm long.

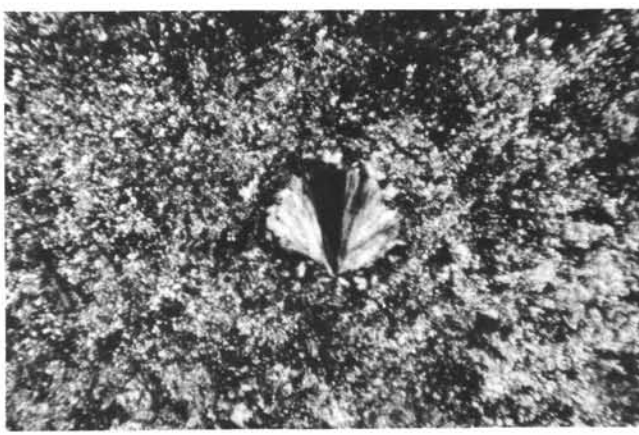


Figure 12. Chalcedonic pore-filling of foraminifera test in microcrystalline chert nodule, 289-1-8-1, 94 cm, Unit 2A, Site 289. Crossed nicols, scale bar is 0.25 mm long.

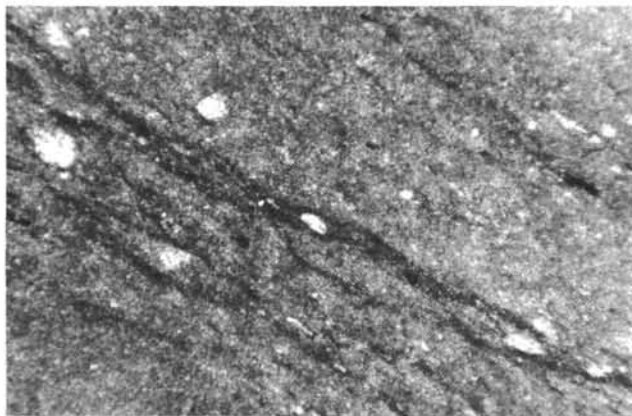


Figure 13. Chalcedonic and chert pore-filling of foraminalifer tests in nanno-foram limestone. Bimodal size distribution of sand-sized and silt-sized foraminiferal tests set in "micritic matrix" of nannofossils. 289-110-1, 134 cm. Unit 2A, Site 289. Crossed nicols; scale bar is 0.25 mm long.

olive-gray chert, whereas below that hiatus bioturbated white limestones with light gray cherts occur. No lithologic change was observed on either side of the other paraconformities in Subunit 2A.

Most of Subunit 2A was deposited in middle bathyal depths. Deposition occurred in a zone of high biological productivity above the foram solution depth. However, in the basal part of the unit deposition fluctuated above and below the foram solution depth, but above the nanno solution depth in Cores 289-128 through 289-131. Periodically, volcanic ash laminae were deposited by bottom currents. Bottom current conditions appear similar to those prevailing during deposition of Unit 1.

Subunit 2B

This unit, recovered from Cores 289-131 and 289-132, consists of 31 meters of ash-bearing and ash-rich limestones interbedded with nodular chert and vitric tuff. The limestones are white, pinkish-gray, orange brown, light olive-gray, and medium gray. Deeper colors are associated with an increase in volcaniclastic components (Appendix A). The limestone becomes yellowish-brown at the base where it is in contact with the basal vitric tuff bed.

The major components in these limestones are nannofossils, fresh and altered volcanic glass, micarb and zeolite. Accessory components include sponge spicules, heavy minerals, and feldspar; trace amounts of pyrite and opaque minerals occur.

These limestones exhibit flaser and lenticular bedding (Figure 14), intense mottling, and bioturbation (Figure 15).

Chert nodules of replacement origin are brownish-black, and dark reddish-brown. They contain limestone blebs, and also interfinger with the enclosing limestone.

Vitric tuffs occur as thin laminae as flaser beds in limestones, and also as two distinct beds in Sections 289-131-1 and 289-131-2. These tuffs are grayish-brown,

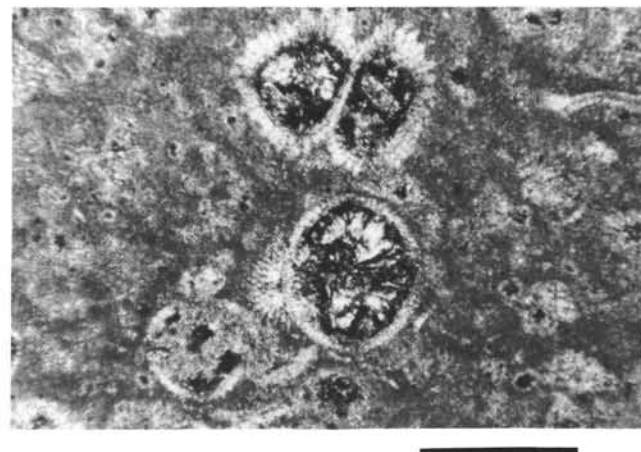


Figure 14. Nanno limestone containing fragments of potassium feldspar and zeolitic clay laminae organized as flaser bedding and clay drapes (darker laminae). 289-131-107, Unit 2B, Site 289. Crossed nicols, scale bar is 0.25 mm long.

with associated blebs of reddish-brown. A third thin tuff consisting of chloritic altered glass is medium green and occurs approximately 5 cm above the base of Subunit 2B. Bioturbation is extremely common in the uppermost tuff layer (Figure 15). The major mineral components are fresh, chloritic and iron-rich glass, zeolites feldspar, attapulgite, palygorskite, opaque minerals, and heavy minerals. Traces of micarb and nannofossils occur. X-ray diffraction (Zemmels, this volume) disclosed the occurrence of significant amounts of palygorskite and quartz, with accessory potassium feldspar and mica in Sample 289-131-1, 106. A separate X-ray analysis of Sample 289-131-1, 107 completed at the clay mineralogy laboratory of the Illinois Geological Survey indicates that attapulgite is also a major constituent in the vitric tuffs. The other ash layers contain significant quantities of potassium feldspar, and montmorillonite (Zemmels, this volume). Palygorskite and montmorillonite dominate the less than two micron grain-size fraction in all ashes and tuffs (Zemmels, this volume).

Foraminifera in Cores 289-131 and 289-132 occur in accessory quantities and are well preserved.

A major hiatus is reported in Core 131-1 (Figure 15) within the uppermost vitric tuff bed (see Paleontology section).

Subunit 2B was deposited under bathyal conditions about the foram solution depth. Carbonate deposition was interrupted periodically by small amounts of altered volcanic ash transported by bottom currents and by volcanic eruptions which blanketed the site with thicker ash beds, now preserved as vitric tuff. These ash beds may represent the terminal phase of basaltic volcanism represented by Unit 3. Bottom currents, with a superimposed tidal component, or periodic storms, reworked most of the sediment, accounting for the wavy bedding and flaser bedding, as in Unit 1.

Unit 3: Basalt

Fresh basalt was encountered at 1262.0 meters below the mudline, and of the 9.2 meters of basalt cored, 4.1



Figure 15. Bioturbated nanno limestone in contact with uppermost vitric tuff (also bioturbated). Contact falls at 63 cm. Uppermost tuff contains 30 m.y. hiatus between Albian to mid-Campanian. 289-131-1, Unit 2B, Site 289.

meters were recovered. The basalt core is in two segments, an upper 3.7 meters and a lower 0.4 meters which are separated by an empty zone of 3.5 meters (Figure 16). The lower basalt appears to be identical with the upper one. The basalt is immediately overlain by a sequence of intercalated limestones and vitric tuffs. The contact with the overlying sediments was not recovered, but the material immediately above the top piece of basalt is a grayish-brown tuff which contains well-preserved nannofossils.

The basalt has a chill zone 10 cm thick. The chill zone changes downwards from a well-developed variolitic texture at the top to an intergranular texture at the bottom. The lava of the top few centimeters was quenched before only a small proportion of the plagioclase was able to crystallize. The chill zone shows small altered phenocrysts of approximately 2% plagioclase and less than 1% olivine. The plagioclase has been replaced by calcite and an unidentified negative, low birefringent mineral with a 2V of approximately 20°. The olivine phenocrysts are replaced by iddingsite and chlorite. The groundmass consists of hollow plagioclase, variolitic quench pyroxene, dendritic quench magnetite, and glass which is extensively chloritized.

The basalt unit consists of alternating coarser intergranular and finer variolitic zones. The intergranular zones show an average grain size of less than 0.3 mm and are composed of acicular plagioclase largely without the hollow habit, and pyroxenes which generally occur as sheaf-like bundles. The intergranular basalt contains approximately equal amounts of plagioclase and pyroxene, approximately 5% magnetite, and a few percent chlorite. The finer variolitic zones show well-developed hollow acicular plagioclase, fine variolitic pyroxene, small dispersed euhedral magnetite, and interstitial brown glass.

Small plagioclase phenocrysts ($An_{70} \pm 5$), usually less than 1 mm, are present throughout the basalt in amounts less than 2%. Altered olivine phenocrysts, less than 1-1/2 mm, are unevenly dispersed throughout and

METERS	CORE SECTION	LITHOLOGY	THICKNESS (m)	Subbottom depth (m)
1	1	EMPTY	1.3	1259.5
2	2	LIMESTONE AND TUFF	1.05	1261.8
3	c	CHILL ZONE		
4	f	BASALT	3.7	
5	c			
6	c			
7				
8		EMPTY	4.6	
9	CC			
10	1	BASALT	0.4	
11	CC		0.5	1271.0
	(133 (2.0 m)			

Figure 16. Summary of lithologic relations in Cores 289-132 and 133. In the basalt column "C" indicates the coarser basalt with an intergranular texture and "f" indicates the finer variolitic basalt.

constitute less than 1% of the unit. Vesicles, less than 2 mm in diameter are sporadically present throughout the basalt, but never exceed about 1% of the rock. Indistinct to distinct thin horizontal flow laminae are present in many parts of the basalt, but appear to be better developed in the intergranular zones.

Veins up to 1-1/2 cm are abundant, particularly in the basalt of Sections 2 and 3 in Core 132. The vein materials consist of various proportions of chlorite, calcite, rare pyrite, and a yellowish-brown material

which is probably siliceous (opaline or jasperoid). Two irregular cavities associated with calcite-chlorite veins contained quartz and calcite crystals.

The basalt probably represents a single flow based on the lack of baking of the overlying sediment and tuff, the textures, and the flow structures which occur throughout the unit. Sufficient petrographic data are not available to adequately classify the basalt, in particular because the pyroxene is too fine grained to allow detection of pigeonite. However, chemical data indicate that the composition is similar to mid-ocean ridge tholeiites (see Stoeser, this volume).

Sequence of Events, Northern Part, Ontong-Java Plateau

Volcanic Phase

Tholeiitic plateau basaltic lava flow was extruded at Site 289 prior to or during Aptian time.

Early Cretaceous

Deposition of volcanic ash and biogenic sediment began during late Aptian time. Following basalt extrusion, deposition of vitric tuff occurred, followed by biogenic sedimentation above the foram solution depth. Biogenic sedimentation continued with minor quantities of volcanic sediment being supplied to the site. A second phase of tuff deposition occurred, followed by a period of nondeposition or erosion. This period ranged from Albian to middle Campanian time.

Late Cretaceous-Paleocene

Biogenic sedimentation resumed during Campanian time below the foram solution depth. Deepening of the foram solution depth or shallowing of the site permitted continued biogenic sedimentation to occur during the Maestrichtian above the foram solution depth. During latest Maestrichtian and earliest Paleocene time a second period of nondeposition or erosion occurred followed by another episode of biogenic sedimentation above the foram solution depth during the late Paleocene. Chert diagenesis postdates the Late Cretaceous-Paleocene biogenic sedimentation. A third period of nondeposition or erosion occurred during latest Danian and Thanetian time (of the Paleocene) followed by a resumption of carbonate sedimentation for a short interval. This sedimentation was followed by a fourth period of nondeposition and erosion during the latest Paleocene which lasted into the early Eocene.

Eocene

A short period of continued biogenic sedimentation above the foram solution depth occurred during the early Eocene followed by a fifth period of nondeposition or erosion. Biogenic sedimentation above the foram solution depth occurred continuously during the middle and late Eocene. A minor period of higher productivity of Radiolaria occurred during the entire Eocene. Chert diagenesis postdates Eocene sedimentation. A sixth period of nondeposition or erosion occurred at the end of Eocene time and lasted into the earliest Oligocene.

Oligocene-Quaternary

From the beginning of the early Oligocene until the Quaternary, continuous biogenic sedimentation of

foraminifera and nannofossils above the foram solution depth has occurred in the northern part of the Ontong-Java Plateau.

GEOCHEMICAL MEASUREMENTS

Table 2 and Figure 17 present pH, alkalinity, and salinity data for Site 289. The sequence was sampled every 50 meters down to 1000 meters, that is down to the late Eocene. Recovery below that level was poor and only one sample was taken from the Late Cretaceous (1167.5 m). The pH remains almost constant at very close to 7 throughout the entire sample interval. The salinity however, remains at normal seawater salinity to 300 meters subbottom depth, then starts to rise slowly as the sediment becomes more lithified. A major excursion to 40.2‰ was recorded in late Eocene rad and micarbon-rich foram-nanno chalk. The alkalinity trend is a more complex one, it increases from the sea floor downward to a depth of 300 meters, then decreases progressively with depth as the salinity increases. The sharp increase in salinity at 1000 meters is not marked by a corresponding excursion in the alkalinity value.

PHYSICAL PROPERTIES

Sample cubes were taken routinely from each section of Cores 289-1 through 289-27 for determination of physical properties. Because of the continuous coring of Site 289 and the excessive time needed to obtain and process cubes for velocity measurements and syringe samples or chips for porosity-density determinations, alternate or even-numbered sections were sampled from Core 289-27 through Core 289-132. Both horizontal and vertical velocity of the sediment cubes were measured and both density and porosity were determined, as in earlier sites, either from a syringe sample proximal to the cube or, in the more indurated sediment, from a sediment chip adjacent to the cube. The results are presented in Figure 18 with acoustic impedance, sonic velocity, wet-bulk density, and grain density shown versus subbottom depth. Bulk density ranges between 1.5 and 2.6 g/cc, and porosity ranges between 75% and almost 5% at Site 289. Bulk density increases and porosity decreases with depth rather uniformly and with only minor fluctuation down to about 1000 meters subbottom. Changes in these physical properties in this interval probably reflect the degree of induration and diagenetic changes within the column. The most severe changes and largest fluctuations in bulk density and porosity occur below 1000 meters and perhaps correlate with the first appearance of a significant amount of quartz and cristobalite in the limestone matrix. Grain density which averages about 2.7 g/cc down to a depth of about 900 meters decreases to a minimum at 1037 meters subbottom perhaps due to decrease in permeability similar to that described and discussed for Site 288. Below 1037 meters the grain density returns to that observed in the upper part of the column (approximately 2.7 g/cc).

Velocities measured in the shipboard laboratory, on samples selected purposely to avoid drilling disturbances, remained below 1.7 km/sec to a depth of over 400 meters subbottom. Only minor fluctuations were observed within this interval, with excursions in velocity invariably less than 0.1 km/sec. In view of the velocity

TABLE 2
Summary of Shipboard Geochemical Measurements, Site 289

Sample (Interval in cm)	Depth Below Sea Floor (m)	Lab Temp (°C)	pH Punch-in/ Flow-through	Alka- linity (meq/kg)	Salinity (°/oo)
Surface seawater			8.37/8.35	2.34	35.2
1-5, 144-150	7.44-7.50	22.0	7.33/7.33	3.22	35.2
5-5, 144-150	45.44-45.50	21.8	7.17/7.18	4.39	35.2
10-4, 144-150	91.44-91.50	21.8	7.10/7.15	4.78	35.2
15-3, 144-150	137.44-137.50	21.8	7.04/7.07	5.07	35.2
20-5, 144-150	188.44-188.50	22.1	7.02/6.96	5.17	35.2
25-3, 144-150	232.44-232.50	22.0	7.07/6.99	5.17	35.2
30-3, 0-6	278.50-278.56	22.2	6.98/6.94	5.27	35.2
35-3, 144-150	327.44-327.50	22.2	7.03/7.01	4.68	35.5
40-5, 144-150	378.44-378.50	22.5	- /7.03	4.29	35.5
45-3, 144-150	422.94-423.00	21.9	6.95/6.96	4.98	35.8
50-5, 144-150	473.44-473.50	21.5	6.91/6.92	4.78	35.8
55-5, 144-150	520.94-521.00	21.8	6.91/6.93	4.59	36.0
60-5, 144-150	567.94-568.00	22.0	6.94/7.02	3.80	36.0
65-2, 144-150	610.94-611.00	22.0	- /7.16	2.73	36.3
70-5, 144-150	633.44-633.50	22.0	6.88/6.95	3.71	36.3
75-3, 144-150	707.44-707.50	21.6	6.92/7.02	3.12	36.3
80-3, 144-150	754.94-755.00	21.6	7.11/7.10	2.93	36.3
86-5, 144-150	814.94-815.00	21.7	7.11/7.28	2.34	36.3
91-3, 144-150	859.44-859.50	21.8	- /7.36	1.85	36.4
99-4, 144-150 ^a	936.94-937.00	21.8	- /7.42	1.46	36.3
99-4, 144-150 ^b	936.94-937.00	21.8	- /7.56	1.37	36.6
106-4, 144-150	1003.44-1003.50	22.4	- /7.35	1.46	40.2
124-2, 144-150	1167.44-1167.50	22.4	- /7.04	1.68	36.6

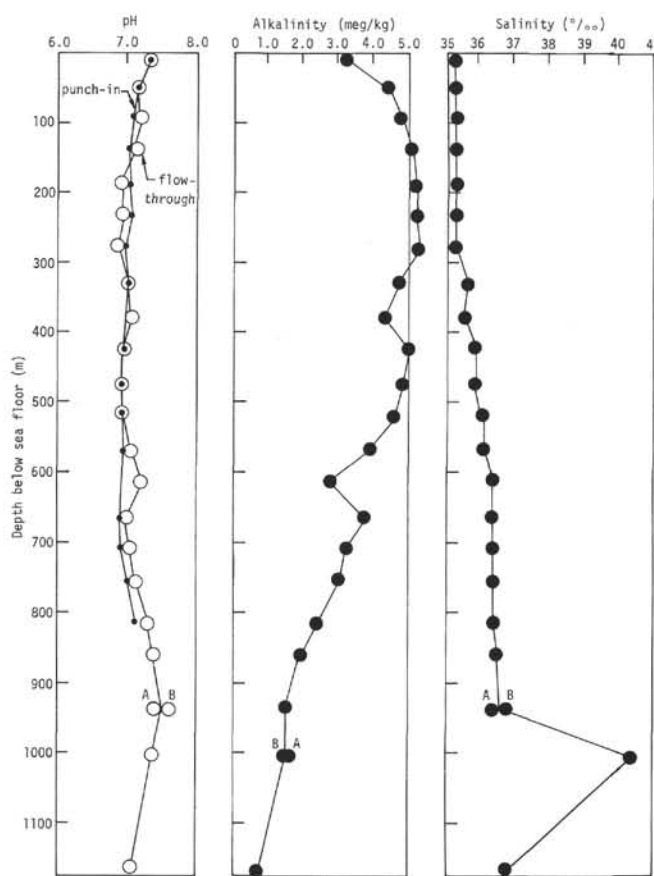
^aSoft sediment.^bHard sediment.

Figure 17. Graphic summary of geochemical data taken at Site 289.

gradients seen at earlier sites, previous experience in extrapolating drilling depths from reflection profiles, and earlier velocity determinations from sonobuoy and wide-angle reflection-refraction profiling nearby, the low velocity gradients encountered in the upper 400 meters of Site 289 were surprising, if not unexpected. These were confirmed, however, through later analysis of sonobuoy wide-angle reflection profile taken during drilling of Site 289.

In the interval, 400 to 550 meters subbottom, average velocity increases from about 1.7 km/sec to about 1.9 km/sec. Within this interval, velocity fluctuation increases markedly with excursions exceeding 0.1 km/sec. Below 550 meters, excursions of more than 0.3 km/sec commonly occur and the curve is more oscillatory (Figure 18). In general the velocity continues to increase, reaching an average of approximately 2.3 km/sec immediately above the chert sequence at about 1015 meters subbottom (Core 289-108). The maximum velocity measured in the siliceous limestones above the basalt at Site 289 is over 4.5 km/sec at about 1143 meters subbottom (Core 289-121-2).

Vertical versus horizontal velocity anisotropy develops for short intervals in the sedimentary column above 600 meters only to repeatedly disappear and reappear. Below 600 meters it becomes pronounced and increases with depth in the hole. The anisotropy seems to be established more abruptly and at a much greater depth in the column at Site 289 than that observed at earlier sites.

Sonic velocity of basalt was also measured at Site 289. Basalt samples were taken wherever possible from regions of Core 132, which were devoid of cracks and

vugs. As was done at previous sites, the basalt was again measured in two mutually perpendicular transverse directions (across the diameter of the core). The average of each pair of measurements is shown plotted in Figure 19. Velocity ranged from 4.75 km/sec to 5.85 km/sec with changes in velocity correlating with variations in texture. Near the top of the basalt, the first sample measured (Core 132-2) is low (4.75 km/sec). The remainder of the core measured below this point ranges about 5.5 km/sec in the seven samples from Core 132, Sections 3 and 4.

This tight grouping of velocity values shown in Figure 19 is in excellent agreement with sonobuoy results reported by Hussong (1972) across the Ontong-Java Plateau and further supports the contention that the basalt cored at Site 289 originated as a single flow.

CORRELATION OF SEISMIC REFLECTION PROFILE WITH DRILLING RESULTS

Site 289 is on the broad surface of the plateau, and reflector depth varies only slightly in the vicinity of the site. The velocity depth curve in Figure 18 was visually smoothed and average vertical interval velocities selected between what appeared to be significant changes in acoustic impedance. These data were then correlated with reflections observed in the profile across the site (Figures 2 and 4). The results are shown in Table 3 and Figure 4. Table 3 shows a qualitative measure of reflectivity and correlatability based on intensity and continuity of the recorded signal on the profile.

The reflector at 1.07 sec correlates with the top of Unit 2, the first appearance of cherts in the section. The 1.26-sec reflector correlates with the top of the basalt at 1249.8 meters, although this reflector cannot be traced with confidence for any distance along the profile. Note that it is difficult to trace these reflectors to Site 288, but as seen in the stratigraphy, Unit 2 is much thicker at Site 288 and the reflector depth to its top is 0.5 sec versus 1.07 sec at Site 289. The thickening of the section occurs entirely on the plateau margin, increasing with depth from the slope break.

PALEONTOLOGY

The primary objective, to obtain a geologic record of planktonic microfossil sedimentation at an equatorial latitude as complete as possible, was successfully met by coring continuously most of the sedimentary sequence present at Site 289 in a single hole. The lower part of the sedimentary sequence at this site was unfortunately punctuated by several substantial stratigraphic hiatuses.

The 132 sedimentary cores recovered represent a sequence that includes a continuous sedimentary column from Pleistocene to lower Oligocene and a broken column from Upper Eocene to Aptian (Lower Cretaceous).

The Pleistocene to Oligocene cores generally contain a diverse microflora and microfauna with excellent to good state of preservation. The downhole change from a primarily biogenous ooze sequence to a largely limestone sequence bearing strings of chert is accompanied by a reduction in the microfossil contents and deterioration of fossil preservation. This trend continues

from Eocene to Cretaceous except near the base of the sequence, where surprisingly well-preserved and diverse Aptian calcareous nannofossils and planktonic foraminifera are encountered. In particular, following the appearance of chert in Core 108 (middle Eocene), Radiolaria rapidly disappear from the sequence and the forms remaining are largely recrystallized.

A combination of biostratigraphic criteria utilizing planktonic foraminifera, calcareous nannofossils, and Radiolaria is used to establish the stratigraphic framework of the recovered sequence (Figure 20). The result for the foraminifera is summarized in Figure 21 by adopting the time-stratigraphic framework of Berggren (1972) for the Cenozoic and of Casey (1964) for the Cretaceous. Because of the consistent occurrence of all three microfossil groups in the upper Eocene through Pleistocene sediments, a high-resolution biostratigraphic control can be achieved for the interval in the future. This report is, however, largely based on the results of examining core-catcher samples. Below the upper Eocene, a combined effect of dissolution of Radiolaria throughout the lower sequence, dissolution of foraminifera in the Campanian and lower Maestrichtian sections, and poor preservation of calcareous nannofossils in the Maestrichtian and some horizons within the Aptian permits utilization of only one or two microfossil groups and will allow a less precise control than that expected for the upper Eocene-Pleistocene sequence. Wherever established, age determinations based on the three microfossil groups are in close agreement except for the positioning of the Pleistocene/Pliocene boundary. This boundary, based on calcareous nannofossils, falls between Cores 289-4 and -5 judged by the last appearance of discoasters in Core 5 and the incoming of *Gephyrocapsa* in Core 4. The foraminiferal boundary occurs between Cores 3 and 4, being the level of the first evolutionary incoming of *G. truncatulinoides* associated with a major left-to-right coiling change in the genus *Pulleniatina*, criteria observed at the Pliocene/Pleistocene boundary of paleomagnetically dated cores from the eastern Equatorial Pacific (Hays et al., 1969).

At least five substantial stratigraphic breaks are detected in the Paleogene sequence at this site, all the Paleogene stage boundaries but one (between Bartonian [upper Eocene] and Lutetian [middle Eocene]) being separated by discontinuities. These breaks occur between: Rupelian (lower Oligocene) and Bartonian; Lutetian and Ypresian (lower Eocene); Ypresian and Thanetian (upper Paleocene); Thanetian and Danian (lower Paleocene); and the lower Danian and middle Maestrichtian (Upper Cretaceous). One additional discontinuity separating the Aptian (Lower Cretaceous) from the Campanian (Upper Cretaceous) is assumed, although the nature and extent of this stratigraphic hiatus is difficult to ascertain due to an extended interval of continuous drilling and coring of 28.5 meters, but with retrieval of core in a single barrel. This 28.5-meter interval, however, seems too short to accommodate all the intervening Cretaceous stages between the Campanian and Aptian, most of which have been encountered at the previous nearby Site 288 as a thick sequence of

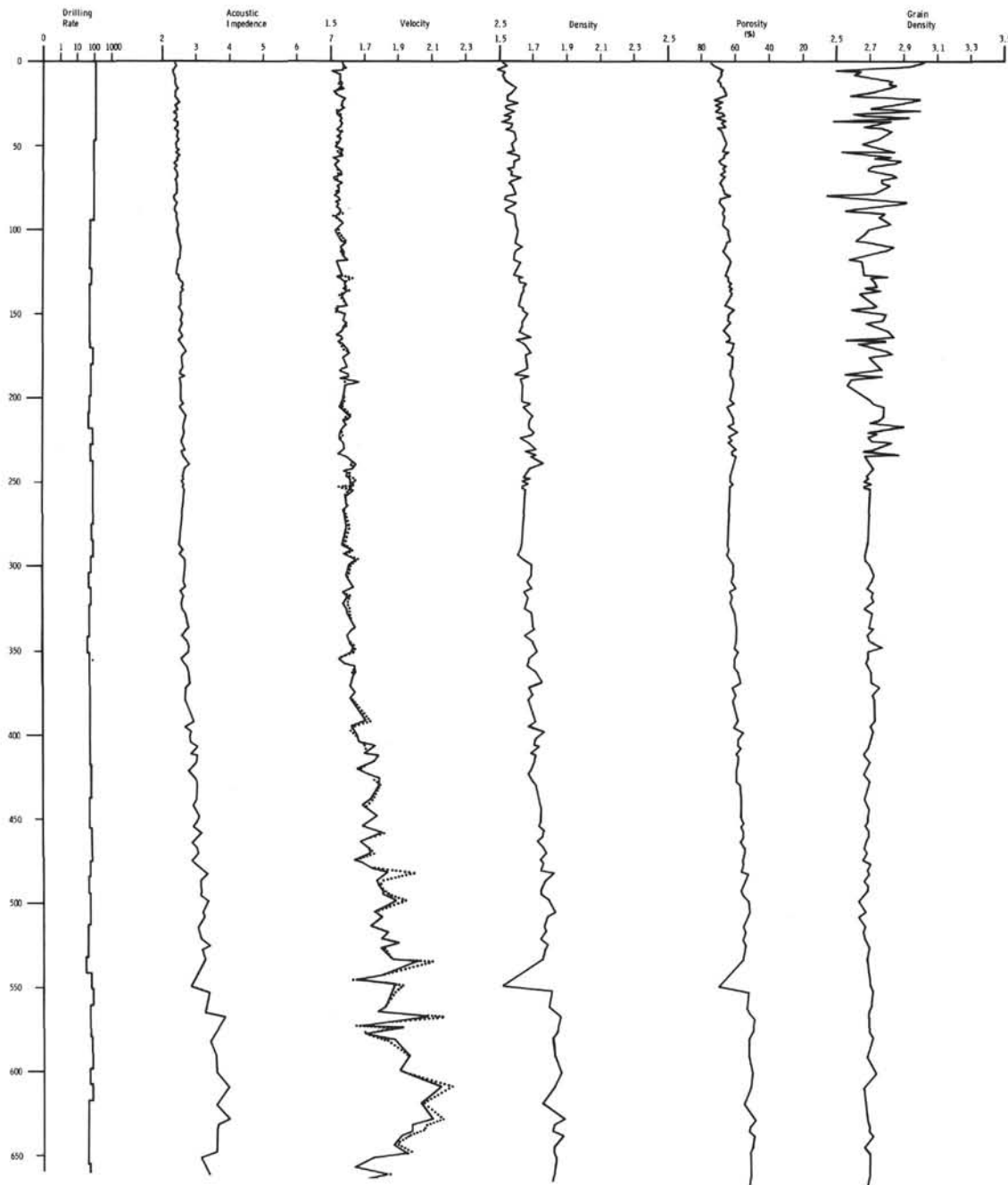


Figure 18. Graphic summary of shipboard physical property measurements. Horizontal acoustic velocity is shown as a dotted line; vertical velocity as a solid line.

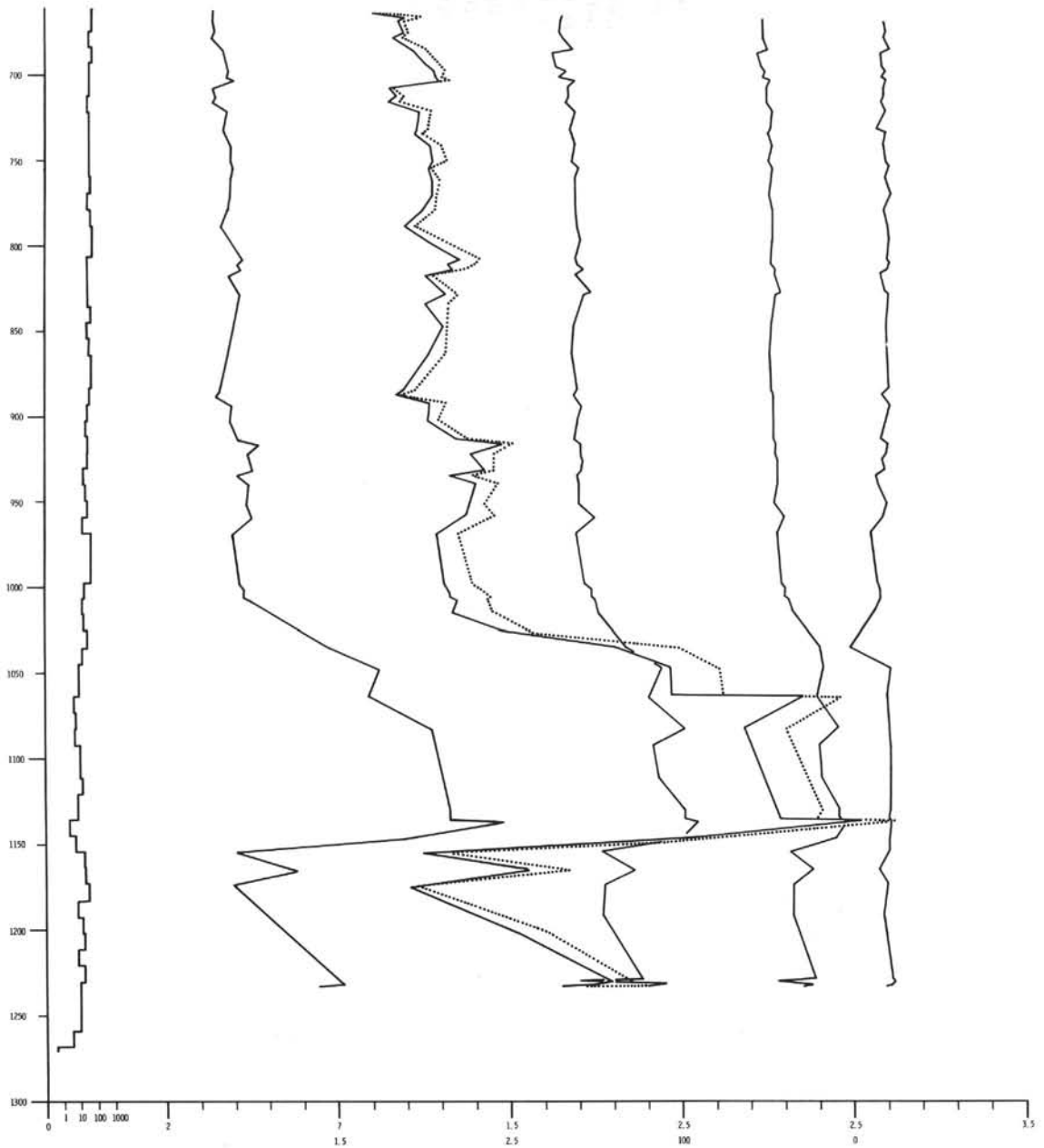


Figure 18. (Continued).

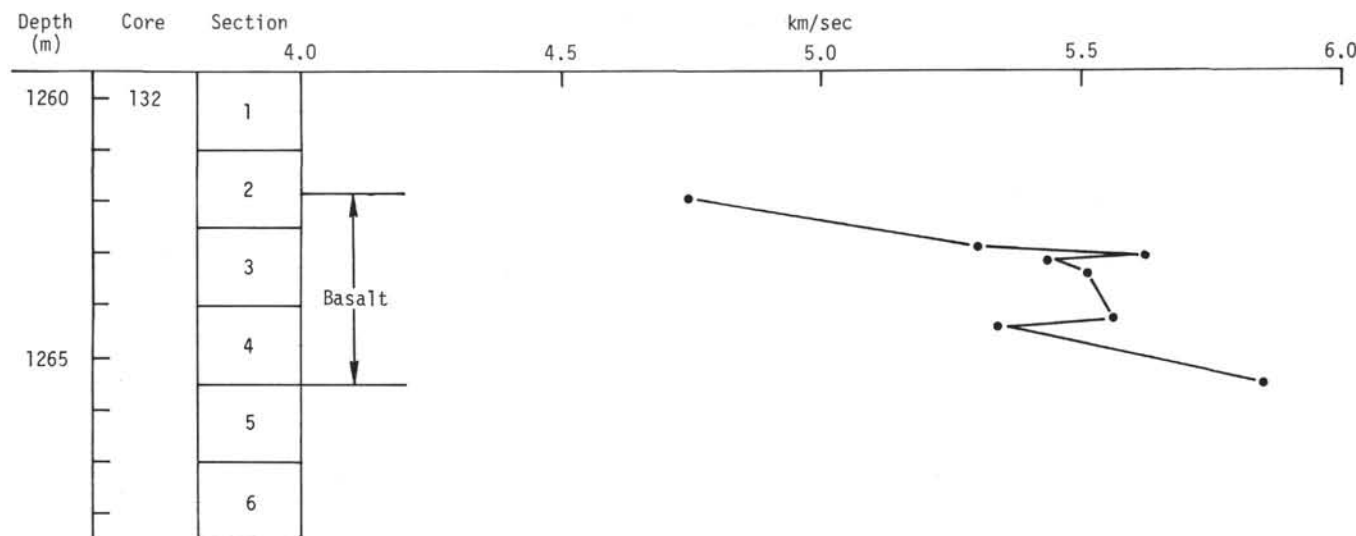


Figure 19. Acoustic velocities measured in Unit 3 (basalt) at Site 289.

TABLE 3
Correlation of Seismic Reflectors, Site 289

Reflec-tor Inten-sity	Cor-relat-ability	Δt (sec)	(m/sec)	z (m)
s	c	0.0	1550	0.0
vw	bc	0.18	1580	139.5
m	bc	0.48	1750	376.5
m	c	0.66	1950	534.0
m	c	0.78	1970	670.5
s	bc	0.84	2050	729.6
s	c	0.94	1970	832.1
s	c	1.00	2200	891.0
m	c	1.07	2150	968.6
m	c	1.12	4000	1022.4
w	c	1.19	2500	1162.4
w	bc	1.26	Basalt	1249.8

Note: s = strong; m = moderate; w = weak;
vw = very weak; c = correlatable; bc = barely correlatable.

limestone with chert. In addition, the Radiolaria sequence suggests a marked condensation of the radiolarian faunal sequence in the upper Eocene.

It is interesting to note that disconformities occurring underneath the Rupelian (lower Oligocene) and Thanetian (upper Paleocene) at this site were also encountered in similar stratigraphic positions at the previous site, 288, located at the northeastern edge of the Ontong-Java Plateau. Thus, it is probable that some of the stratigraphic hiatuses encountered at this site are of considerable magnitude extending over vast distances in the western Equatorial Pacific region. A widespread unconformity centered in the lower Oligocene, with upper Oligocene sediments overlying upper Eocene, has been reported by Kennett et al. (1972) in the neighboring region of the Tasman Sea-Coral Sea areas. The timing of this unconformity is surprisingly similar to that of the

lower Oligocene/upper Eocene discontinuity encountered over the Ontong-Java Plateau at Sites 288 and 289.

In spite of the tropical location of Site 289 and the excellent preservation of foraminifera, several diagnostic species of the planktonic foraminiferal zones widely in use today are conspicuously missing or occur only in greatly reduced numbers in the Oligocene-Recent sequence. Conspicuously absent are all the species belonging to the genus *Praeorbulina* (important group for delineating boundaries in the mid-Miocene sequence) and those species occurring in unusual scarcity are *Globigerina nepenthes* Todd (marker species for the Zone N14 and the top of the Cochiti Geomagnetic Event of early Pliocene) and species of the genus *Sphaeroidinellopsis* (marker for the N12/N13 zonal boundary and the top of the Mammoth Geomagnetic Event of late Pliocene). On the other hand, Oligocene-Pleistocene faunas are dominated throughout the sequence by species of the genus *Globoquadrina*. Such faunal characteristics may suggest planktonic foraminiferal assemblages living within a narrow belt along the Equator.

A similar absence of a number of diagnostic calcareous nannofossils used for the Neogene zonal scheme is also noted at this site. *Discoaster tamalis* and the cosmopolitan *Ceratolithus tricorniculatus* are virtually absent in the Pliocene sediments. *C. tricorniculatus* is a species generally used for delineating the lower/upper Pliocene boundary. Furthermore, *Helicopontosphaera ampliapertura*, whose extinction level marks the zonal boundary between NN4 and NN5 is absent in the lower Miocene sediment. All of these zonal species appear elsewhere in the Pacific within their proper stratigraphic intervals.

Foraminifera

Planktonic foraminifera are present in all the cores recovered from this site except in Cores 128 through 130

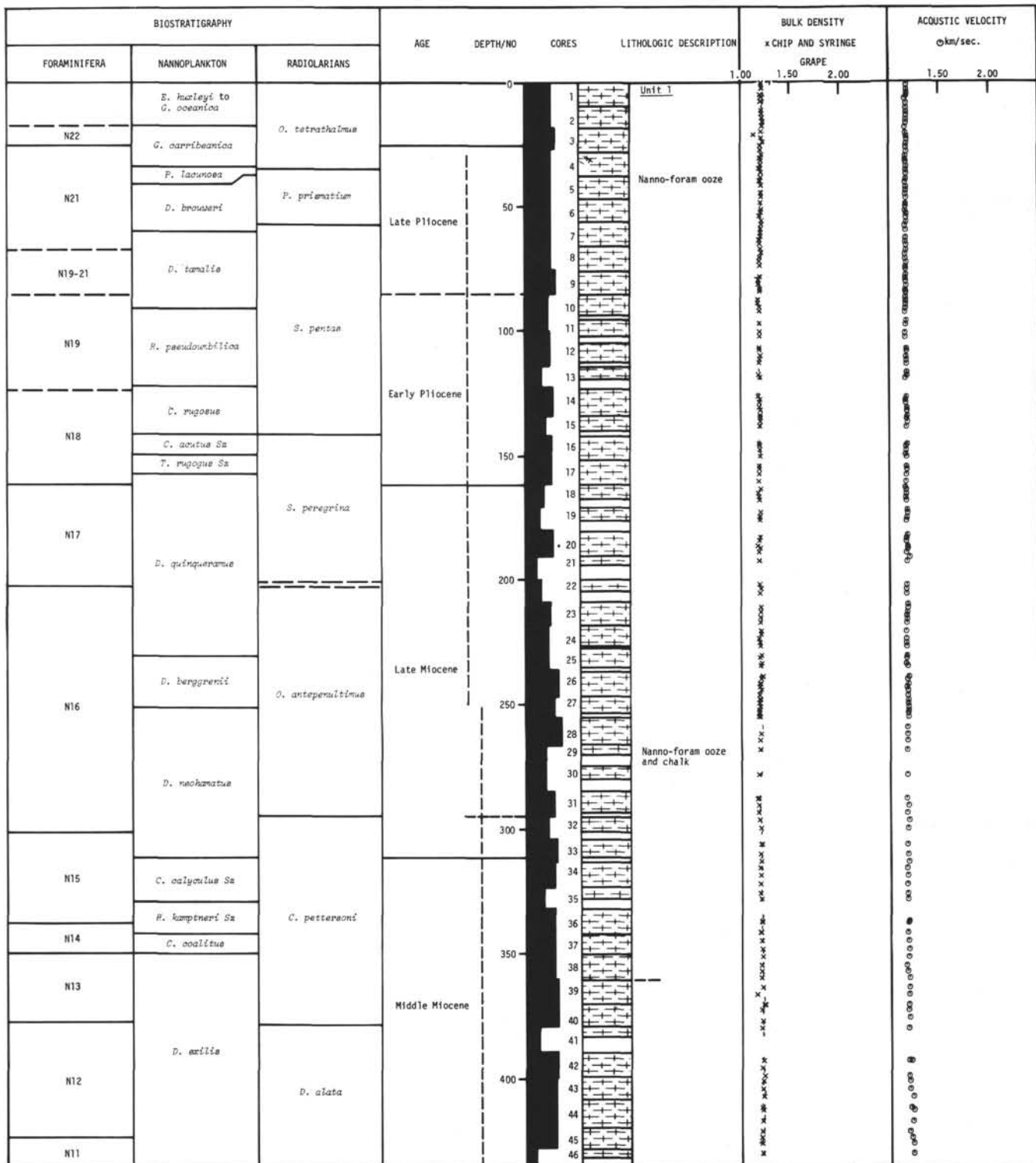


Figure 20. Composite biostratigraphy, lithology, and physical properties, Site 289.

Cenozoic and of Casey (1964) for the Cretaceous are adopted for the construction of the table.

Foraminifera investigations reveal that a continuous sequence of Pleistocene through lower Oligocene exists at this site underlain by a broken sequence of upper

from the lower part of the sequence. The distribution of biostratigraphically significant planktonic foraminiferal species and the standard foraminiferal zones recognized at this site are summarized in Figure 21. The time-stratigraphic framework of Berggren (1972) for the

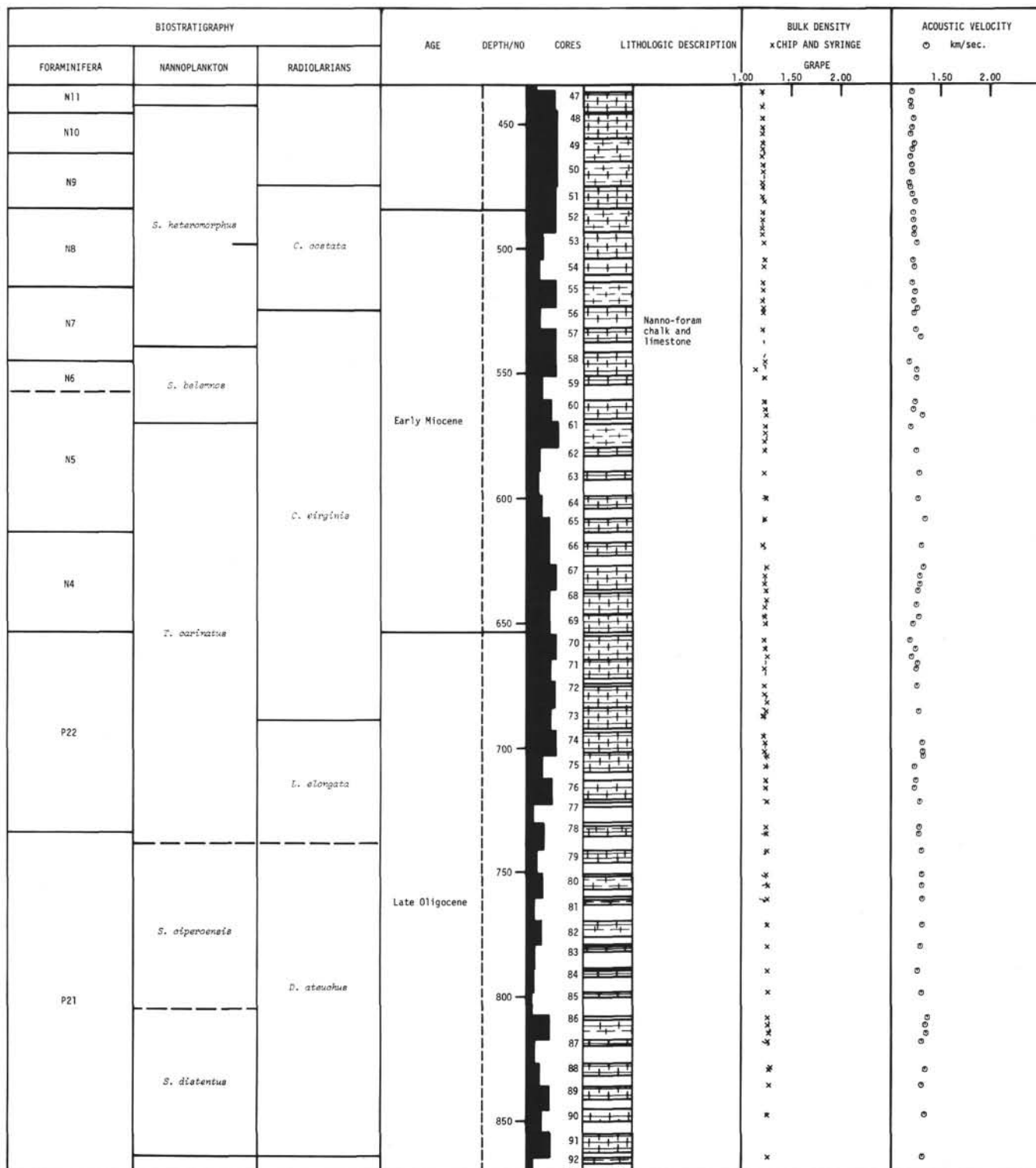


Figure 20. (Continued).

Eocene to Aptian. Well-preserved foraminifera occur in great abundance in the continuous Pleistocene-Oligocene sequence of Cores 289-1 through 289-101. No apparent reworked faunas nor evidence of marked foraminiferal solution are detected in this interval. Most

of the zonally diagnostic species recorded by Blow (1969) are present at this site and occur in successions similar to those established by him, thus enabling rather precise application of Blow's zonal scheme to the continuously cored sequence. Furthermore, the availability

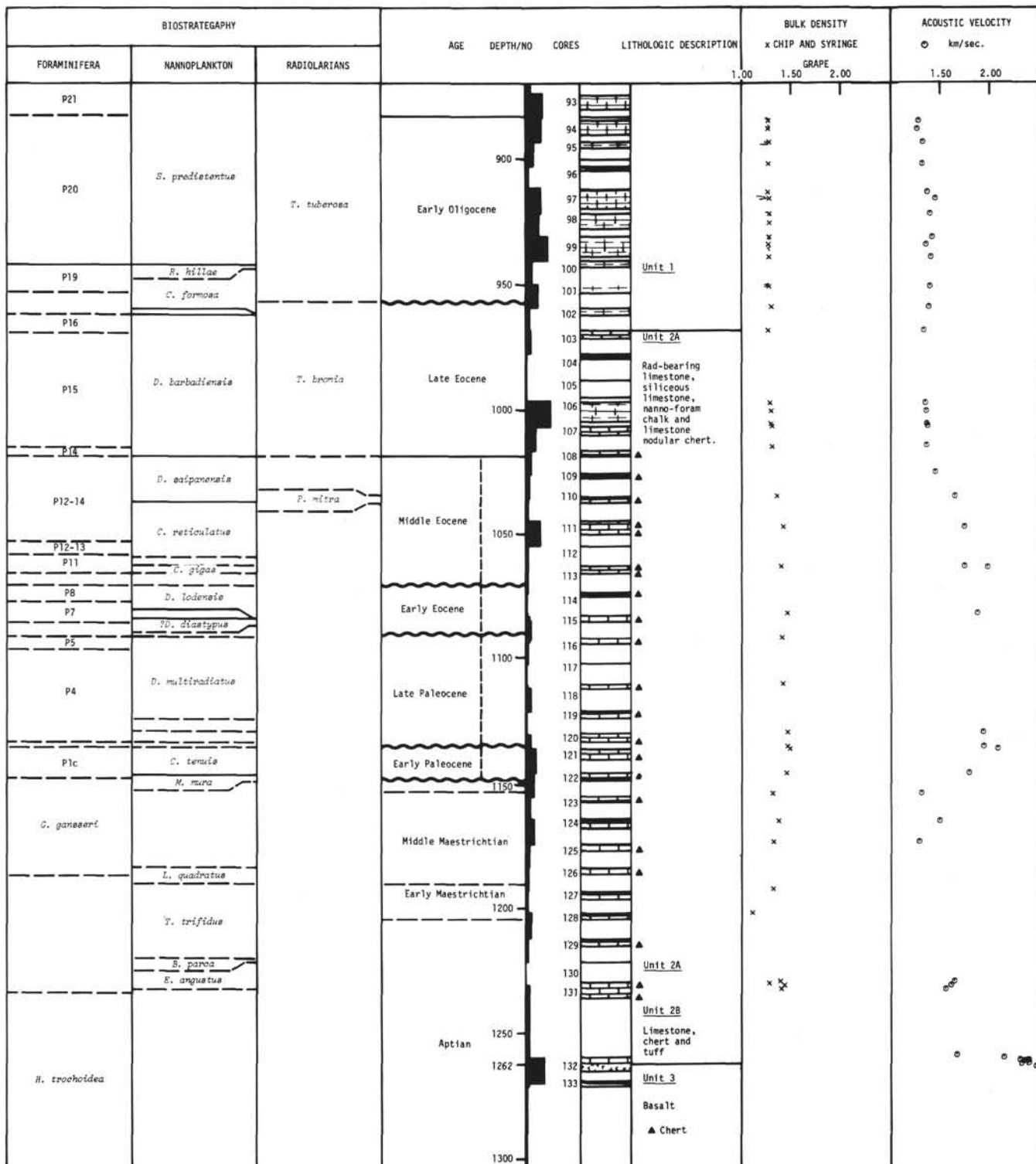


Figure 20. (Continued).

of a continuous record of sedimentation in an apparently stable depositional environment above the carbonate compensation depth should provide a means of assessing the duration of each planktonic foraminiferal zone. The duration of these zones has been fixed only approximately on the basis of a few radiometrically dated zones dispersed through the sequence.

The post-Miocene sequence at this site can also be correlated rather precisely with the paleomagnetically dated deep-sea sequence from the eastern Equatorial Pacific (Hays et al., 1969; Saito et al., 1975). Such a correlation indicates an approximate time span represented by each of the upper 16 cores to be on the order of 300,000 years.

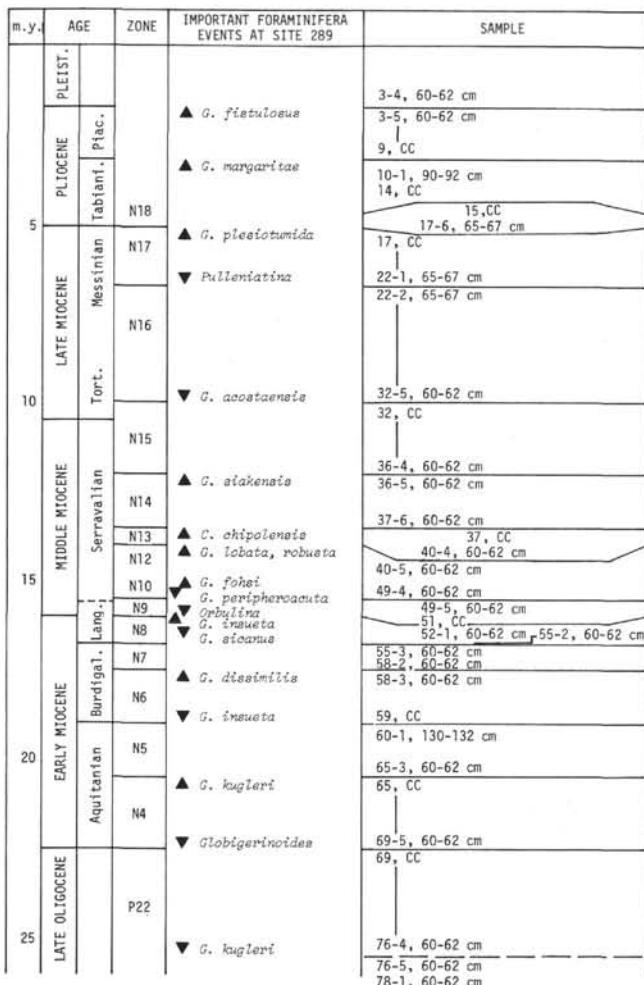


Figure 21. Important foraminiferal events at Site 289.

The downhole transition from a primarily nonlithified biogenous ooze sequence to a largely limestone sequence bearing strings of chert is nearly coincident with the discontinuity separating the upper, continuous column of the Pleistocene-Oligocene from the lower, hiatus-laden column of upper Eocene-Aptian. Some indications of lithification occur as high as Core 289-59 where processed foraminifera assemblages still include many specimens encrusted with sediment particles. Concomitant with the increasing lithification of sediments below the Oligocene/Eocene discontinuity, preservation of foraminifera deteriorates drastically and foraminifera become totally recrystallized. The poor preservation of foraminifera and several disconformities within the lower column make it difficult to establish the precise zonal subdivision of the upper Eocene-Aptian sequence. However, surprisingly well-preserved foraminifera are found within the lower sequence in Cores 125 and 126 (both middle Maestrichtian age) and in Cores 131 and 132 (both late Aptian age).

The Tertiary/Cretaceous boundary at this site is apparently a discontinuity involving a considerable time span, in which the latest Maestrichtian fauna characterized by *Abathomphalus mayaroensis* (Bolli) and

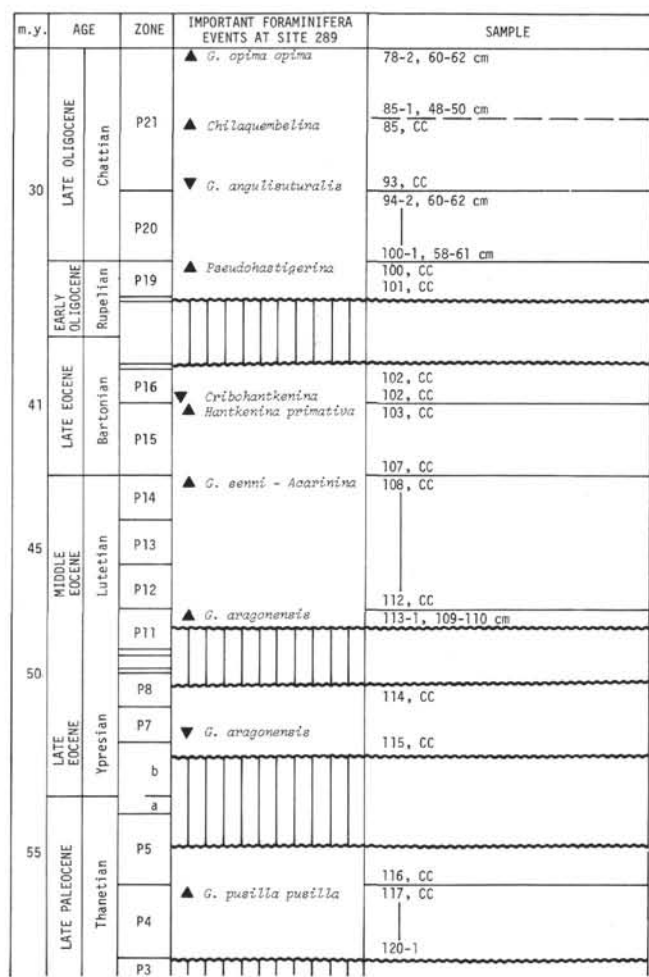


Figure 21. (Continued).

the earliest Danian fauna typified by *Globigerina eugubina* Luterbacher and Premoli-Silva are missing. This discontinuity occurs in the seemingly continuous limestone sequence of Core 289-122 between 5-7 cm and 133-135 cm depth. Its exact position has yet to be determined, but no obvious lithological change which might suggest the stratigraphic hiatus occurs within this interval.

As was also observed at the previous site, 288, the lower Maestrichtian-upper Campanian sequence (Cores 128-130) at this site is devoid of planktonic foraminifera. A similar interpretation of the deposition depth of these sediments can be made, indicating a sedimentation depth close to or below the carbonate compensation depth but above the calcareous nannoflora solution depth.

The stratigraphic relationship between Aptian and Campanian sediments is very likely to be disconformable but whether sediments representing any other Cretaceous stage exist between the two at this site cannot be determined with the available data. The maximum possible interval of 28.5 meters allowable in this core between the Campanian and Aptian sediments seems too short to accommodate any substantial part of

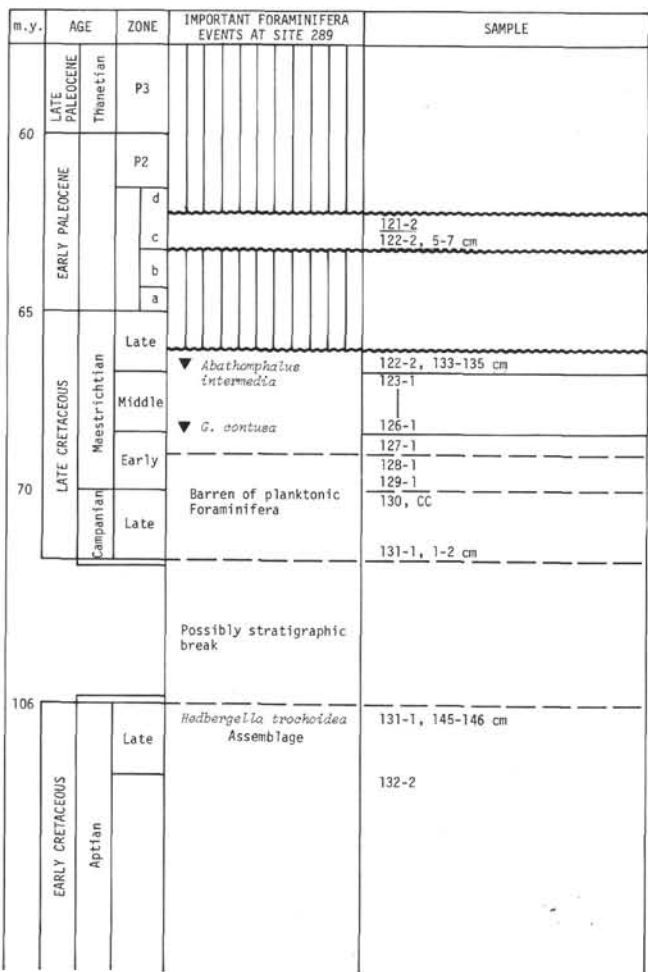


Figure 21. (Continued).

other Cretaceous stages. The Aptian fauna includes abundant planktonic species and is interpreted as having been deposited above the calcium carbonate compensation depth.

Calcareous Nannofossils

The sequence ranges in age from Early Cretaceous to Quaternary. Nannofossils are abundant through most of the section. Preservation is excellent in the upper part of the section, but deteriorates gradually, with a parallel decrease in abundance, from the lower Miocene downwards. The Oligocene-Quaternary part of the sequence is complete insofar as its nannofossil zones are all present and well developed. In contrast, the Lower Cretaceous-Eocene section is broken and several hiatuses are recognized.

The nannostratigraphy of this site is dealt with in more detail by Shafik (this volume). Figure 22 is a summary of the biostratigraphy as deduced from the study of the nannofossils.

Radiolaria

Radiolaria assemblages adequate for biostratigraphic purposes were found in all of the upper 110 continuous cores recovered at this site, with the exception of Core

Series or Subseries	Nannofossil Zones/Subzones	Site 289 Samples
HOLOCENE PLEISTOCENE	<i>Emiliania huxleyi</i> - <i>Gephyrocapsa oceanica</i>	1-1, 30-31 cm 2-6, 30-31 cm
	<i>Gephyrocapsa caribbeanica</i>	2, CC 4-3, 110-111 cm
	<i>Pseudoemiliania lacunosa</i>	4-4, 30-31 cm 4-6, 30-31 cm
PLIOCENE	<i>Discoaster brouwerii</i>	4, CC 7-2, 35-36 cm
	" <i>Discoaster</i> " <i>pentaradiatus</i>	7-2, 120-121 cm 7-6, 30-31 cm
	<i>Discoaster tamalis</i>	7, CC 10-3, 30-31 cm
Lower	<i>Reticulofenestra pseudoumbilica</i>	10-4, 30-31 cm 13, CC
	<i>Ceratolithus rugosus</i>	14-1, 30-31 cm 15, CC
	<i>Ceratolithus tricorniculatus</i>	16-1, 120-121 cm 16-4, 30-31 cm
Upper	<i>Ceratolithus acutus</i>	16-5, 30-31 cm 17-3, 120-121 cm
	<i>Triquetrorhabdulus rugosus</i>	17-4, 120-121 cm 25-1, 120-121 cm
	<i>Discoaster quinqueramus</i>	25-2, 120-121 cm 27-3, 120-121 cm
Middle	<i>Discoaster berggrenii</i>	27-4, 30-31 cm 33-4, 120-121 cm
	<i>Discoaster neohamatus</i>	33-5, 30-31 cm 35-4, 120-121 cm
	<i>Catinaster calyculus</i>	35, CC 36, CC
Lower	<i>Discoaster hamatus</i>	37-1, 30-31 cm 37-6, 35-36 cm
	<i>Helicopontosphaera kampfneri</i>	37-6, 120-121 47-4, 30-31 cm
	<i>Catinaster coalitus</i>	47-5, 30-31 cm 53-3, 120-121 cm
OLIGOCENE	<i>Discoaster exilis</i>	53-4, 120-121 cm 57, CC
	<i>Sphenolithus heteromorphus</i>	58-1, 30-31 cm 60, CC
	<i>Discoaster druggii</i>	61-1, 30-31 cm
Upper	<i>Triquetrorhabdulus carinatus</i>	<i>Discoaster deflandrei</i>
		<i>Cyclicargolithus abisectus</i>
		78, CC
Middle	<i>Sphenolithus ciperoensis</i>	79-1, 60-61 cm 85, CC
	<i>Sphenolithus distentus</i>	86-2, 120-121 cm 91, CC
	<i>Sphenolithus predistentus</i>	92-1, 120-121 cm 100-1, 50-51 cm
Lower	<i>Reticulofenestra hillae</i>	100-1, 122-123 cm 100, CC
	<i>Cyclococcolithina formosa</i>	101-1, 65-66 cm 102-1, 112-113 cm
	<i>Discoaster barbadiensis</i>	102, CC 104, CC
EOCENE		105, CC 108-1, 74-75 cm
	<i>Discoaster saipanensis</i>	108, CC 110-1, 107-108 cm
	<i>Cyclicargolithus reticulatus</i>	110, CC 112, CC
Middle	<i>Reticulofenestra umbilica</i>	
	<i>Chiasmolithus gigas</i>	113-1, 117-118 cm
	<i>Nannotetra fulgens</i>	
Lower	<i>Discoaster sublodoensis</i>	<i>Rhabdosphaera inflata</i>
		<i>Discoasteroides kuepperi</i>
	<i>Discoaster lodoensis</i>	114-1, 148-150 cm 115-1, 55-56 cm
Lower	<i>Tribrachiatis orthostylus</i>	
	<i>Discoaster diastypus</i>	7115, CC

Figure 22. Nannofossil biostratigraphy at Site 289.

Series or Subseries	Nannofossil Zones/Subzones	Site 289 Samples
PALEOCENE	<i>Discoaster multiradiatus</i>	116-1, 140-143 cm 119, CC
	<i>Discoaster nobilis</i>	
	<i>Discoaster mohleri</i>	120-1, 80-81 cm 120-1, 148-150 cm
	<i>Heliolithus kleinpellii</i>	120, CC
	<i>Fasciculithus tympaniformis</i>	
	<i>Cyclococcolithina robusta</i>	121-1, 125-126 cm 121-2, 62-63 cm
	<i>Cruciplacolithus tenuis</i>	122-1 (top)
MAESTRICHIAN	<i>Micula mura</i>	122, CC
	<i>Lithraphidites quadratus</i>	126-1, 135-136 cm 126 (bottom)
	<i>Tetralithus trifidus</i>	127-1, 131-132 cm 129, CC
CAMPANIAN	<i>Brownsonia parca</i>	130, CC
	<i>Eiffellithus augustus</i>	131-1, 1-2 cm 131-1, 30-31 cm
SANTONIAN	<i>Gartnerago obliquum</i>	
CONIACIAN	<i>Marthasterites furcatus</i>	
TURONIAN	<i>Micula decussata</i>	
ALBIAN	<i>Eiffellithus turrisiffell</i>	
	APTIAN	131-1, 149-150 cm 132-2, 68-70 cm

Figure 22. (Continued).

289-109 which proved totally barren. Below Section 289-110-1 only traces on extremely poorly preserved Radiolaria were encountered at a few Cretaceous levels, apart from a rich *T. bromia* Zone assemblage downworked in a drilling sand of Sample 289-112, CC.

Throughout this succession Radiolaria are preserved in gray to white nanno-foram oozes, chalks, and limestones. Down to Sample 289-107, CC abundance of Radiolaria, though subject to fluctuation, is high. Peak abundance is probably in Cores 289-103 and 289-104, the longest section showing consistently relatively low return per sample is Cores 289-1 through 289-14. With very few marked exceptions, preservation and diversity of assemblages are good. A slightly more detailed discussion of abundance, preservation, and diversity of radiolarians is included in Holdsworth and Harker (this volume).

Between Samples 289-107, CC and 289-108-1, 72-75 cm there occurs a drastic change, taking place within a depth interval which is at maximum 14 meters, at minimum 0.72 meter, but most probably only slightly more than 6.0 meters. Radiolarians become very scarce and show corrosion and darkening. In Section 289-110-1 only fragmentary, robust species have survived and Core 289-109 revealed no evidence of radiolarians. Change in abundance, preservation, and diversity coincides rather closely with a sharp increase in the degree of chertification of rock recovered.

Zonal Allocation

Some difficulties were encountered in placing zone boundaries (see Holdsworth, this volume, for details.) Final allocations may be summarized:

O. tetrathalmus Zone: 289-1-4, 70-72 through 4-4, 70-72

P. prismatum Zone: 289-4, CC through 6, CC

S. pentas Zone: 289-7-3, 70-72 through 15, CC

S. peregrina Zone: 289-16-4, 70-75 through 22-3, 70-75

O. penultimus Zone: Not recognizable

O. antepenultimus Zone: 289-22, CC through 31, CC

C. petterssoni Zone: 289-32-3, 70-75 through 40-5, 70-75

D. alata Zone: 289-40, CC through 50, CC

C. costata Zone: 289-51-3, 70-75 through 56-2, 70-75

C. virginis Zone: 289-56, CC through 73-3, 70-75

L. elongata Zone: 289-73, CC through 78, CC

D. ateuchus Zone: 289-79-1, 70-75 through 91, CC

T. tuberosa Zone: 289-92-1, 125-130 through 101, CC

T. bromia Zone: 289-102-1, 91-95 through 108-1, 72-75

P. goetheana Zone: Not recognizable in material recovered

P. chalara Zone: Not recognizable in material recovered

P. mitra Zone: 289-110-1, 106-108

For tabulation of Radiolaria, see Holdsworth (this volume).

SEDIMENTATION RATES

The excellent foraminiferal age determinations in the Cenozoic at this site have made it possible to draw up an accurate sediment accumulation column. Saito has used the thickness of the Miocene foraminiferal zones to modify the time scale devised by Berggren (1972), assuming a roughly uniform rate of sedimentation.

In Figure 23 the sediment accumulation curve has been drawn using the scale of Vincent (1974). The sharp increase in gradient in the early middle Miocene and the lower gradient in the later early Miocene is almost certainly an indication that the 14 m.y. early/middle Miocene boundary is too young. The 16 m.y. boundary suggested by Saito is more acceptable.

The sedimentation rates are given in Table 4, calculated on the basis of an initial 70% porosity. Sufficient age points to give a reliable curve are available in the intervals from the early Oligocene to the present, the mid to late Eocene and the Campanian-Maestrichtian.

From the early Oligocene to Pleistocene, the depositional rate fluctuates between a high of 67 m/m.y. in the late Oligocene to 15 m/m.y. for the Pleistocene. Using Saito's modified Miocene scale, most of the rates fall between 30 and 50 m/m.y. without exhibiting any clear overall trend that might be associated with latitudinal motion of the Ontong-Java Plateau.

The middle to late Eocene rate of deposition is a little over 30 m/m.y. and is hence on the low side of the range of later rates. The Campanian-Maestrichtian rate (23 m/m.y.) is less than that of the Eocene, but is about half

TABLE 4
Sedimentation Rates, Site 289

Unit	Depth (m)	Thickness (m)	Porosity (%)	Thickness Corrected to 70% Porosity	Age (m.y.)	Duration (m.y.)	Sedimentation Rate (m/m.y.)	
							Observed Thickness	Thickness Corrected to 70% Porosity
I	0-25-5	25.5	69	26	0-1.75	1.75	15	15
	25.5-85.5	60	68	64	1.75-3.0	1.25	48	51
	85.5-161	75.5	64	91	3.0-5.0	2	38	46
	161-317	156	62	198	5-10.5	5.5	28	36
					5-11.0	6	26	33
	317-421.5	104.5	61	136	10.5-16 ^a	5.5	29	41
	421.5-484	62.5	56	92	11.0-14	3.0	56	72
	484-655	171	53	268	16-22.5 ^a	6.5	26	41
					14-22.5	8.5	20	32
	655-702	47	52	75	22.5-24.7	2.2	21	34
	702-885	183	48	354	24.7-30	5.3	35	67
	885-955	70	46	126	30-32.5	2.5	28	50
	955-1015	60	41	118	40.0-43.0	3.0	20	40
	1015-1070	55	21	145	43.0-48	5.0	11	29
	1070-1090	20	11	59	(51.3-52.7)	(1.4)	(14)	(42)
I-2A	1090-1135	45	18	123	(55.5-58)	(2.5)	(18)	(49)
	1135-1148	13	11	39	(62.7-63.5)	(0.8)	(16)	(49)
	1148-1250	102	30	238	65.5-76	10.5	10	23
	2B	1250-1262	12	20 ^b	(107-108)	(1)	(12)	(32)

Note: Values in parentheses are based on an assumed gradient of the sediment accumulation curve.

^aRevised Miocene time scale of Saito (unpublished data).

^bEstimated value.

of that found at Site 288 for the same interval. This suggests that undetected breaks in sedimentation may exist in the Late Cretaceous at this site.

SUMMARY AND CONCLUSIONS

Summary

Site 289 was located on the north central portion of the Ontong-Java Plateau to sample a presumably continuous biostratigraphic sequence. Continuous coring resulted in recovery of 56% of the section to a depth of 1271 meters subbottom (basalt was encountered at 1262 m). The section proved to be complete in the Neogene and incomplete in the Paleogene.

The section consists of:

Unit 1 (0-969 m): Pleistocene to late Eocene nanno-foram ooze and chalk.

Unit 2 (969-1262 m): Late Eocene to Early Cretaceous Radiolaria-bearing limestone, siliceous limestone, nanno-foram chalk, nodular chert, and tuff.

Unit 3 (1262-1271 m): Basalt (pre-early Aptian).

The continuous Pleistocene to early Oligocene sediments contain a diverse microflora and microfauna with excellent to good preservation. Material in the deeper limestone sequences is more poorly preserved, save for the surprisingly diverse and well-preserved Aptian.

At least six substantial stratigraphic breaks are present in the section. These occur between Rupelian (lower Oligocene) and Bartonian; Lutetian (middle Eocene) and Ypresian; Ypresian and Thanetian (upper Paleocene); Thanetian and Danian (lower Paleocene);

lower Danian and Maestrichtian; and late Aptian and Campanian. The Eocene/Oligocene break is similar to that reported by Kennett et al. (1972) in the Tasman and Coral seas.

Very minor chert was detected in the lower Miocene with the major appearance in late Eocene accompanied by the loss of Radiolaria from the sediments. Less chert was observed at this site than at Site 288.

The sequence of events recognized at Site 289 began during or prior to early Aptian time with the extrusion of tholeiitic basaltic lava flows. Following basalt extrusion, deposition of vitric tuff occurred, followed by biogenic sedimentation above the foram solution depth. A period of nondeposition or erosion followed from late Aptian into Campanian.

Biogenic sedimentation during Campanian time was below the foram solution depth, but fluctuations in depth of the plateau (or of the foram solution depth) permitted continued biogenic sedimentation to occur during the Maestrichtian above the foram solution depth. During latest Maestrichtian and earliest Paleocene time, a second period of nonaccumulation occurred. Biogenic sedimentation above the foram solution depth continued during the late Paleocene. A third period of nonaccumulation occurred during the latest Paleocene, and persisted into the early Eocene.

A short period of continued biogenic sedimentation above foram solution depth occurred during the early Eocene followed by a fourth hiatus. Biogenic sedimentation above the foram solution depth occurred continuously during the middle and late Eocene. A minor period of higher productivity of Radiolaria occurred

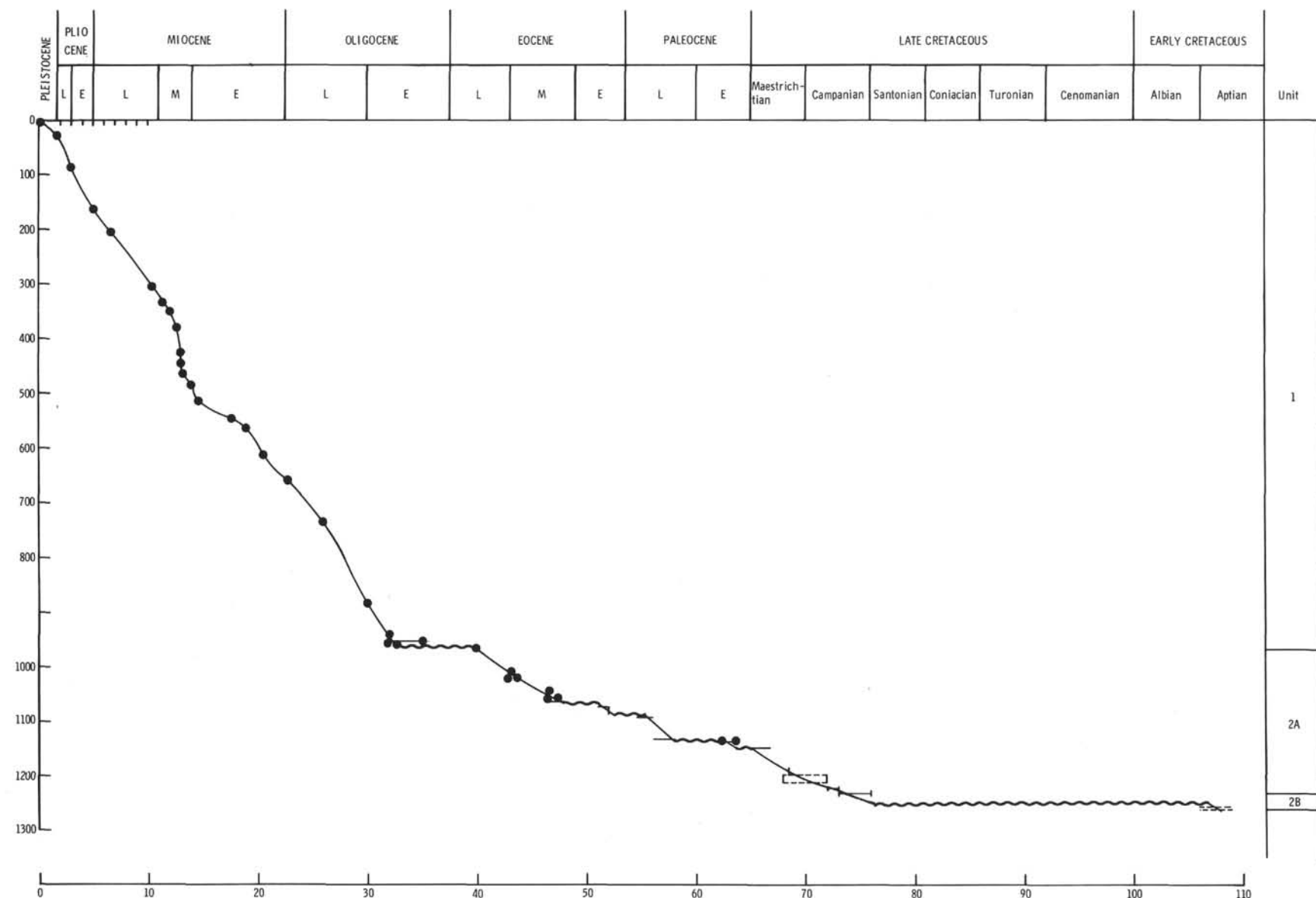


Figure 23. Sedimentation accumulation curve for Site 289 based on foraminiferal age determinations for the Cenozoic and foraminiferal and nannofossil determinations for the Cretaceous. (Time scale from Vincent, 1974; van Hinte, 1972.)

during the entire late Eocene. A fifth period of nonaccumulation occurred at the end of Eocene time and persisted into the earliest Oligocene (the Eocene/Oligocene regional unconformity of Leg 21).

From the beginning of the early Oligocene until the Holocene, continuous biogenic sedimentation of foraminifera and nannofossils above the foram solution depth has occurred on the northern part of the Ontong-Java Plateau.

The Early Cretaceous age for Site 288 fits well at the western end of the original Phoenix spreading center based on magnetic trend of Larson and Chase (1972). The age at Site 289 requires a fracture zone between Sites 288 and 289 which appears to have been crossed very near Site 288.

Comparison of Site 289 With Sites 64 and 288

The stratigraphic sequences and sedimentary features at Site 289 show close similarities to those at Sites 64 and 288. Some major differences occur, probably because Sites 289 and 64 (160 km south of Site 289) are on the Ontong-Java Plateau and have been so located for most of their histories, whereas Site 288 is 550 km to the southeast of Site 289 at the western end of the Stewart Basin on the southeastern flank of the Ontong-Java Plateau. At all three sites biogenic ooze comprises almost all of the sediment. Ash is reported as a minor constituent throughout the column at both Sites 288 and 289. Breaks in the sedimentary record occur at both sites, but are more marked at Site 288 where the presence of derived faunas together with the included hiatuses, may be the result of the site's position on the flank of the plateau.

Unit 1, as defined at Site 289, can be traced to Sites 64 and 288, although it is considerably thinner at Site 288 (Figure 24) due largely to the less complete Neogene

sequence. This thinning is accompanied by the occurrence of chert-bearing younger limestones at Site 288, and thus Unit 2 is thicker than at Site 289 (Figure 24). The overall volume of chert at Site 288 appears to be far greater than at Site 289.

Two other differences are present in Unit 1 at these three sites. H₂S gas occurs at Site 289, whereas an unidentified gas with a "sweet-smelling" odor (Winterer, Riedel, et al., 1971, p. 552) occurs at Site 64. No gas was observed at Site 288. The foraminifera content at Site 289 appears to be greater than at Sites 64 and 288.

Unit 2, as defined at Site 289, is traceable to Sites 64 (where only the uppermost 20 meters was recovered) and 288. The thickness of Unit 2 at Site 288 is twice that at 289 because of the greater thickness of the Upper Cretaceous section. The basal subunit of mixed volcanic ash, vitric siltstone and carbonates is considerably thicker at Site 288 in spite of there being five breaks in the depositional record. At Site 289, five major stratigraphic discontinuities were also observed in Unit 2 (Figure 25) (see also Paleontology Section). The vitric

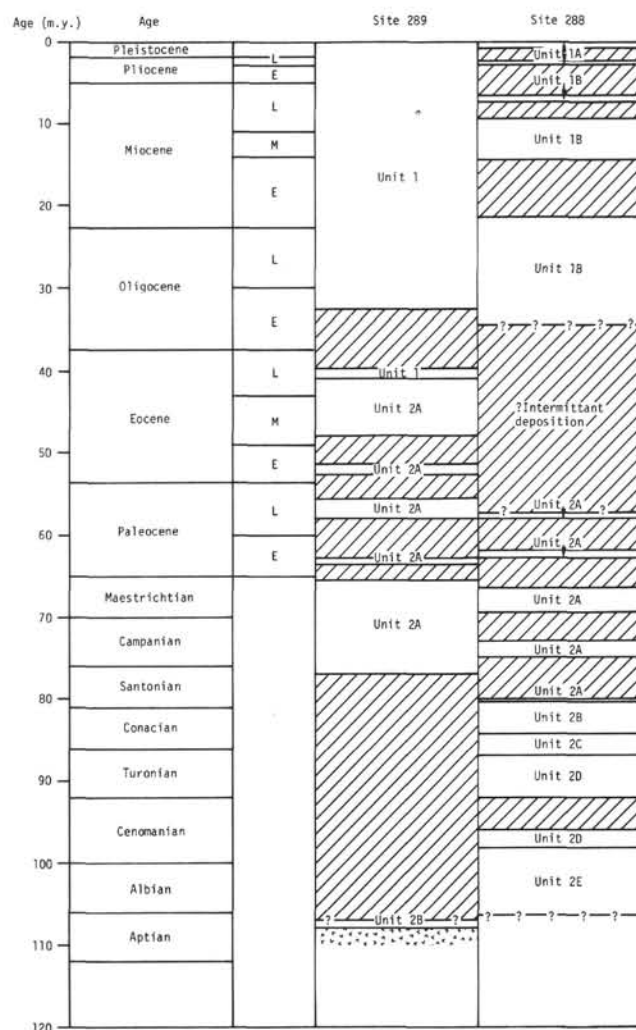
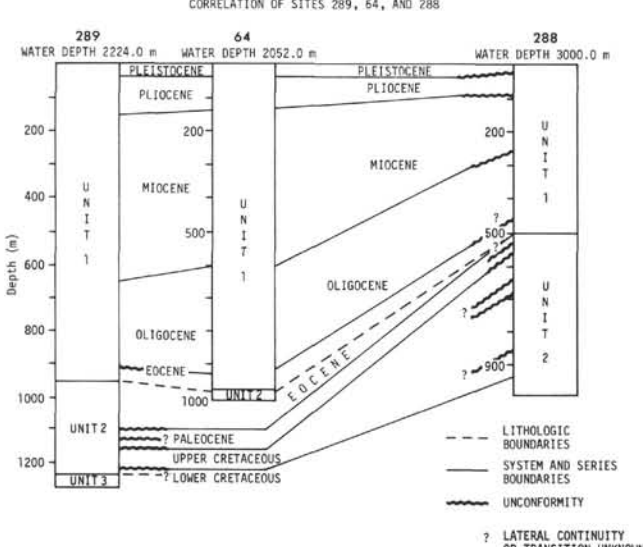


Figure 25. Time-stratigraphic correlation of Sites 289 and 288. (Time scale after Berggren, 1972; van Hinte, 1972.)

Figure 24. Correlation of Sites 289, 64, 288.



siltstone-carbonate rhythmic sequences observed at Site 288 in Turonian sediments are absent at Site 289 (Turonian rocks are not represented). Large chert nodules occur in rocks older than Oligocene at all three sites, although scattered chert fragments of fine pebble size occur in the Miocene at Site 289 and 288. Whether this chert diagenesis should be a function of progressive burial and depth-controlled remobilization of silica, or whether other factors are more significant at Sites 289, 64, and 288 remains open.

Although close physical similarity exists among the recovered sediments at all three sites, sharp differences in the thicknesses of major time-stratigraphic units occur (Figure 24). The section of Upper Cretaceous sediments is thicker at Site 288 by a five-fold factor than at Site 289 where a long Upper Cretaceous hiatus in deposition occurred. The Paleocene is represented at both sites by nearly equally thick sections; an upper Paleocene hiatus being common to both sites also. The Eocene at Site 288 may be present in a recovery gap but would be thin; it was partly recovered at Site 64, and is represented incompletely at Site 289 where three hiatuses occur. The Oligocene section reaches its maximum thickness at Site 64, and thins slightly towards Sites 289 and 288. The Miocene thickens progressively when traced from Sites 288 to 64 to 289. The Pliocene thickens gradually in the same direction; the Pleistocene appears to be uniformly thick over all three sites, but only part of the Pleistocene is represented at Site 288.

REFERENCES

- Berggren, W.A., 1972. A Cenozoic time-scale—some implications for regional geology and paleobiogeography: *Lethaia*, v. 5, p. 195-215.
- Blow, W.H., 1969. Late middle Eocene to Recent planktonic foraminiferal biostratigraphy. In Bronnimann, P. and Renz, H.H. (Eds.), *Plankt. Microfossils 1st Internatl. Conf. Proc.*: Leiden, Netherlands (Brill): v. 1, p. 199-421.
- Casey, R., 1964. The Cretaceous period. In Harland, W.B., Smith, A.G., and Wilcock, B. (Eds.), *The Phanerozoic Time Scale*: Geol. Soc. London, Quart. J., v. 120S, p. 193-202.
- Greenwood, R., 1973. Cristobalite: its relationship to chert formation in selected samples from the Deep Sea Drilling Project: *J. Sediment. Petrol.*, v. 43, p. 700-708.
- Hays, J.D., Saito, T., Opdyke, N.P., and Burckle, L.H., 1969. Pliocene-Pleistocene sediments of the equatorial Pacific: their paleomagnetic, biostratigraphic and climatic record: *Geol. Soc. Am. Bull.*, v. 80, p. 1481.
- Heath, G.R., 1973. Cherts from the eastern Pacific, Leg 16, Deep Sea Drilling Project. In Van Andel, T.H., Heath, G.R., et al., *Initial Reports of the Deep Sea Drilling Project, Volume 16*: Washington (U.S. Government Printing Office), p. 609-614.
- Heath, G.R. and Moberly, R., 1971. Cherts from the western Pacific, Leg 7, Deep Sea Drilling Project. In Winterer, E.L., Riedel, W.R., et al., *Initial Reports of the Deep Sea Drilling Project, Volume 7*: Washington (U.S. Government Printing Office), p. 991-1007.
- Hussong, D.M., 1972. Complex structure of the South Fiji Basin as shown by ASPER refraction data (abstract): *Geol. Soc. Am. Abstracts with Programs*, v. 4, p. 175.
- Kennett, J.P., Burns, R.E., Andrews, T.E., Churkin, M., Davies, T.A., Dumitrica, P., Edwards, A.R., Galehouse, J.S., Packham, G.H., and van der Lingen, G.J., 1972. Australia-Antarctic continental drift, paleocirculation changes and Oligocene deep sea erosion: *Nature Phys Sci.*, v. 289, p. 51.
- Kroenke, L.W., 1972. Geology of the Ontong-Java Plateau, Hawaii Institute of Geophysics Pub. HIG-72-5, 119p.
- Larson, R.F. and Chase, C.G., 1972. Late Mesozoic evolution of the western Pacific Ocean: *Geol. Soc. Am. Bull.*, v. 83, p. 3627.
- Lonsdale, P., Malfait, B.T., and Spiess, F.N., 1972a. Abyssal sand waves on the Carnegie Ridge: *Geol. Soc. Am. Abstract with Programs*, v. 4, p. 579-580.
- Lonsdale, P., Normark, W.R., and Newman, W.A., 1972b. Sedimentation and erosion on Horizon Guyot: *Geol. Soc. Am. Bull.*, v. 83, p. 289-316.
- McCave, I.N., 1970. Deposition of fine-grained suspended sediment from tidal currents: *J. Geophys. Res.*, v. 75, p. 4151-4159.
- Saito, T., Burckle, L.H., and Hays, J.D., 1975. Late Miocene to Pleistocene biostratigraphy of equatorial Pacific sediments. In Saito, T. and Burckle, L.H. (Eds.), *Late Neogene Epoch Boundaries* (24th International Geological Congress, Montreal, 1972, Sump. 109). Am. Mus. Nat. Hist., Micropal. Press, Spec. Publ. no. 1, p. 226-237.
- Van Hinte, J.E., 1972. The Cretaceous time-scale and planktonic foraminiferal zones: *Ned. Akad. Wetensch. Proc. Ser. B.*, v. 75, p. 61-68.
- Vincent, E., 1974. Cenozoic planktonic biostratigraphy and paleoceanography of the western Indian Ocean. In Fisher, R.L., Bunce, E.T., et al., *Initial Reports of the Deep Sea Drilling Project, Volume 24*: Washington (U.S. Government Printing Office), p. 1111-1150.
- Winterer, E.L., Riedel, W.R., et al., 1971. Initial Reports of the Deep Sea Drilling Project, Volume 7: Washington (U.S. Government Printing Office).

APPENDIX A
Smear-Slide Determination, Site 289 (values in percent)

Sample (Interval in cm)	Depth (m)	Feldspar	Heavy minerals	Mica	Volc. glass	Pyrite + Opaques	Micronodules	Zeolite	Micarb.	Calcareous spicules	Forams	Nannos	Radiolaria	Sponge spicules	Diatoms	Silicoflag.	Lithologic Unit
1-1, 75	0.75	tr								55 45	tr	tr					
1-2, 32	1.82	1								64 40							
1-3, 3	3.03	tr								55 45							
1-3, 75	3.75									55 45		tr	tr				
1-5, 75	6.75	tr								60 40	tr		tr				
1, CC	9.10									52 48							
2-1, 75	10.25									54 45	1		tr				
2-1, 120	10.70		1							53 45		tr	1				
2-4, 76	14.76			1 24						40 35	tr		tr				
2-5, 47	15.97	tr								55 45	tr		tr				
2, CC	18.60			1						45 53	1		tr				
3-1, 75	20.05									60 37	2	tr	tr	1			
3-3, 75	23.05	tr								63 30	5			2			
3-5, 75	26.05				tr	tr				59 40	1			tr			
3-6, 123	28.03	tr	tr							59 40	1	tr	tr				
3, CC	28.40	tr			2					52 46				tr			
4-2, 92	30.92	tr								54 45	1	tr	tr	tr			
4-4, 75	33.75		tr							65 32	2	1	tr	tr			
4, CC	37.60			tr						50 46	2	tr	tr	2			
5-1, 120	39.20	1	1	tr					tr	55 43	tr	tr	tr	1			
5-3, 75	41.75			tr	tr					55 41	2	2	tr	tr			
5-5, 62	44.62				1					55 42	1	tr	tr	1			
5, CC	47.10			tr						50 46	2	1	tr	1			
6-1, 93	48.43	tr		tr						60 39	1	tr	tr	tr			
6-3, 75	55.30			tr	tr					65 35	tr	tr	tr				
6-4, 75	52.75	tr			tr					54 45	1	tr	tr				
6, CC	56.60	tr			tr					57 40	2	1	tr	tr			
7-1, 75	57.75	tr	tr			2				60 37	1	tr	tr	tr			
7-4, 75	56.25	tr			tr					55 43	1	tr	tr				
7, CC	66.10			tr	1					50 45	2	2	tr				
8-1, 75	67.75			tr	tr					60 38	1	tr	1		1		
8-4, 75	72.25	tr			tr					55 45	tr	tr	tr				
8, CC	76.10	tr			tr					50 47	1	1	tr	1			
9-1, 72	77.12	tr			tr					60 39	1	tr	tr				
9-4, 75	81.65	tr			tr	tr				65 34	1	tr	tr	tr			
9, CC	85.50				tr	tr			tr	50 48	1	tr	tr	1			
10-1, 85	86.35				tr					54 46	tr	tr	tr				
10-2, 10	87.10				100												
10, CC	93.10	tr			tr					55 44	tr	tr	tr				
11-1, 75	95.75	tr		1						69 26	2	2	tr	tr			
11, CC	102.60				1					55 47	1		1				
12-2, 75	106.75	1								60 38		tr	1				
12, CC	113.60				tr	tr				55 45	tr	tr	tr				
13-2, 75	116.25	4		tr						60 34	2	tr					
13, CC	120.10			1	1					55 38	1	1	1	2			
14-2, 75	126.05	tr			tr					55 42	1	2	tr	tr			
14, CC	132.90	tr			tr					55 42	2	1	tr	tr			
15-1, 100	134.00	1								55 41	2	1	tr	tr			
15, CC	139.10	1								55 40	2			1			
16-2, 75	144.85	1			tr					55 39	3	1	tr	1			
16, CC	151.70			1	1					55 40	1	1		1			
17-2, 75	154.25	tr			tr	tr				55 43	1	1					
17, CC	161.10	tr			tr					55 42	2	1	tr				
18-2, 75	163.75	tr			tr	tr				60 36	3	1	tr	tr			
18, CC	169.10	1	tr		2					55 39	3						
19-3, 75	174.75	1								55 39	3	1	1				
19, CC	171.10				1	tr				55 43	1	tr	tr				
20-2, 75	182.85				tr					50 46	3	1	tr	tr			
20, CC	189.70				1	tr				65 32	2	tr	tr				
21, CC	193.10	tr								55 44	1	tr	tr				
22-2, 75	201.75	tr			tr	tr				55 45	tr	tr					

APPENDIX A - *Continued*

Sample (Interval in cm)	Depth (m)	Feldspar	Heavy minerals	Mica	Volc. glass	Pyrite + Opaques	Micronodules	Zeolite	Micarb	Calcareous spicules	Forams	Nannos	Radiolaria	Sponge spicules	Diatoms	Silicoflag.	Lithologic Unit
22, CC	205.60	1									60 38 1						
23-1, 90	209.90	tr									50 49 1	tr					
23, CC	218.10	tr									50 48 2	tr					
24-2, 75	220.75	tr									50 48 1	1					
24-5, 88	225.38	tr									45 50 1	1					
24, CC	227.60										50 47 3	tr				tr	
25-2, 75	330.25	tr			tr						50 49 1	tr					
25, CC	237.10	1			tr						60 39	tr	tr				
26-1, 75	238.65										50 49 1	tr					
26, CC	247.00	tr			tr						54 44 1	1				tr	
27-1, 100	248.00	tr			tr						50 47 1	1					
27-3, 75	250.75	tr			tr						49 48 1	2					
27-3, 76	250.76	tr			tr						50 44 3	3					
27-3, 76	250.76							tr			53 45 1	1					
27, CC	256.10	1						tr			60 36 2	1	tr	tr			
28-1, 75	257.65	tr						1			55 41 2	1	tr	tr			
28, CC	266.00										65 29 5	1	tr	tr			
29-1, 75	266.75	1									60 36 2			1			
29, CC	270.60	tr									60 35 4	1	tr	tr			
30-2, 75	277.75	tr			tr						60 35 3	1	1	tr			
30-2, 128	278.25	tr			1						55 37 5	1		1			
30, CC	280.10	tr			1	2					58 36 2	1	tr	tr			
31-2, 75	287.25	tr				tr					55 40 3	1		1			
31, CC	249.10					tr					60 36 3	1	tr	tr			
32-2, 75	296.75	1									55 39 3	1	tr	1			
32, CC	302.10	tr									59 37 4	tr	tr	tr			
33-1, 75	304.85										60 37 2	1					
33, CC	313.20				tr						55 44	tr	1				
34-1, 75	314.25										50 48 1	tr					
34-6, 75	321.75				tr	tr					47 50 3	1					
34, CC	322.60	tr									50 48 2	tr				1	
35-3, 62	326.62										45 53 1	tr					
35, CC	329.10	1									55 40 2	1	tr	1			
36-2, 75	335.05										50 47 2	tr					
36, CC	341.90				tr						55 41 2	1	tr	1			
37-2, 75	346.65				tr						50 45 3	tr					
37, CC	351.50	tr			1						60 36 1	1		1			
38-1, 75	352.75										50 47 1	1					
38, CC	361.10				tr						60 38 1	1					
39-1, 75	362.25	tr									43 55 2	tr					
39, CC	370.60	tr					1				55 42 1	1		tr			
40-1, 75	371.65	tr									52 45 2	1					
40, CC	380.00	tr									60 36 3	1		tr			
41-1, 90	380.90	tr				tr					65 32 2	1	tr	tr			
41, CC	383.10	tr				1					55 37 4	1	1	1			
42-2, 75	392.25	tr									50 46 2	2	tr	tr			
42, CC	399.10	1									55 37 5	1	1	tr			
43-1, 75	400.15	tr									60 37 2	1		tr			
43, CC	408.50										50 47 1	2					
44-1, 75	409.55	tr									60 38 2	tr	tr	tr			
44, CC	417.90	tr									65 32 3	tr					
45-1, 75	419.05										70 21 5	2	tr				
45, CC	427.40	tr			tr	tr	tr				50 46 1	3					
46-2, 75	429.75										70 23 3	1					
46, CC	430.60	tr			tr						55 41 2	2					
47-3, 75	440.75										45 48 3	1					
47, CC	446.10	tr			tr	tr					60 38 1	1					
48-1, 75	447.75										55 38 1	1					
48, CC	456.10										1 55 38 4	1		1			
49-1, 75											4 45 48 3	tr					
49, CC	465.50										55 39 3	1	tr	1			

APPENDIX A - *Continued*

Sample (Interval in cm)	Depth (m)	Feldspar Heavy minerals Mica Volc. glass Pyrite + Opaques Micromodules Zeolite Micarb	3	Forams Nannos Radiolaria Sponge spicules Diatoms Silicoflag.	Lithologic Unit
50-1, 75	466.75			55 39 3	
50, CC	475.10			55 39 4 1 tr	
51-1, 90	475.90			55 38 2 1 1 1	
51, CC	484.10			55 40 3 1 1	
52-1, 75	485.75			50 43 3 3 1	
52, CC	496.10	tr		55 41 3 1	
53-2, 75	406.25	tr		55 42 2 1	
53, CC	500.10	3 2	2	55 37 1 tr	
54-2, 75	505.75	tr	1	55 41 2 1 tr tr	
54, CC	509.60	tr	3	30 64 3 tr	
55-1, 75	514.15		1	51 43 3 1 1	
55, CC	522.50		3	36 40 20 1	
56-2, 75	524.75	tr	3	10 77 10	
56, CC	528.60		3	60 34 3 tr	
57-1, 80	532.90	tr	3	60 35 2	
57, CC	541.20	tr	3	65 28 3 1	
58-1, 75	542.75		3	40 56 1	
58, CC	551.10	tr	3	60 34 3 tr	
59, CC	554.10	tr tr	3	70 23 3 1	
60-2, 75	562.75	tr	3 1	50 43 2	
60, CC	569.60	tr	3 1	60 35 1	
61-1, 75	571.25		3	60 32 5 tr	
61-3, 105	574.55	tr	5	55 37 3 tr	
61, CC	579.60	tr	3	40 56 1 tr	
62-2, 75	581.75		3	50 44 3	
62, CC	582.60	tr		40 54 3 tr	
63-1, 80	589.80	tr	tr	50 49 1 tr	
63, CC	592.10		4 2	55 38 1 tr	
64-2, 100	601.00	1	1	2 44 36 15 1 tr	
64, CC	603.10		tr	4 2 55 38 1	
65-2, 62	610.12		tr	1 60 37 2 tr	
65, CC	612.60	tr tr	2	55 42 1 tr	1
66-1, 75	618.25	tr		60 37 2 1	
66, CC	622.10	tr		55 44 1 tr	
67-1, 75	628.25	tr		60 34 6 tr tr	
67, CC	636.60	tr		60 40 tr tr	
68-2, 75	638.75	tr		tr 55 43 2 tr	
69-1, 82	646.82		3	50 45 2	
69, CC	653.60	tr	tr	60 38 2 tr tr	
70-1, 75	656.75		3	60 36 1	
70, CC	665.10	tr	tr	50 48 1 1	
71-1, 75	665.75		4	50 38 8	
71, CC	672.60	tr	3	60 33 3 1	
72-2, 75	676.75		5	45 47 3	
72, CC	683.60		3 3	55 34 5	
73-2, 75	686.25		3 8	50 37 11 1	
73, CC	691.60		3 10	55 27 5	
75-2, 75	705.25		3 10	35 50 2 tr	
75, CC	709.10	tr		3 50 46 1	
76-1, 75	713.25		3 5	50 30 11 1	
76-2, 75	714.75	tr		3 30 44 20 1 1	
76, CC	720.10			3 50 44 1 1 1	
77, CC	723.60	1		2 55 39 1 1 1	
78-2, 75	733.75	tr		5 45 38 15 1 1	
78, CC	736.10	tr		3 55 40 1 1	
79-1, 10	741.10			30 58 10 1 1	
79, CC	745.60	tr		1 55 42 tr 2 tr	
80-2, 80	752.80			3 20 72 4 1 tr	
80, CC	756.60	1	tr	55 41 1 1 1	
81, CC	763.10	1	1	55 40 1 1 1	
82-1, 75	770.25		3 2	2 30 52 10 1	

APPENDIX A - *Continued*

Sample (Interval in cm)	Depth (m)	Feldspar	Heavy minerals	Mica	Volc. glass	Pyrite + Opaques	Micromodules	Zeolite	Micarb.	Calcareous spicules	Forams	Nannos	Radiolaria	Sponge spicules	Diatoms	Silicoflag.	Lithologic Unit
82, CC	774.10	tr								1	55	40	2	1			
83-1, 140	780.40	tr		tr						1	40	47	10	1			
83, CC	782.10	tr		1						1	55	38	2	1			
84-1, 110	789.60									3	45	46	5	1			
84, CC	781.60	1			1						55	42	tr	1			
85-1, 75	798.75					tr				5	60	30	5				
85, CC	799.60						tr				51	46	2	1			
86-2, 75	809.75									4	50	42	3	1			
86, CC	816.60									10	45	43	2				
87-2, 75	819.25									5	50	43	2	tr			
87, CC	820.10					tr				5	60	33	2				
88-2, 75	828.75						tr			5	50	41	3	1			
88, CC	831.10							tr		5	55	37	3	tr			
89-2, 76	838.26	tr								4	45	50	tr	1			
89, CC	842.10									5	50	43	2	tr			
90-1, 100	846.50	tr								5	10	68	15	2			
90, CC	850.10										52	46	2	tr			
91, CC	862.60	1		tr							60	36	8	1			1
92, CC	866.10				3						55	37	4	1			
93, CC	880.10	tr			tr						55	40	3	2			
94-2, 77	885.77				1	tr					46	50	3				
94, CC	889.60									3	60	35	1	1			
95-2, 75	895.25	tr				tr				2	53	42	3	tr			
95, CC	896.10									3	50	44	2	1			
96, CC	904.10									4	65	26	5				
97-1, 11-	913.10	tr								2	48	47	3	tr			
98-2, 75	923.75									5	60	27	8				
98, CC	927.60									5	70	20	5				
99-1, 72	931.72	tr		7	3					15	5	58	10	2			
99, CC	938.60									5	40	46	8	1			
100-1, 104	941.54				5	tr				15	15	48	•	2			
100, CC	942.10					tr				5	50	39	5	1			
101-1, 87	950.87	tr				tr				15	40	37	8				
101, CC	953.10									5	50	40	4	1			
102-1, 100	960.50						tr			15	50	27	8	tr			
102, CC	961.10									5	60	29	5	1			
103-1, 80	969.80									15	30	13	40	2			
103, CC	970.60									6	45	38	11				
104, CC	978.60									3	40	27	30				
105, CC	988.10									2	35	31	2	tr			
106-2, 103	1000.03									20	20	45	15				
106, CC	1005.10										10	79	10	1			
107-2, 75	1009.25	3		tr						2	40	39	15	1			
107, CC	1010.10	tr									20	42	30	1	1		
108, CC	1018.10	tr								8	20	70			2A		
109, CC	1027.60									15	30	52	3				
110, CC	1037.10					tr				15	20	45	20				
111, CC	1049.60						tr			10	10	70	10				
112, CC	1054.60									20	10	70					
117, CC	1102.10	1			tr						60	38					
118, CC	1113.10	3								15	40	42					
119, CC	1121.10	2								15	40	43					
121-2, 84	1138.34				tr	3	50	27			20						
126-1, 140	1184.90					tr				10	2	88					
131-1, 5	1231.05						1	5	10		5	79					
131-1, 48	1231.48	2	3	30	1			7	10		47						
131-1, 100	1232.06	3	5	74	10			5			3						
131-2, 12	1232.62	2	1	10				10	5		67						
131-2, 76	1233.26			5	1			3	7		84						
132-2, 50	1262.50		3	71	5	2	15				3	1					
132-2, 76	1262.76	5		87	5			1			2				2B		

Site 289 Hole Core 1 Cored Interval: 0.0-9.5 m

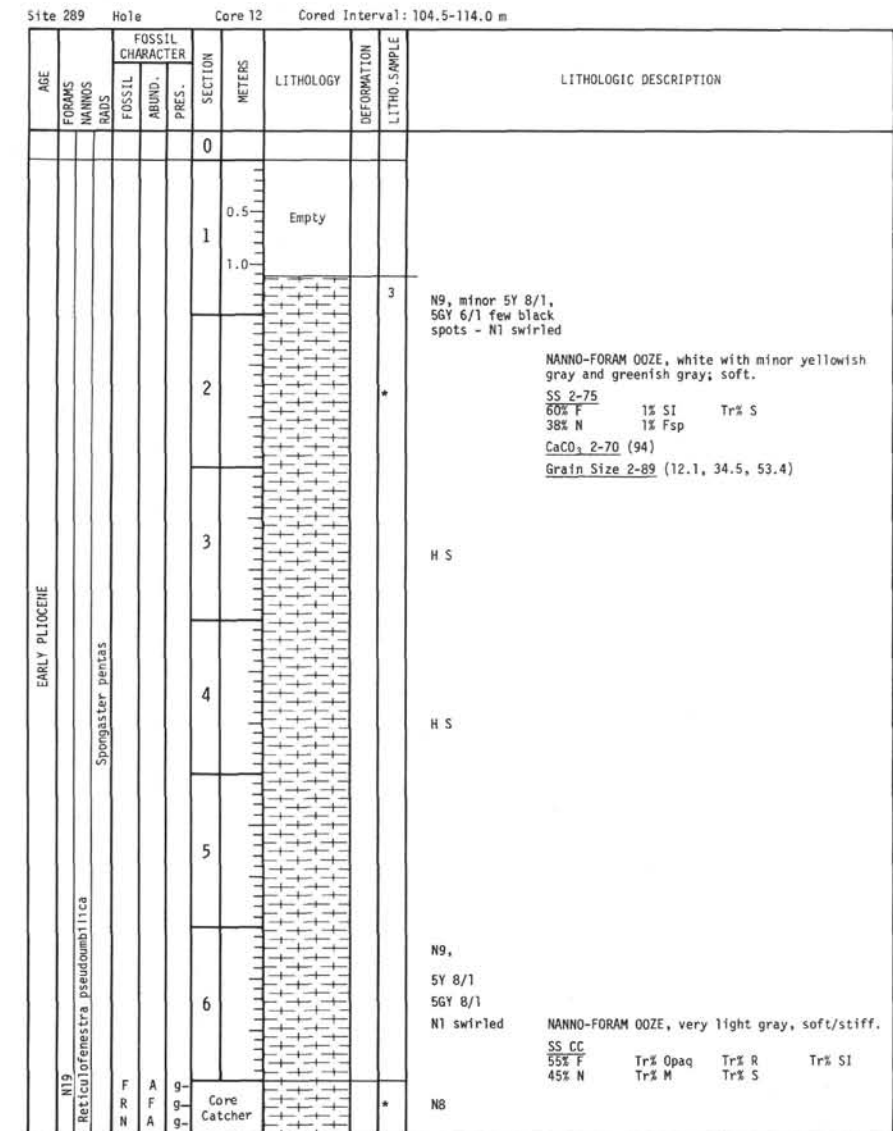
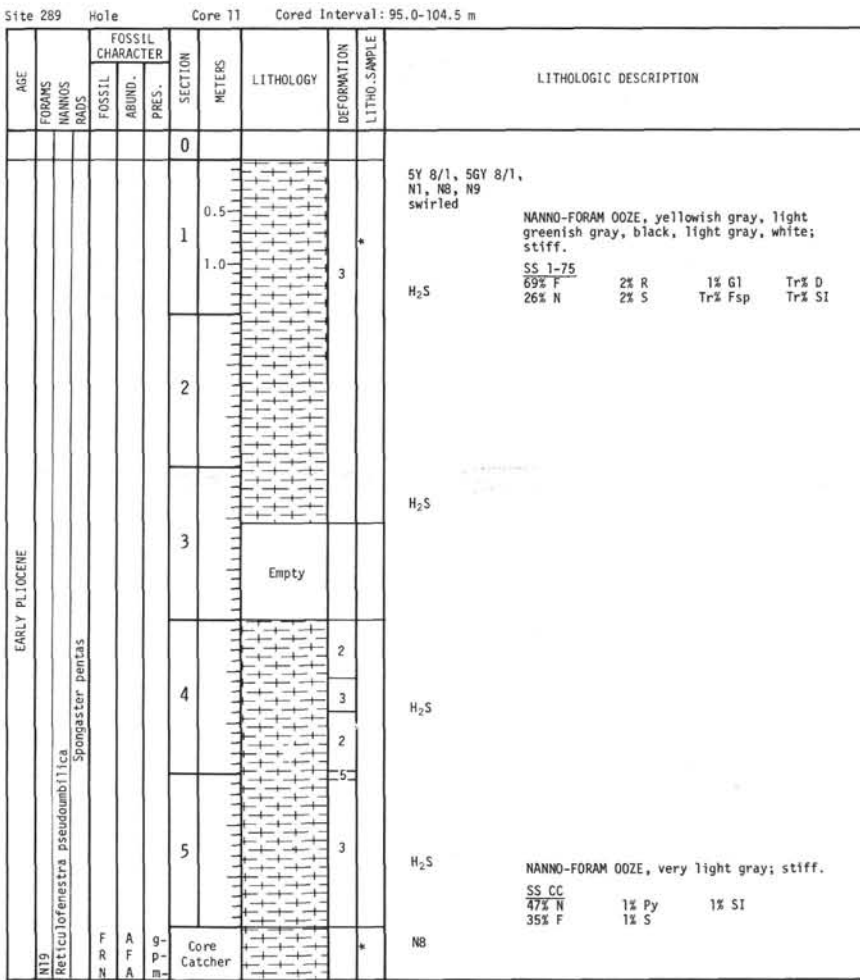
Site 289 Hole Core 2 Cored Interval: 9.5-19.0 m

Explanatory notes in Chapter 2

Site 289		Hole	Core 5	Cored Interval: 38.0-47.5 m				
AGE	FOSSIL CHARACTER	SECTION	METERS	LITHOLOGY	DEFORmATION	LITHOLOGIC DESCRIPTION		
						FoSSIL ABUND.	PRES.	Litho. Sample
		0						
		N A g-	0.5		3	SB 9/1, SG 8/1, N1 swirled SY 8/1 + SG 6/1		
		N A g-	1.0		*	NANNO-FORAM OOZE, white, yellowish gray, greenish gray, black spots; soupy to soft. SS 1-120 55% F 1% G1 Tr% R 43% N 1% SI Tr% S 1% Fsp Tr% Py Tr% Calc S.		
		N A g-	2		*	pyrite abundant		
		N A g-	3		*	NANNO-FORAM OOZE, colors as above; soft. SS 3-75 55% F 2% R Tr% G1 Tr% D 41% N 2% S Tr% Opag Tr% SI		
		N A g-	4		*	SY 7/3 (pale yellow) N8 N1 SG 6/1 swirled		
		N A g-	5		*	NANNO-FORAM OOZE, pale yellow, very light gray, greenish gray, with black spots; soft. SS 5-62 55% F 1% Py 1% SI Tr% S 42% N 1% R Tr% D		
		N A g-	6		*	NANNO-FORAM OOZE, very light gray; soft. SS CC 50% F 2% R 1% SI Tr% D 46% N 1% S Tr% G1		
N21	Discaster brouweri Pterocanium prasinatum	F R F g- R F g- N A g- Core Catcher			N9			
					NB			

Explanatory notes in Chapter 2

Explanatory notes in Chapter 2



Site 289		Hole	Core 14	Cored Interval: 123.5-133.0 m							
AGE	FORAMS NANNO- RADS	FOSSIL CHARACTER	SECTION	METERS	LITHOLOGY	DEFOR- MATION	LITHOLOGIC DESCRIPTION				
							FOS- SIL	ABUND.	PRES.	LITHO. SAMPLE	
EARLY PLIOCENE	N18	Spongaster pentas		0		3	NANNO-FORAM OOZE				
			N	-	-	N9					
				0.5							
				1							
				1.0							
				-		3					
				2		*					
				3			N9	NANNO-FORAM OOZE, white, yellowish gray,			
				4			N1	greenish gray, black spots; soft/soupy.			
				5			5Y 8/1	SS 2-75			
				6			5GY 8/1	55% F	2% S	Tr% Fsp	Tr% SI
				7			swirled	42% N	1% R	Tr% D	
				8			H ₂ S	Grain Size 2-10 (4.0, 32.1, 63.9)			
				9				CaCO ₃ 2-13 (94)			
				10							
				11			H ₂ S - stiff				
				12							
				13			H ₂ S				
				14							
				15			H ₂ S				
				16							
				17			H ₂ S				
				18							
				19			NANNO-FORAM OOZE, very light gray, stiff.				
				20							
				21			SS CC				
				22			55% F	2% R	Tr% Fsp	Tr% D	
				23			42% N	1% S	Tr% Opaq	Tr% SI	
				24							
				25							
				26							
				27							
				28							
				29							
				30							
				31							
				32							
				33							
				34							
				35							
				36							
				37							
				38							
				39							
				40							
				41							
				42							
				43							
				44							
				45							
				46							
				47							
				48							
				49							
				50							
				51							
				52							
				53							
				54							
				55							
				56							
				57							
				58							
				59							
				60							
				61							
				62							
				63							
				64							
				65							
				66							
				67							
				68							
				69							
				70							
				71							
				72							
				73							
				74							
				75							
				76							
				77							
				78							
				79							
				80							
				81							
				82							
				83							
				84							
				85							
				86							
				87							
				88							
				89							
				90							
				91							
				92							
				93							
				94							
				95							
				96							
				97							
				98							
				99							
				100							
				101							
				102							
				103							
				104							
				105							
				106							
				107							
				108							
				109							
				110							
				111							
				112							
				113							
				114							
				115							
				116							
				117							
				118							
				119							
				120							
				121							
				122							
				123							
				124							
				125							
				126							
				127							
				128							
				129							
				130							
				131							
				132							
				133							

Explanatory notes in Chapter 2

Site 289		Hole	Core 18	Cored Interval: 161.5-171.0 m				
AGE	FOSSIL FORMS NANNO- RADAS	FOSSIL CHARACTER		SECTION	LITHOLOGY	DEFORMATION	LITHO-SAMPLE	LITHOLOGIC DESCRIPTION
		Fossil	Abund.					
LATE Miocene	N17	Discaster cf. indigeramus		0	Empty			
				1	0.5	3	N9	
				1	1.0		N9, 5Y 8/1 N1 swirled H ₂ S +5GY 8/1	
				2		*	RAD BEARING NANNO-FORAM DOZE, white, yellowish gray, greenish gray, with black spots; stiff. SS 2-75 60% F 1% S Tr% Py 36% N Tr% Fsp Tr% D 3% R Tr% G1 Tr% SI CaCO ₃ 2-35 (95) Grain Size 2-40 (8.5, 35.0, 56.5)	
				3			H ₂ S	
				4			H ₂ S	
				5			H ₂ S	
					Core Catcher	*	N8	RAD BEARING NANNO-FORAM DOZE, very light gray; stiff. SS CC 55% F 3% R 1% Fsp 39% N 2% G1 Tr% HM

Explanatory notes in Chapter 2

• (0. penultimate zone not recognizable)

Explanatory notes in Chapter 2

Site 289 Hole		Core 24		Cored Interval: 218.5-228.0 m					
AGE	FOSSIL CHARACTER	SECTION	METERS	LITHOLOGY	DEFORmATION	LITHOLOGIC DESCRIPTION			
						FOSSIL BODS	FOSSIL ABUND.	PRES.	LITHO. SAMPLE
		0							
				Empty					
		1	0.5						
		1	1.0						
		2	1.0						
		2	1.5						
		2	2.0						
		2	2.5						
		3	2.5						
		3	3.0						
		4	3.0						
		4	3.5						
		5	3.5						
		5	4.0						
		6	4.0						
		6	4.5						
		6	5.0						
		6	5.5						
		6	6.0						
		6	6.5						
		6	7.0						
		6	7.5						
		6	8.0						
		6	8.5						
		6	9.0						
		6	9.5						
		6	10.0						
		6	10.5						
		6	11.0						
		6	11.5						
		6	12.0						
		6	12.5						
		6	13.0						
		6	13.5						
		6	14.0						
		6	14.5						
		6	15.0						
		6	15.5						
		6	16.0						
		6	16.5						
		6	17.0						
		6	17.5						
		6	18.0						
		6	18.5						
		6	19.0						
		6	19.5						
		6	20.0						
		6	20.5						
		6	21.0						
		6	21.5						
		6	22.0						
		6	22.5						
		6	23.0						
		6	23.5						
		6	24.0						
		6	24.5						
		6	25.0						
		6	25.5						
		6	26.0						
		6	26.5						
		6	27.0						
		6	27.5						
		6	28.0						
		6	28.5						
		6	29.0						
		6	29.5						
		6	30.0						
		6	30.5						
		6	31.0						
		6	31.5						
		6	32.0						
		6	32.5						
		6	33.0						
		6	33.5						
		6	34.0						
		6	34.5						
		6	35.0						
		6	35.5						
		6	36.0						
		6	36.5						
		6	37.0						
		6	37.5						
		6	38.0						
		6	38.5						
		6	39.0						
		6	39.5						
		6	40.0						
		6	40.5						
		6	41.0						
		6	41.5						
		6	42.0						
		6	42.5						
		6	43.0						
		6	43.5						
		6	44.0						
		6	44.5						
		6	45.0						
		6	45.5						
		6	46.0						
		6	46.5						
		6	47.0						
		6	47.5						
		6	48.0						
		6	48.5						
		6	49.0						
		6	49.5						
		6	50.0						
		6	50.5						
		6	51.0						
		6	51.5						
		6	52.0						
		6	52.5						
		6	53.0						
		6	53.5						
		6	54.0						
		6	54.5						
		6	55.0						
		6	55.5						
		6	56.0						
		6	56.5						
		6	57.0						
		6	57.5						
		6	58.0						
		6	58.5						
		6	59.0						
		6	59.5						
		6	60.0						
		6	60.5						
		6	61.0						
		6	61.5						
		6	62.0						
		6	62.5						
		6	63.0						
		6	63.5						
		6	64.0						
		6	64.5						
		6	65.0						
		6	65.5						
		6	66.0						
		6	66.5						
		6	67.0						
		6	67.5						
		6	68.0						
		6	68.5						
		6	69.0						
		6	69.5						
		6	70.0						
		6	70.5						
		6	71.0						
		6	71.5						
		6	72.0						
		6	72.5						
		6	73.0						
		6	73.5						
		6	74.0						
		6	74.5						
		6	75.0						
		6	75.5						
		6	76.0						
		6	76.5						
		6	77.0						
		6	77.5						
		6	78.0						
		6	78.5						
		6	79.0						
		6	79.5						
		6	80.0						
		6	80.5						
		6	81.0						
		6	81.5						
		6	82.0						
		6	82.5						
		6	83.0						
		6	83.5						
		6	84.0						
		6	84.5						
		6	85.0						
		6	85.5						
		6	86.0						
		6	86.5						
		6	87.0						
		6	87.5						
		6	88.0						
		6	88.5						
		6	89.0						
		6	89.5						
		6	90.0						
		6	90.5						
		6	91.0						
		6	91.5						
		6	92.0						
		6	92.5						
		6	93.0						
		6	93.5						
		6	94.0						
		6	94.5						
		6	95.0						
		6	95.5						
		6	96.0						
		6	96.5						
		6	97.0						
		6	97.5						
		6	98.0						
		6	98.5						
		6	99.0						
		6	99.5						
		6	100.0						
		6	100.5						
		6	101.0						
		6	101.5						
		6	102.0						
		6	102.5						
		6	103.0						
		6	103.5						
		6	104.0						
		6	104.5						
		6	105.0						
		6	105.5						
		6	106.0						
		6	106.5						
		6	107.0						
		6	107.5						
		6	108.0						
		6	108.5						
		6	109.0						
		6	109.5						
		6	110.0						
		6	110.5				</td		

Explanatory notes in Chapter 2

Explanatory notes in Chapter 2

Explanatory notes in Chapter 2

Explanatory notes in Chapter 2

Site 289 Hole Core 34 Cored Interval: 313.5-323.0 m

Site 289 Hole Core 35 Cored Interval: 323.0-332.5 m

Explanatory notes in Chapter 2

• *Helfcopontosphaera kampfneri*

Site 289 Hole Core 36 Cored Interval: 332.5-342.0 m									
AGE	FOSSIL CHARACTER			SECTION	METERS	LITHOLOGY	DEFORmATION	LITHO SAMPLE	LITHOLOGIC DESCRIPTION
	FORAMS	NANNO.	RADS						
MIDDLE Miocene				0					
N14				1	0.5				N9, N1
				2	1.0				NANNO-FORAM OOZE, white (N9), black (N1) spots; no laminae; stiff.
	F	A	e-	3	2				Same as in Section 1. NANNO-FORAM OOZE, white; stiff/semi-lithified. SS 2-75 50% F 2% R Tr% S 47% N 1% M
				4	0				Same as in Section 2. <u>CaCO₃ 3-63 (94)</u> <u>Grain Size 3-66 (6.1, 50.4, 43.5)</u> X-ray 3-70 7% Amor 93% Cryst 100% Calc
				5	0				Section 4: white (N9), black (N1) spots, greenish gray (SG 8/1) and pale purple (SRP 7/2) in parallel laminae; semi-lithified/stiff; parallel laminae at 4/80, 4/90, and 4/100.
				6	0				Section 5: white (N9) only; no parallel laminae.
	F	A	e-						Section 6: 6/0-100, like Section 5; 6/100-150, white (N9), black (N1) spots, greenish gray (SG 6/1) parallel laminae; very light gray (N8) band, parallel laminae at 6/104.
	R	A	g-						NANNO-FORAM OOZE, white. SS CC 55% F 2% R 1% SI Tr% D 41% N 1% S Tr% Py
	N		f-						White (N9)

Site 289 Hole Core 37 Cored Interval: 342.0-351.5 m									
AGE	FOSSIL CHARACTER			SECTION	METERS	LITHOLOGY	DEFORmATION	LITHO SAMPLE	LITHOLOGIC DESCRIPTION
	FORAMS	NANNO.	RADS						
MIDDLE Miocene				0					
N13				1	0.5				N9, N7, N8
				2	1.0				SG 6/1 SRP 7/2
	F	A	e-	3	0				Section 2: white (N9), black (N1) spots, light gray (N8) in bands (2-4 cm thick), greenish gray (SG 6/1) and pale purple (SRP 7/2) in parallel laminae; semi-lithified/soft; light gray banding at 2/23-34.
				4	0				RAD BEARING NANNO-FORAM OOZE, white. SS 2-75 50% F 3% R Tr% G1 45% N 2% M Tr% S
				5	0				parallel laminae at 2/10-18, 2/58, 2/97-100, 2/119-124, 2/130, and 2/142
				6	0				Section 3: same as Section 2; parallel laminae at 3/30-32.
									Section 4: white (N9), black (N1) spots; no laminae.
									Section 5: like Section 4.

Explanatory notes in Chapter 2

Site 289 Hole		Core 38		Cored Interval: 351.5-361.0 m								
AGE	FOSSIL CHARACTER	SECTION	METERS	LITHOLOGY	DEFORATION	LITHOLOGIC DESCRIPTION						
						FORAMS	NANNO	RADS	FOSILL	ABUND.	PRES.	LITHO SAMPLE
N13	<i>Discosaster exilis</i>	0	0									NANNO-FORAM OOZE, white (N9).
		0.5	0			N9						NANNO-FORAM OOZE/CHALK, white (N9), black (N1) spots, greenish gray (SG 6/1) and light gray (N7) parallel laminae.
		1	0/1		*	N1						NANNO-FORAM OOZE, white.
		1.0	1			N7						SS 1-75 50% F 1% M 1% S 47% N 1% R
		2	0/1			SG 6/1						Stiff/semilithified, parallel laminae at 1/4, 1/9, 1/14-27, 1/44-46, 1/75-77, and 1/92-94.
		3	1									Section 2: white (N9), black (N1) spots; semilithified/soft; no laminae.
		4	0			N9						
		5	0									Section 3: like Section 1, parallel laminae at 3/72, 3/78; gray bands at 3/99. <u>CaCO₃ 3-62 (93)</u> <u>Grain Size 3-67 (7.8, 45.9, 46.3)</u>
		6	1/0									N9 + N1 spots semilithified/stiff
												+SG 6/1 in parallel laminae at 5/144, 147
												parallel laminae at 6/104
												NANNO-FORAM OOZE, white.
												SS CC 60% F 1% R Tr% Py 38% N 1%
												Core Catcher White (N9)

Explanatory notes in Chapter 2

Site 289 Hole Core 42 Cored Interval: 389.5-399.0 m

AGE	FORAMS	NANNO- RAD'S	FOSSIL CHARACTER	SECTION	METERS	LITHOLOGY	DEFOR- MATION	LITHO. SAMPLE	LITHOLOGIC DESCRIPTION					
									FOS- SIL	ABUND.	PRES.			
MIDDLE MIocene	N12	Discaster exilis		0										
		Dorcaspyris alata		1	0.5	N9 N1 spots SG 6/1 SRP 6/2	0/1	NANNO-FORAM OOZE/CHALK in parallel laminae						
				2	1.0		0/1	semilithified/soft						
				3			*	semilithified/stiff						
				4			0/1	NANNO-FORAM OOZE, white, black spots, greenish gray and pale purple in parallel laminae; semilithified/stiff. SS 2-75 50% F 2% R Tr% Fsp Tr% SI 46% N 2% S Tr% D						
				5			0/1	Parallel laminations at: Section 1-10 to 14, 40 to 50, 64 to 66, 125 to 134 Section 2-2 to 5 Section 3-71 to 76 Section 4-65 to 67, 103 Section 5-40 to 56, 77 to 83 Section 6-10 to 14, 36 to 42, 50 to 56, 144 to 148						
				6			0/1	CaCO ₃ 4-67 (93) Grain Size 4-90 (15.3, 44.3, 40.5)						
								RAD BEARING NANNO-FORAM OOZE, white; semilithified/stiff. SS CC 55% F 5% R 1% D 1% S Tr% SI 37% N 1% Fsp 1% S						
						N9	*							

Site 289 Hole Core 43 Cored Interval: 399.0-408.5 m

AGE	FORAMS	NANNO- RAD'S	FOSSIL CHARACTER	SECTION	METERS	LITHOLOGY	DEFOR- MATION	LITHO. SAMPLE	LITHOLOGIC DESCRIPTION					
									FOS- SIL	ABUND.	PRES.			
MIDDLE MIocene	N12	Discaster exilis		0					N9					
		Dorcaspyris alata		1	0.5		0/1	NANNO-FORAM OOZE/CHALK N9, N1 spots SG 6/1 SRP 6/2 in parallel laminae						
				2	1.0		*	NANNO-FORAM OOZE, white, black spots, greenish gray and pale purple in parallel laminae; semilithified/stiff. SS 1-75 60% F 2% R 37% N 1% S Tr% SI						
				3			0/1	Parallel laminae at: Section 1-52 to 60, 75 to 82, 96 to 101, 113 to 121 Section 2-111 to 114, 144 to 146 Section 3-146 to 148 Section 4-35 Section 5-109 Section 6-33 to 35, 98 to 102, 121 to 123, 144 to 149						
				4			0/1							
				5			0/1							
				6			0/1							
								NANNO-FORAM OOZE, white; semilithified/stiff. SS CC 50% F 2% S 47% N 1% R						
						N9	*							

Explanatory notes in Chapter 2

Site 289 Hole		Core 44		Cored Interval: 408.5-418.0 m		LITHOLOGIC DESCRIPTION						
AGE	FOSSIL CHARACTER	SECTION	METERS	LITHOLOGY	DEFORmATION	LITHO. SAMPLE	LITHOLOGIC DESCRIPTION					
							FIDGBAMS	NANNO- RAKS	Fossil	Absurd.	PRES.	
MIDDLE Miocene	Dorcaspyris alata		0									
N12	Discaster exilis		0.5				N9	5Y 8/1 blebs	NANNO-FORAM OOZE/CHALK			
			1		0/1 *				NANNO-FORAM CHALK, white, with yellowish gray blebs; semilithified/stiff.			
			1.0				SS 1-75	60% F	2% R	Tr% D	Tr% SI	
			2		0/1		38% N	Tr% Fsp	Tr% S			
			3		0		Parallel laminae at:					
			4		0/1		N1 spots	Section 2-34 to 36, 48, 109				
			5		3		SG 6/1	Section 3-42 to 43				
			6		0		5RP 7/2	laminae Section 4-10 to 12, 18 to 20, 26 to 29, 49 to 51				
							N7 bands					
							+ 5Y 8/1 blebs					
								<u>CaCO₃ 3-17 (91)</u>				
								<u>Grain Size 3-20 (22.0, 43.6, 34.4)</u>				
							N9	soft				
								semilithified at 62-68				
								RAD BEARING NANNO-FORAM OOZE, white; semilithified/soft.				
							Core Catcher	SS CC	3% R	Tr% S		
								65% F	Tr% Fsp			
								32% N				

Explanatory notes in Chapter 2

Explanatory notes in Chapter 2

Explanatory notes in Chapter 2

Explanatory notes in Chapter 2

Site 289 Hole Core 56 Cored Interval: 522.5-532.0 m													
AGE	FORAMS NANNO RAD'S	FOSSIL CHARACTER	FOSSIL ABUND. PRES.	SECTION	METERS	LITHOLOGY	DEFORATION	LITHO. SAMPLE	LITHOLOGIC DESCRIPTION				
									0	5	10	1/0	
EARLY MIocene	N7 Sphenolithus heteromorphus Calocycletta virginis	R	A	0	0.5	Void							
				1	0.5	N8 very light gray chalk ooze							
				1	1.0	N9 white							
				2	0.5	N8							
				2	1.0	N1 black spots, N1 and SG 6/1 black and greenish gray laminae.							
				2	1.5	RAD AND FORAM BEARING NANNO CHALK, white; semilithified/stiff.							
				2	2.0	SS 2-75 77% N 10% F	10% R 3% M	Tr% G1					
				3	0.5	Grain Size 3-66 (5.7, 64.7, 29.6) <u>CaCO₃ 3-83 (94)</u>							
				3	1.0	Parallel laminae at: Section 2-111 to 113, 120 to 126 Section 3-3 to 7, 21 to 23 Section 4-26 to 27 (56 6/1), 69 to 72 (56 6/1)							
				4	0.5	MICARB AND RAD BEARING NANNO-FORAM CHALK, white.							
				4	1.0	SS CC 60% F 34% N	3% M 3% R	Tr% S					
			f	Core Catcher	0.5	*	N9						

Site 289 Hole Core 57 Cored Interval: 532.0-541.5 m													
AGE	FORAMS NANNO RAD'S	FOSSIL CHARACTER	FOSSIL ABUND. PRES.	SECTION	METERS	LITHOLOGY	DEFORATION	LITHO. SAMPLE	LITHOLOGIC DESCRIPTION				
									0	5	10	1/0	
EARLY MIocene	N7 Sphenolithus heteromorphus Calocycletta virginis	F N A f	A f	0	0.5								
				1	0.5								
				1	1.0								
				2	0.5								
				2	1.0								
				3	0.5								
				3	1.0								
				4	0.5								
				4	1.0								
				5	0.5								
				5	1.0								
				6	0.5								
				6	1.0								
				Core Catcher	0.5	*	N9						
					0.5								
					1.0								
					1.5								
					2.0								
					2.5								
					3.0								
					3.5								
					4.0								
					4.5								
					5.0								
					5.5								
					6.0								
					6.5								
					7.0								
					7.5								
					8.0								
					8.5								
					9.0								
					9.5								
					10.0								
					10.5								
					11.0								
					11.5								
					12.0								
					12.5								
					13.0								
					13.5								
					14.0								
					14.5								
					15.0								
					15.5								
					16.0								
					16.5								
					17.0								
					17.5								
					18.0								
					18.5								
					19.0								
					19.5								
					20.0								
					20.5								
					21.0								
					21.5								
					22.0								
					22.5								
					23.0								
					23.5								
					24.0								
					24.5								
					25.0								
					25.5								
					26.0								
					26.5								
					27.0								
					27.5								
					28.0								
					28.5								
					29.0								
					29.5								
					30.0								
					30.5								
					31.0								
					31.5								
					32.0								
					32.5								
					33.0								
					33.5								
					34.0								
					34.5								
					35.0								
					35.5								
					36.0								
					36.5								
					37.0								
					37.5								
					38.0								
					38.5								
					39.0								
					39.5								
					40.0								
					40.5								
					41.0								
					41.5								
					42.0								
					42.5								
					43.0								
					43.5								
					44.0								
					44.5								
					45.0								
					45.5								
					46.0								
					46.5								
					47.0								
					47.5								
					48.0								
					48.5								
					49.0								
					49.5								
					50.0								
					50.5								
					51.0								
					51.5								
					52.0								
					52.5								
					53.0								
					53.5								
					54.0								
					54.5								
					55.0								
					55.5								
					56.0								
					56.5								
					57.0								
					57.5								
					58.0								
					58.5								
					59.0								
					59.5	</td							

Site 289 Hole Core 58 Cored Interval: 541.5-551.0 m

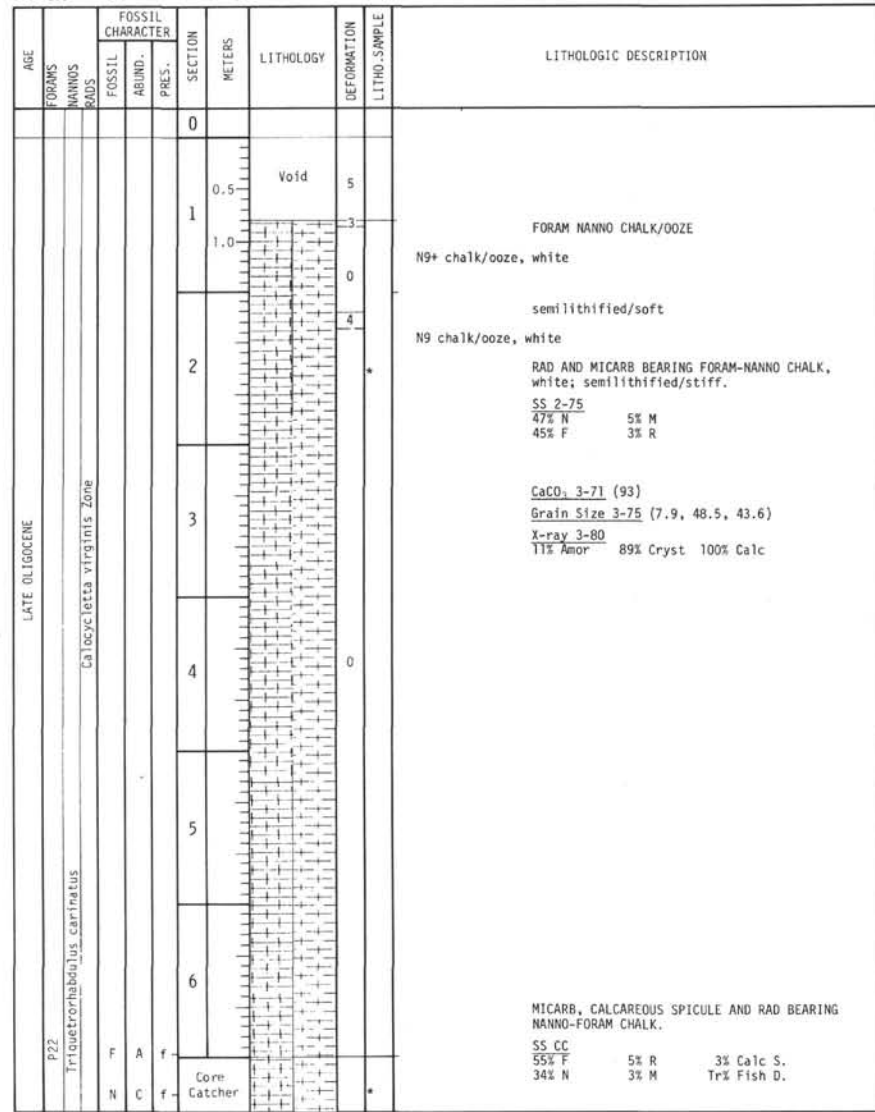
Site 289 Hole Core 59 Cored Interval: 551.0-560.5 m

Explanatory notes in Chapter 2

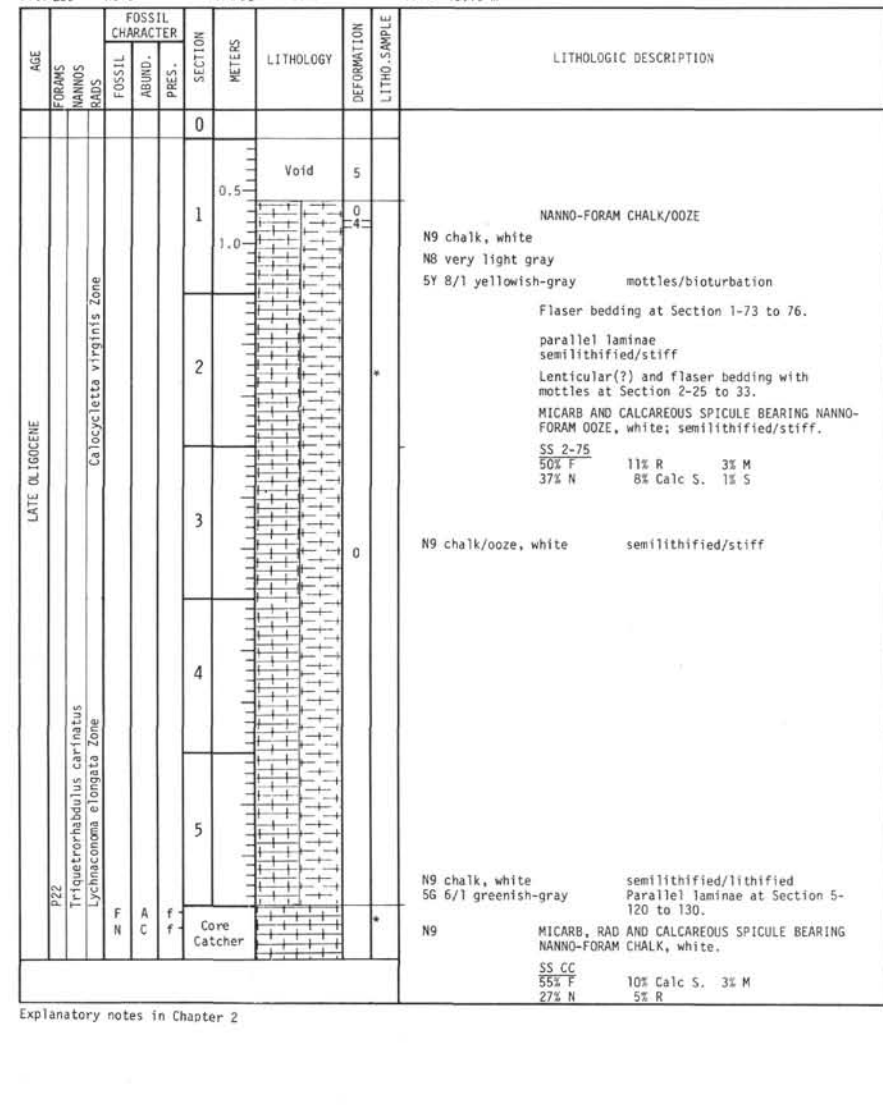
Explanatory notes in Chapter 2

Site 289		Hole	Core 69	Cored Interval: 646.0-655.5 m							
AGE	FORAMS NANNO RAD.	FOSSIL CHARACTER		SECTION	METERS	LITHOLOGY	DEFOR. LITHO. SAMPLE	LITHOLOGIC DESCRIPTION			
		FOSIL ABUND.	PRES.								
LATE OLIGOCENE	N4			0		Void	5				
EARLY MIocene					0		0	FORAM-NANNO CHALK/OOZE			
					0.5			N9 chalk/ooze, white SG 8/1 light greenish gray			
					1.0		0	MICARB-BEARING NANNO-FORAM CHALK, white; semilithified/stiff; mottling (bioturbation).			
							*	N1 black spots SS 1-82 50% F 3% M 45% N 2% R			
				2				Parallel laminae at: Section 1-31 to 33, 60 to 62, 70 to 72, 65-90, 105 to 106			
				3				Parallel laminae at: Section 2-12 to 20, 100 to 106, 130 to 150 (sparse) Section 3-15, 80 to 84, 108, 138			
				4			0	semilithified/stiff			
				5				N9 chalk/ooze, white N1 black spots			
								NANNO-FORAM CHAK, white; semilithified.			
								SS CC 60% F 2% R 38% N Tr% Fsp Tr% Py Tr% S Tr% SI			
								N9			
								Core Catcher			

Site 289 Hole Core 72 Cored Interval: 674.5-684.0 m



Site 289 Hole Core 73 Cored Interval: 684.0-693.5 m



Explanatory notes in Chapter 2

Site 289 Hole		Core 80		Cored Interval: 750.5-760.0 m			
AGE	FOSSIL CHARACTER	SECTION		LITHOLOGY	DEFORMATION LITHO. SAMPLE	LITHOLOGIC DESCRIPTION	
		METERS	PRES.				
		0					
LATE OLIGOCENE							
#	P21						
	=	Sphenolithus cipriensis					
		Dorcasoduspis attenuatus					
F N	C C	f f	Core Catcher		*	N9	
						</td	

Explanatory notes in Chapter 2

Explanatory notes in Chapter 2

Explanatory notes in Chapter 2

Site 289 Hole Core 90 Cored Interval: 845.5-855.0 m

AGE	FORAMS	NANNO-	RADIA.	FOSSIL CHARACTER		SECTION	METERS	LITHOLOGY	DEFORMATION	LITHO. SAMPLE	LITHOLOGIC DESCRIPTION
				PRES.	ABUND.						
LATE OLIGOCENE						0		Empty			
P21	Sphenolithus distentus					1	0.5				
	Dorcadopsisyr's atenuatus					2	1.0	N9 chalk/ooze, white			
N	C	f				3	1.5	NANO CHALK/OOZE MICARB AND FORAM BEARING, RAD RICH NANNO CHALK, from dark gray laminae. SS 1-100 68% N 10% F 2% S 15% R 5% M Tr% Py			
							2	N5 medium gray Parallel laminae at: Section 1-107 to 111, 145 Section 2-throughout Section 3-50 to 52, 59 to 61 Wavy-flaser-lenticular bedding at: Section 2-96, 135 to 137 Section 3-26 to 31, 135 to 140 Bioturbated at: Section 1-126 to 138, 146 to 154 Section 2-throughout Section 3-32 to 48, 120 to 136, 134 to 150 CaCO ₃ 3-60 (90) Grain Size 3-64 (4.8, 44.7, 50.6)			
							3	N9 white			
							4	NANNO-FORAM CHALK, white. SS CC 52% F 2% R 46% N Tr% S			
							5				

Site 289 Hole Core 91 Cored Interval: 855.0-864.5 m

AGE	FORAMS	NANNO-	RADIA.	FOSSIL CHARACTER		SECTION	METERS	LITHOLOGY	DEFORMATION	LITHO. SAMPLE	LITHOLOGIC DESCRIPTION
				PRES.	ABUND.						
LATE OLIGOCENE						0		Empty			
P21	Sphenolithus distentus					1	0.5				
	Dorcadopsisyr's atenuatus					2	1.0				
N	F	C				3	1.5				
	R	C				4	2.0				
						5	2.5				
							3				
							4				
							5				

(core shattered by punch corer)
RAD BEARING NANNO-FORAM CHALK, white.
SS CC
60% F 3% R 1% Fsp 1% S
36% N Tr% G1

Explanatory notes in Chapter 2

Site 289 Hole		Core 97		Cored Interval: 912.0-921.5 m				
AGE	FOSSIL CHARACTER	SECTION	METERS	LITHOLOGY		DEFORMATION	LITHO. SAMPLE	LITHOLOGIC DESCRIPTION
				FOSSIL ABUND.	PRES.			
		0						
EARLY OLIGOCENE	Thecocystis tuberosa	1	0.5	Empty				NANNO-FORAM CHALK
P20	Sphenolithus predistinctus	1	0.5					Bioturbated throughout.
T	C	1	1.0			0/4	*	RAD BEARING NANNO-FORAM CHALK, white, with medium to very light gray; semilithified; bioturbated.
		2	1.0	Void				SS 1-101 48% F 3% R 47% N 2% M Tr% Fsp Tr% S
		2	1.5			0/4		N9, NB, NG
		3	2.0	Void				N9, NB bioturbated
		3	2.5			0/4		N1 black area with rings around black spot
		3	3.0			0/4		X-ray 3-77 (greenish gray) 36% Amor 96% Calc 1% Mont 64% Cryst 3% Plag
		4	3.5			0/4		N9 (SG 6/1 band at Section 3-74 N8)
		4	4.0					Bioturbated throughout. +N4 flaser(?) beds

Explanatory notes in Chapter 2

Site 289		Hole	Core 98	Cored Interval: 921.5-931.0 m				
AGE	FORAMS	NANNO. RAD.	FOSIL CHARACTER	METERS	SECTION	DEFORMATION	LITHO. SAMPLE	LITHOLOGIC DESCRIPTION
EARLY OLIGOCENE	P20 Sphenolithus predistensus			0				
R F N	A C C			0.5		4/3		N9 NANNO-FORAM CHALK/OOZE, white; soft; (disturbed by drilling?).
				1.0		0		
				1.4		0		
				1.4		0		
				1.4		0		
				2		*		
				2		0		N9 chalk/ooze, white semilithified/soft
				2		0		N8 very light gray
				2		0		N6 medium gray
				3		5		MICARB AND RAD BEARING NANNO-FORAM CHALK, white. SS 2-75 60% F 8% R 27% N 5% M
				3		5		Bioturbation at: Section 1-140 to 150 Section 2-1 to 5, 24 to 70, 108 to 114 Section 3-105 to 112, 125 to 131
				3		5		X-ray 3-127 15% Amor 86% Cryst 100% Calc Grain Size 3-131 (3.0, 45.5, 51.5) CaCO ₃ 3-135 (91) Section 3 semilithified/stiff.
				4		0		NB ooze, semilithified, very light gray
				4		0		N7 ooze, light gray
				4		0		MICARB AND RAD BEARING NANNO-FORAM CHALK, white. SS CC 70% F 5% M 20% N 5% R
				4		*		
				Core Catcher				

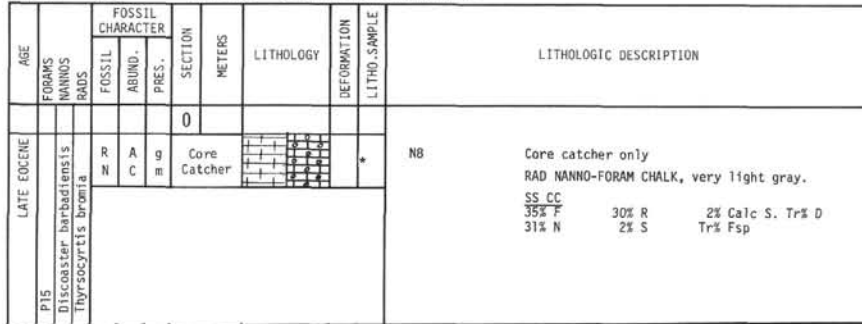
Site 289		Hole	Core 99	Cored Interval: 931.0-940.5 m				
AGE	FORAMS	NANNO. RAD.	FOSIL CHARACTER	METERS	SECTION	DEFORMATION	LITHO. SAMPLE	LITHOLOGIC DESCRIPTION
EARLY OLIGOCENE	P20 Sphenolithus predistensus			0				
R F N	F C C	m f f		0.5		6/4		N9 FORAM-NANNO CHALK/OOZE, white, very light gray, medium gray; semilithified/stiff, abundant bioturbation.
				1.0		*		N8 PYRITE, VOLCANIC GLASS, FORAM AND RAD BEARING, MICARB RICH, NANNO CHALK, from gray laminae.
				1.0		*		SS 1-72 58% N 5% G1 2% Fe-O Tr% G 15% M 5% F 2% S 10% R 3% Py Tr% Fsp
				2				N7 light gray N5 medium gray
				2				semilithified/stiff
				2				abundant bioturbation
				3				N9 white chalk ooze N7 light gray N5 medium gray
				3				
				4				
				4				
				5				
				5				
				Core Catcher				

Explanatory notes in Chapter 2

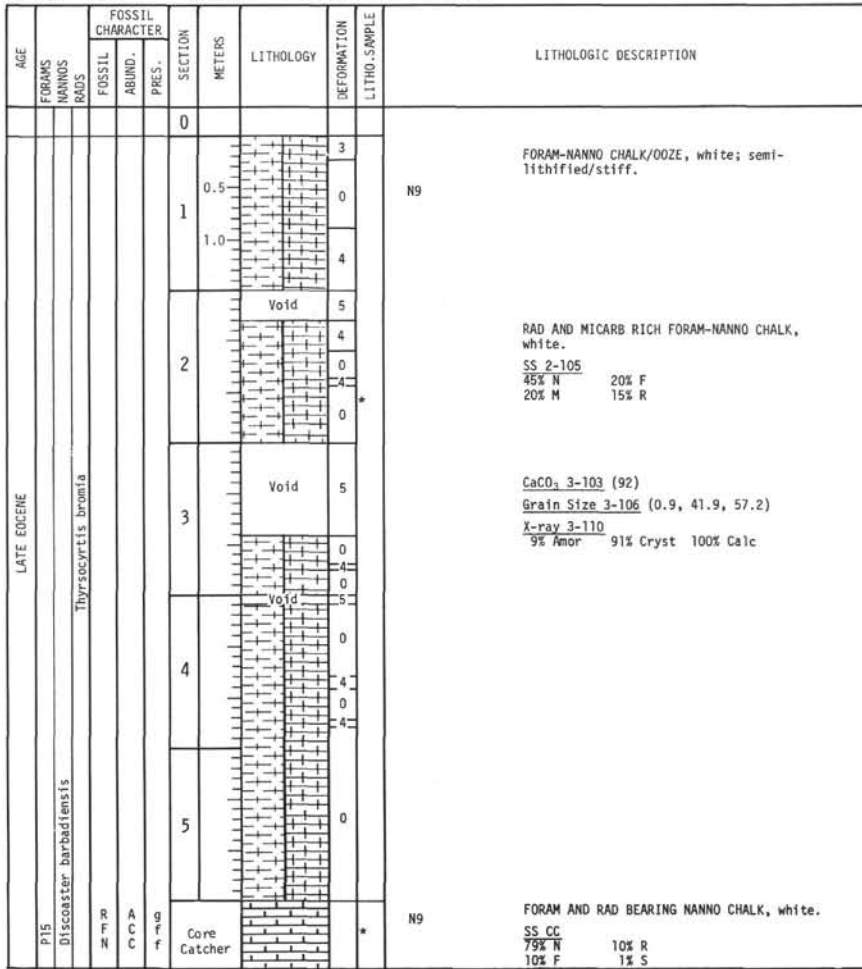
Site 289		Hole	Core 101	Cored Interval: 950.0-959.5 m
AGE		FOSIL CHARACTER		LITHOLOGIC DESCRIPTION
		FOSSIL CHARACTER		
		FOSSIL CHARACTER		
		FOSSIL CHARACTER		
P19	EARLY OLIGOCENE	FORAMS NANNO- RAD'S	SECTION	METERS
Z F 20	Cyclococcolithina formosa <i>Thecocystis tuberosa</i>	FOSSIL ABUND.- PRES.		DEFORMATION
				LITHO-SAMPLE
			0	
				Empty
				3
				0
				3
				0
				0
				4*
				0
				4/0
				0
				4/0
				4
				4/0
				0
				4/0
				*
	N		1	
				N9
				N8
			2	
				N9/N8
	A C C	m f f	Core Catcher	

Explanatory notes in Chapter 2

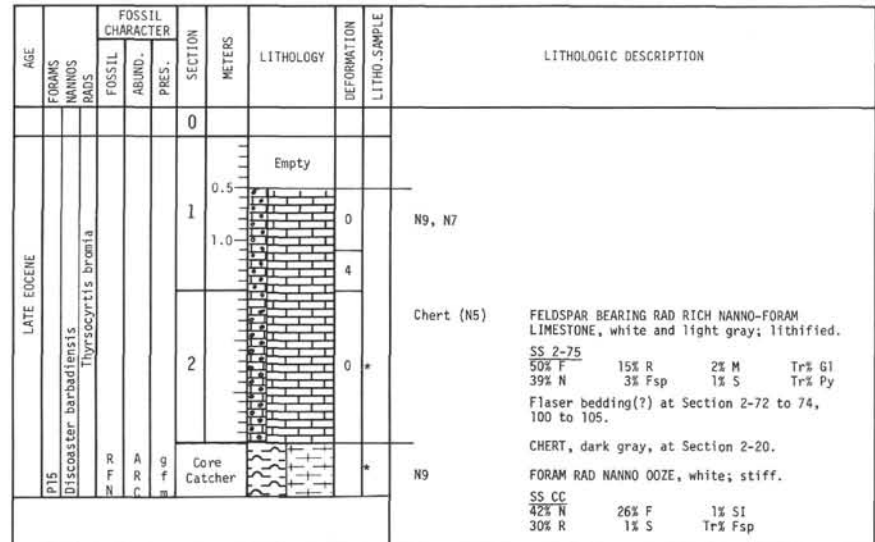
Site 289 Hole Core 105 Cored Interval: 988.0-997.5 m



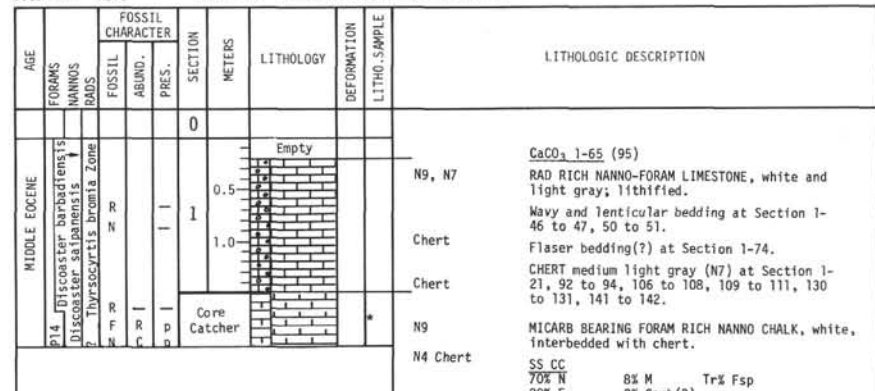
Site 289 Hole Core 106 Cored Interval: 997.5-1007.0 m



Site 289 Hole Core 107 Cored Interval: 1007.0-1016.5 m

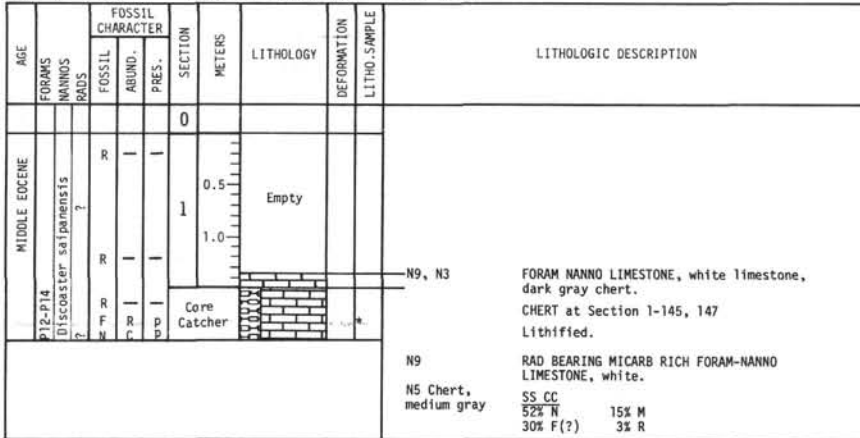


Site 289 Hole Core 108 Cored Interval: 1016.5-1026.0 m

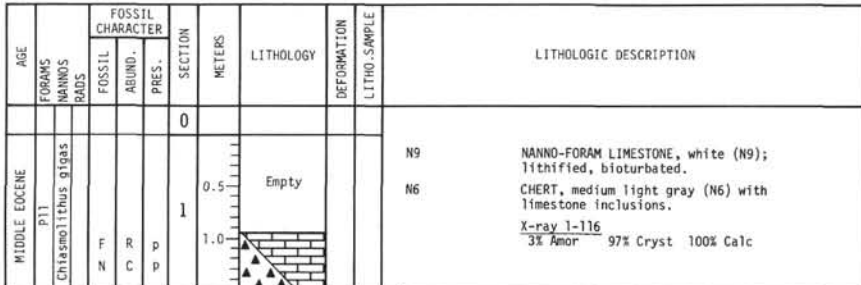


Explanatory notes in Chapter 2

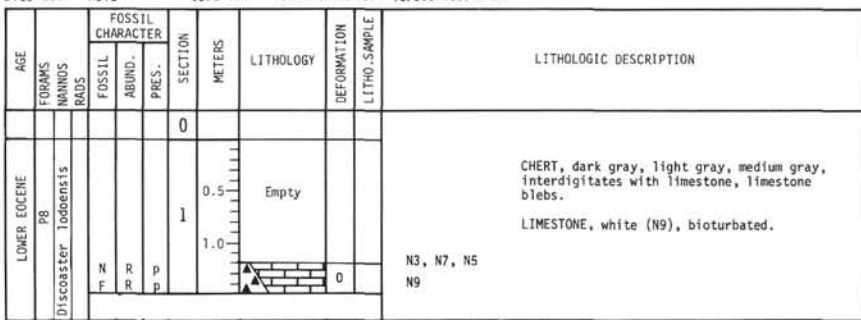
Site 289 Hole Core 109 Cored Interval: 1026.0-1035.5 m



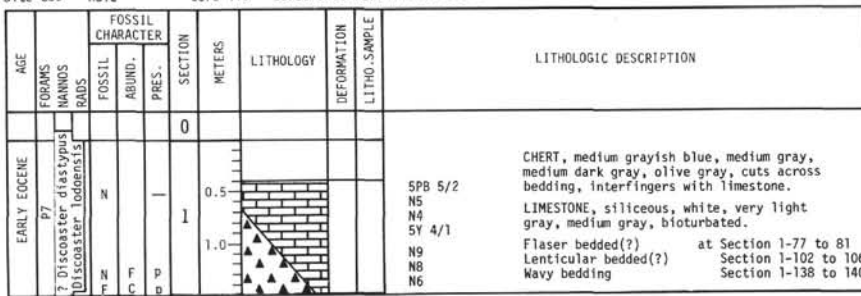
Site 289 Hole Core 113 Cored Interval: 1064.0-1073.5 m



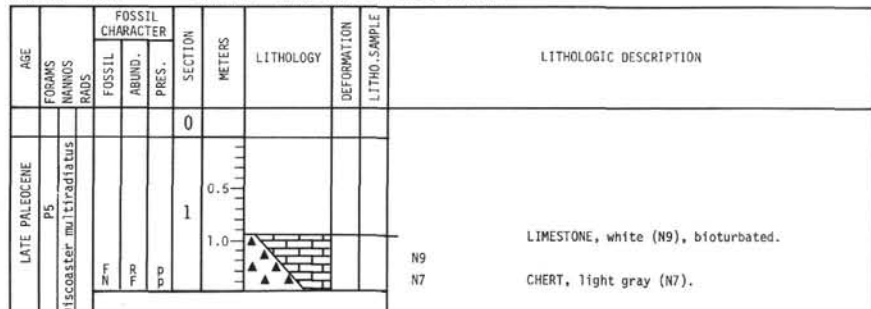
Site 289 Hole Core 114 Cored Interval: 1073.5-1083.0 m



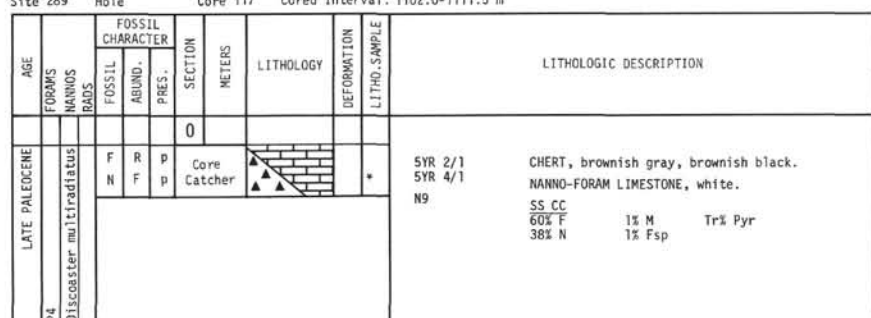
Site 289 Hole Core 115 Cored Interval: 1083.0-1092.5 m



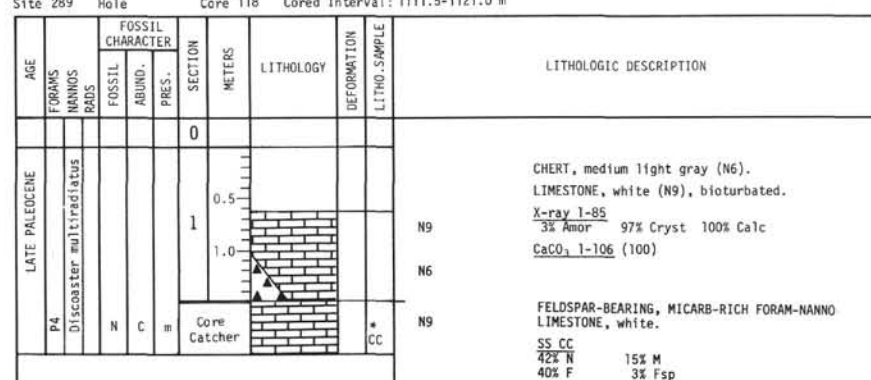
Site 289 Hole Core 116 Cored Interval: 1092.5-1102.0 m



Site 289 Hole Core 117 Cored Interval: 1102.0-1111.5 m



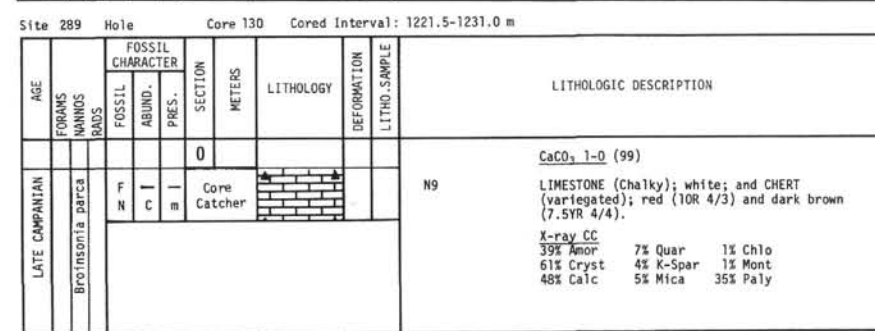
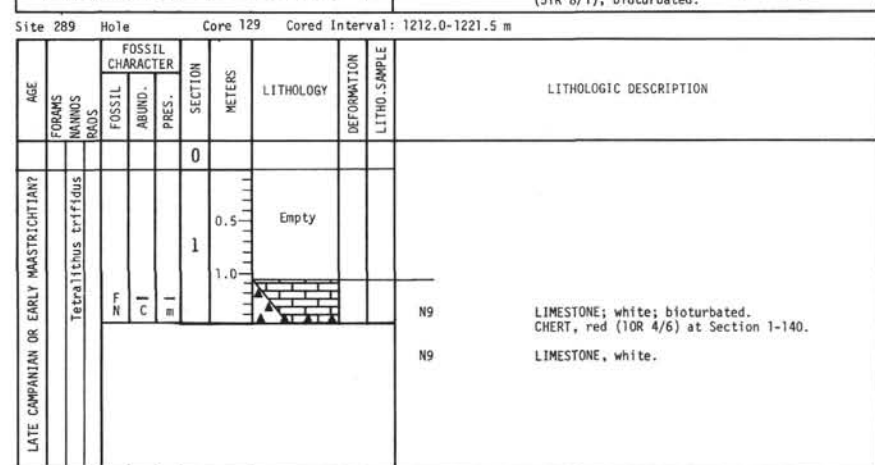
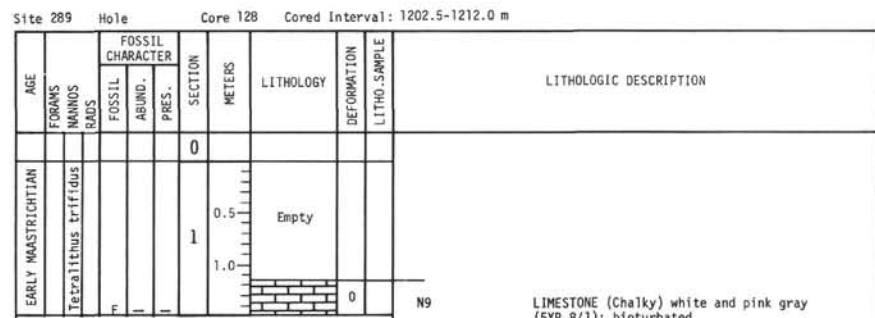
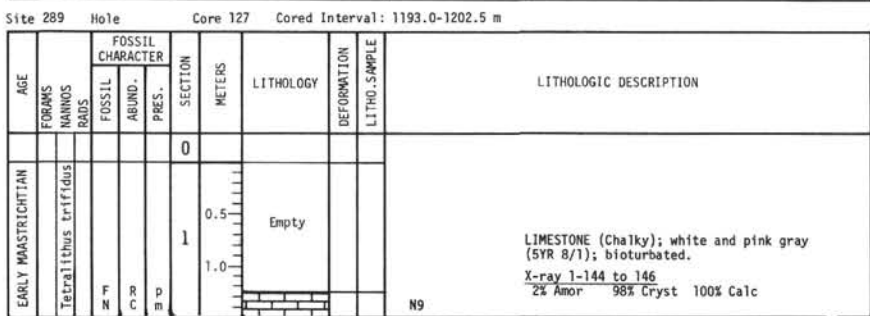
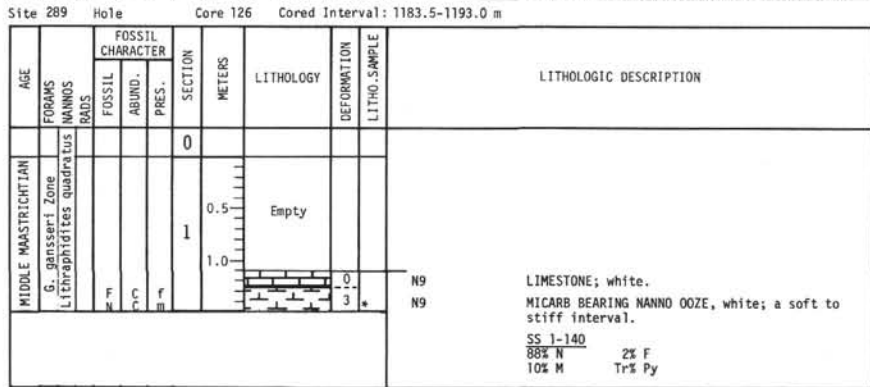
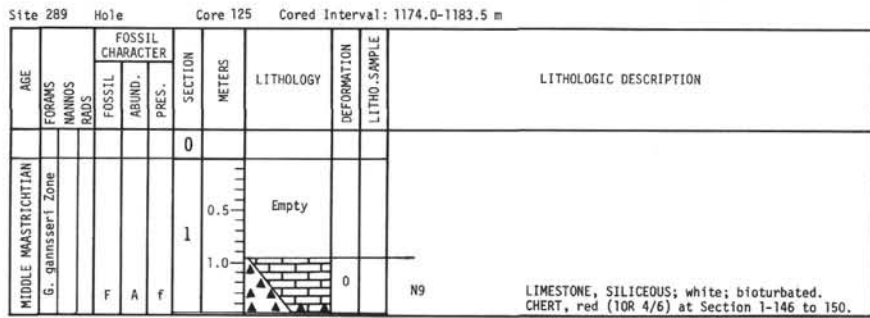
Site 289 Hole Core 118 Cored Interval: 1111.5-1121.0 m



Explanatory notes in Chapter 2

Site 289		Hole	Core 123	Cored Interval: 1155.0-1164.5 m				
AGE	FORAMS NANOMS RADLS	FOSSIL CHARACTER	SECTION	METERS	LITHOLOGY	DEFOR. LIT.	LITHO. SAMPLE	LITHOLOGIC DESCRIPTION
		FOSSIL ABUND. PRES.						
M. MASTRICHTIAN	G. ganister Zone		0		Empty			
			1	0.5 1.0	0.5 1.0	0	N9	LIMESTONE; white; bioturbated; stylolites at Section 1-29 and 101. CHERT, red (10R 4/6) at Section 1-55 to 60.
F N	C C	f f						

Explanatory notes in Chapter 3



Explanatory notes in Chapter 2

Site 289 Hole Core 131 Cored Interval: 1231.0-1259.5 m

Site 289 Hole Core 132 Cored Interval: 1259.5-1269.0 m

Explanatory notes in Chapter 2

